

AD-774 192

SEISMIC DECOUPLING EXPERIMENT: A COM-  
PARISON OF SEISMIC MEASUREMENTS TAKEN  
IN THE DIAMOND DUST, DIAMOND MINE, AND  
MINE DUST HE SERIES OF EVENTS

James W. Adams, et al

Environmental Research Institute of Michigan

Prepared for:

Air Force Office of Scientific Research

February 1973

DISTRIBUTED BY:

**NTIS**

National Technical Information Service  
U. S. DEPARTMENT OF COMMERCE  
5285 Port Royal Road, Springfield Va. 22151

SECURITY CLASSIFICATION OF THIS PAGE (When Data Entered)

REPORT DOCUMENTATION PAGE		READ INSTRUCTIONS BEFORE COMPLETING FORM	
1. REPORT NUMBER <b>AFOSR - TR - 74 - 0148</b>	2. GOVT ACCESSION NO.	3. RECIPIENT'S CATALOG NUMBER <b>AD 774192</b>	
4. TITLE (and Subtitle) COMPARISON OF <del>THE</del> SEISMIC MEASUREMENTS TAKEN IN THE DIAMOND DUST, DIAMOND MINE, AND MINE DUST HE SERIES OF EVENTS		5. TYPE OF REPORT & PERIOD COVERED Interim	
7. AUTHOR(s) James W. Adams Rowland H. McLaughlin		6. PERFORMING ORG. REPORT NUMBER 197200-1-T (POR 6664)	
9. PERFORMING ORGANIZATION NAME AND ADDRESS Environmental Research Institute of Michigan P. O. Box 618 Ann Arbor, Michigan 48107		8. CONTRACT OR GRANT NUMBER (s) F44620-71-C-0033	
11. CONTROLLING OFFICE NAME AND ADDRESS Advanced Research Projects Agency/NMR 1400 Wilson Blvd. Arlington, VA 22209		10. PROGRAM ELEMENT, PROJECT, TASK AREA & WORK UNIT NUMBERS 62701 D AO 2104	
14. MONITORING AGENCY NAME AND ADDRESS Air Force Office of Scientific Research 1400 Wilson Boulevard NP Arlington, VA 22209		12. REPORT DATE February 1973	
16. DISTRIBUTION STATEMENT (of this Report) Approved for public release. Distribution unlimited.		13. NUMBER OF PAGES 94	
17. DISTRIBUTION STATEMENT (of the abstract entered in Block 20, if different from Report)		15. SECURITY CLASS. (of this report) Unclassified	
18. SUPPLEMENTARY NOTES		16. DECLASSIFICATION/DOWNGRADING SCHEDULE	
Reproduced by <b>NATIONAL TECHNICAL INFORMATION SERVICE</b> U S Department of Commerce Springfield VA 22151			
19. KEY WORDS (Continue on reverse side if necessary and identify by block number)			
Seismic measurements		Seismic spectral ratios	
Nuclear device		Seismic energy	
Azimuthal effects		Tectonic strain release	
Seismograms			
20. ABSTRACT (Continue on reverse side if necessary and identify by block number)			
The MINE DUST HE shot of May 10, 1972 was recorded at a number of seismograph stations operated by the University of Michigan, the U. S. Geological Survey, and by the NOAA Special Projects Group. The recordings obtained at the close-in University of Michigan stations disclosed that this shot was a factor of 1.30 larger than the previous HE shot of this series, based on particle velocity measurements. The geometric means of an energy ratio measure indicated that MINE DUST HE was 1.23 times larger than DIAMOND MINE HE; that DIAMOND DUST was 5.67 times larger than MINE DUST HE; that DIAMOND MINE was 6.32 times larger than DIAMOND DUST.			

DD FORM 1 JAN 73 1473 EDITION OF 1 NOV 65 IS OBSOLETE

SECURITY CLASSIFICATION OF THIS PAGE (When Data Entered)

SECURITY CLASSIFICATION OF THIS PAGE (When Data Entered)

20.

The latter may be questionable because there is evidence that tectonic strain release may have occurred at the time of DIAMOND MINE. Energy ratios are comparable to the square of particle velocity ratios. Coda length magnitudes were 0.23 magnitude units larger for MINE DUST HE than those for the earlier HE shot. MINE DUST HE did not generate large enough signals to be detected at 200 km so body wave magnitudes could not be determined.

ia  
SECURITY CLASSIFICATION OF THIS PAGE (When Data Entered)

COMPARISON OF ~~SEISMIC~~ SEISMIC MEASUREMENTS TAKEN IN THE  
DIAMOND DUST, DIAMOND MINE, AND MINE DUST HE SERIES OF EVENTS

ANNUAL REPORT

ARPA ORDER NO.	2104
PROGRAM CODE NO.	2F10
NAME OF CONTRACTOR:	Environmental Research Institute of Michigan, Ann Arbor
EFFECTIVE DATE OF CONTRACT:	15 December 1970
CONTRACT EXPIRATION DATE:	14 March 1973
AMOUNT OF CONTRACT:	\$165,893
CONTRACT NUMBER:	F44620-71-C-0033
PRINCIPAL INVESTIGATOR:	Rowland H. McLaughlin
PHONE:	Area Code 313, 483-0500, Ext. 321
REPORT PREPARED BY:	James W. Adams Rowland H. McLaughlin
PROGRAM MANAGER:	Donald W. Klick, Lt. Col., USAF
PHONE:	AFOSR (AFSC), Area Code 202, 694-5456
SHORT TITLE OF WORK:	Seismic Decoupling Experiment
REPORT NUMBER:	197200-1-T (POR 6664)
DATE:	February 1973

"This research was supported by the Advanced Research  
Projects Agency of the Department of Defense and was  
monitored by the U. S. Air Force Office of Scientific  
Research under Contract No. F44620-71-C-0033."

AFOSR

SECURITY CLASSIFICATION OF THIS PAGE (When Data Entered)

REPORT DOCUMENTATION PAGE		READ INSTRUCTIONS BEFORE COMPLETING FORM									
1. REPORT NUMBER <b>TR-74-0148</b>	2. GOVT ACCESSION NO.	3. RECIPIENT'S CATALOG NUMBER									
4. TITLE (and Subtitle) COMPARISON OF SEISMIC MEASUREMENTS TAKEN IN THE DIAMOND DUST, DIAMOND MINE, AND MINE DUST HE SERIES OF EVENTS		5. TYPE OF REPORT & PERIOD COVERED Interim									
7. AUTHOR(s) James W. Adams Rowland H. McLaughlin		6. PERFORMING ORG. REPORT NUMBER 197200-1-T (POR 6664)									
9. PERFORMING ORGANIZATION NAME AND ADDRESS Environmental Research Institute of Michigan P. O. Box 618 Ann Arbor, Michigan 48107		8. CONTRACT OR GRANT NUMBER(s) F44620-71-C-0033									
11. CONTROLLING OFFICE NAME AND ADDRESS Advanced Research Projects Agency/NMR 1400 Wilson Blvd. Arlington, VA 22209		10. PROGRAM ELEMENT, PROJECT, TASK AREA & WORK UNIT NUMBERS 62701 D AO 2104									
14. MONITORING AGENCY NAME AND ADDRESS (if different from Controlling Office)		12. REPORT DATE February 1973									
		13. NUMBER OF PAGES 94/100									
		15. SECURITY CLASS. (of this report) Unclassified									
		15a. DECLASSIFICATION/DOWNGRADING SCHEDULE									
16. DISTRIBUTION STATEMENT (of this Report) Approved for public release. Distribution unlimited.											
17. DISTRIBUTION STATEMENT (of the abstract entered in Block 20, if different from Report)											
18. SUPPLEMENTARY NOTES											
19. KEY WORDS (Continue on reverse side if necessary and identify by block number)											
<table border="0"> <tr> <td>Seismic measurements</td> <td>Seismic spectral ratios</td> </tr> <tr> <td>Nuclear device</td> <td>Seismic energy</td> </tr> <tr> <td>Azimuthal effects</td> <td>Tectonic strain release</td> </tr> <tr> <td>Seismograms</td> <td></td> </tr> </table>				Seismic measurements	Seismic spectral ratios	Nuclear device	Seismic energy	Azimuthal effects	Tectonic strain release	Seismograms	
Seismic measurements	Seismic spectral ratios										
Nuclear device	Seismic energy										
Azimuthal effects	Tectonic strain release										
Seismograms											
20. ABSTRACT (Continue on reverse side if necessary and identify by block number)											
<p>The MINE DUST HE shot of May 10, 1972 was recorded at a number of seismograph stations operated by the University of Michigan, the U. S. Geological Survey, and by the NOAA Special Projects Group. The recordings obtained at the close-in University of Michigan stations disclosed that this shot was a factor of 1.30 larger than the previous HE shot of this series, based on particle velocity measurements. The geometric means of an energy ratio measure indicated that MINE DUST HE was 1.23 times larger than DIAMOND MINE HE; that DIAMOND DUST was 5.67 times larger than MINE DUST HE; that DIAMOND MINE was 6.32 times larger than DIAMOND DUST.</p>											

DD FORM 1473 EDITION OF 1 NOV 65 IS OBSOLETE  
1 JAN 73

SECURITY CLASSIFICATION OF THIS PAGE (When Data Entered)

SECURITY CLASSIFICATION OF THIS PAGE (When Data Entered)

20.

The latter may be questionable because there is evidence that tectonic strain release may have occurred at the time of DIAMOND MINE. Energy ratios are comparable to the square of particle velocity ratios. Coda length magnitudes were 0.23 magnitude units larger for MINE DUST HE than those for the earlier HE shot. MINE DUST HE did not generate large enough signals to be detected at 200 km so body wave magnitudes could not be determined.

SECURITY CLASSIFICATION OF THIS PAGE (When Data Entered)

CONTENTS

Abstract

1. Introduction
2. Field Measurement Data and Results
  - 2.1. University of Michigan Participation
  - 2.2. USGS
  - 2.3. NOAA/ESL
  - 2.4. Magnitude Calculations
3. Recommendations and Conclusions

References

- Appendix A: MINEDUST HE Spectral Analyses
- Appendix B: Composite Spectral Curves as a Function of Event, Site and Wave Type
- Appendix C: Spectral Ratios of MINE DUST HE/DIAMOND MINE HE as a Function of Wave Type and Site
- Appendix D: Spectral Ratios of DIAMOND MINE/DIAMOND DUST as a Function of Wave Type and Site
- Appendix E: FORTRAN-SABR Program for Body Wave Energy Calculations
- Appendix F: Energy Program Results as a Function of Site and Event
- Appendix G: Energy Spectrum Ratios

COMPARISON OF ~~SEISMIC~~ SEISMIC MEASUREMENTS TAKEN IN THE DIAMOND DUST,  
DIAMOND MINE, AND MINE DUST HE SERIES OF EVENTS

1

INTRODUCTION

This POR complements the previously issued technical report (ref. 5) for the MINE DUST HE event and contains the final results of the analyses which have been performed on all of the MIGHTY MITE events but which have not been reported previously (refs. 3, 4, 5).

The Geophysics Section of the Infrared and Optics Division, Willow Run Laboratories, University of Michigan established six portable seismograph stations to record this event. The same close-in locations used for the previous events of this series were reoccupied (fig. 1). In addition, a station was established near Meadville, Arizona about 225 km southeast of ground zero.

Stations of the Nevada seismograph net were also used through the cooperation of the National Oceanic and Atmospheric Administration (NOAA), and the United States Geological Survey (USGS). Figure 2 is a map showing the locations of stations in the various nets.

2

FIELD MEASUREMENT DATA AND RESULTS

2.1. UNIVERSITY OF MICHIGAN PARTICIPATION

The Geophysics Section of the Infrared and Optics Division, Willow Run Laboratories, University of Michigan established six portable seismograph stations to obtain data for the MINE DUST HE event. The five close-in stations (fig. 1) were located in the same positions as used for DIAMOND DUST, DIAMOND MINE, and the DIAMOND MINE HE shot of February 4, 1971. All stations were equipped with matched three-component short-period seismometers and magnetic tape recorders. An additional high frequency vertical seismometer, a low frequency seismometer, and a microphone were used at the Pahute Mesa

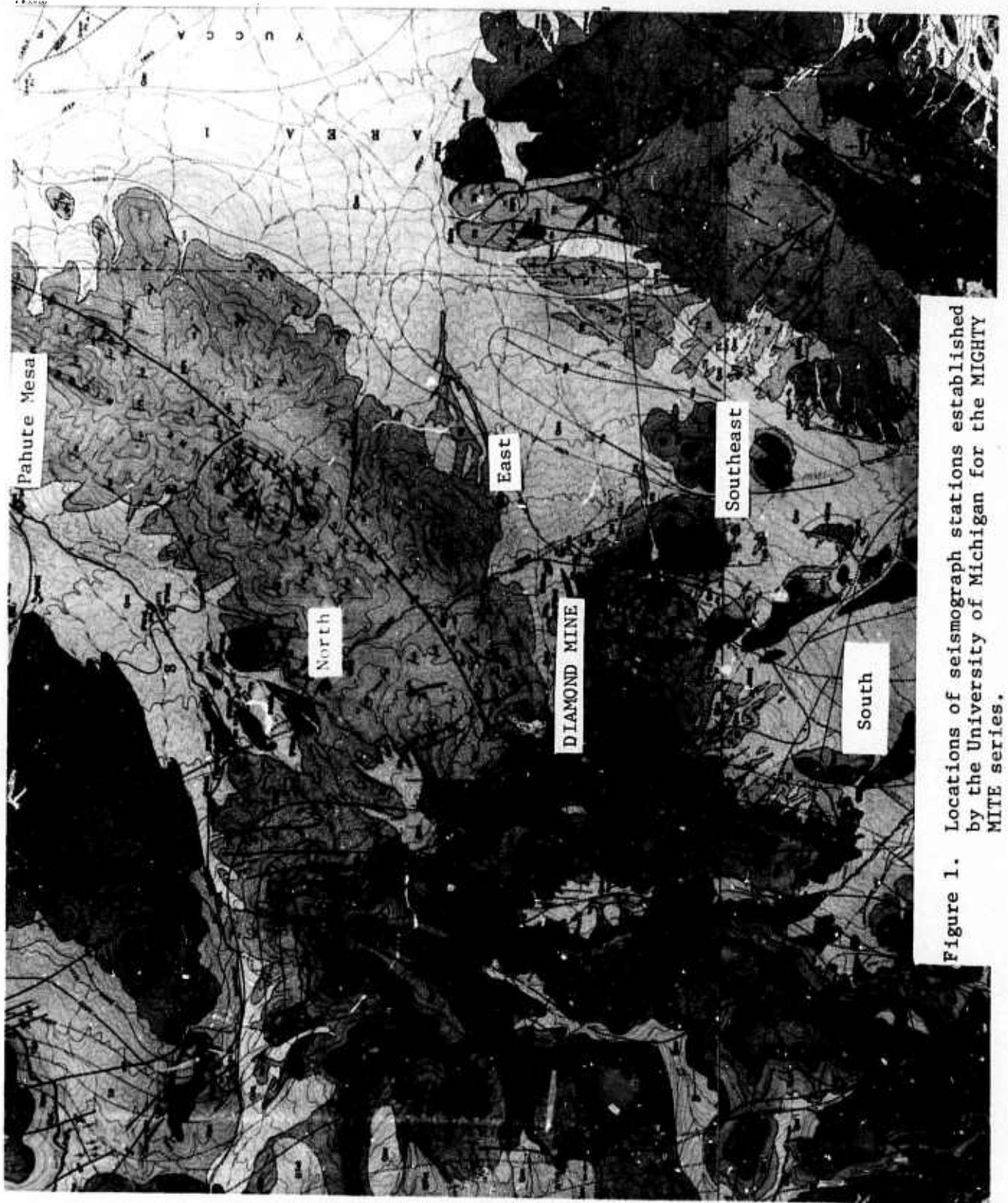


Figure 1. Locations of seismograph stations established by the University of Michigan for the MIGHTY MITE series.

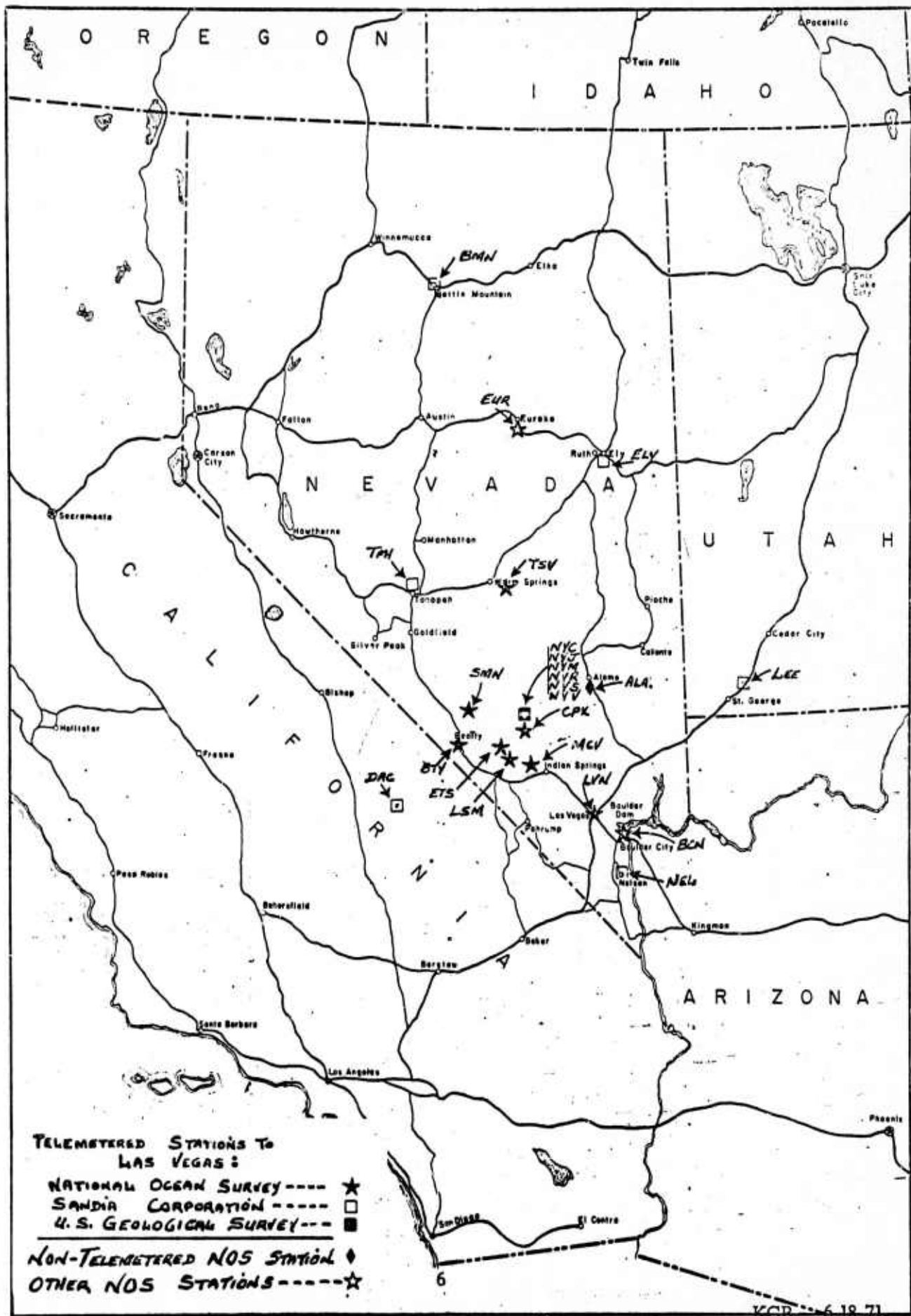


Figure 2. NOAA/ERL CGS Net

site located about 6 km north-northeast of ground zero. A sixth station equipped with a three-component short-period seismometer and a tape recorder was located near Meadsville, Arizona at a distance of about 225 km southeast of ground zero.

A summary of information about the sites appears in Table 1. The horizontal distances and bearings are with respect to the MINE DUST HE working point and magnetic North. The values were obtained from Holmes and Narver at NTS who did the surveying. The values for the North site are only an estimate. The surveyors located a point which was northwest of the North site. The elevations are estimated from Department of Interior Geological Survey maps (Tippah Spring and Mine Mountain). The geology of the stations are a result of on-site inspections, the above mentioned geological maps and seismic refraction profiles conducted as described below.

TABLE 1. RECORDING STATIONS

<u>Station</u>	<u>Bearing</u>	<u>Distance</u> (km)	<u>Elevation</u> (ft)	<u>Station Geology</u>
South	183°57'	2.64	5190	Upper Miocene or Pliocene Tiva Canyon Member of Paintbrush Tuff
Southeast	119°59'	2.59	5005	Paintbrush Tuff
East	68°10'	2.48	4890	Alluvium over Miocene Tuff, Indian Trail formation (older than Paintbrush)
Northeast	12°0'	2.82	5250	Pa. or Permian Tippah Limestone
Pahute Mesa	21°30'	6.05	4794	Alluvium

Reversed refraction profiles were made for each site. Three-component seismometers were located at each end of a 76 m line and the seismic source was moved along the line at eleven equally spaced locations. The line ran from the site back toward the working points. Thus, for example, the North site used for the events was at the north end of the refraction profile for that site. A summary of the results are given in figure 3 and the accompanying table. They were derived using standard refraction techniques (Dobrin, pp. 81-84). The two northerly sites and the East site have unconsolidated dry sand at the surface that accounts for the low velocities. The other two sites have bedrock at or very near the surface and at the South site the surface rock was badly fractured. This, along with the cracked regions from previous shots (fig. 4), caused lower transmission velocities. In addition to the layers revealed in these profiles, there is another below them which has a velocity in the neighborhood of 4 km per second. This was inferred from the first compressional arrival time of the various events. The greater part of the propagation path is probably through the Indian Trail Formation tuff beds.

Good data were obtained at nearly every site for all events. However, for DIAMOND DUST the transverse component at the East site was slightly over-recorded and the tape recorder speed at the North site was not constant. The East site overrecorded data are considered unreliable above 10 Hz and the North site data considered unreliable below 10 Hz. WWVB was not recorded at the East site for DIAMOND MINE HE and hence, could not be used in analysis where timing was critical. The output from the vertical seismometer at the Southeast site for DIAMOND MINE gave evidence of malfunction and was, therefore, not included in the data analyzed. All other recordings were good.

The azimuthal asymmetry noted in Willis and Hand (1971) for the DIAMOND DUST event was observed for the other three events as well; the wave train duration increases and the frequency content decreases from north clockwise to south. The East site consistently had about double the signal level which would be expected based on the data gathered at the other sites. At the

	D m	P-wave velocity km/sec		i degrees
		$\alpha_1$	$\alpha_2$	
Pahute Mesa	7.6	.363	1.05	3.0
North	0.9	.290	1.22	-0.5
East	15.5	.472	1.62	2.5
Southeast	10.4	.671	1.10	7.3
South	18.0	.655	1.15	5.2

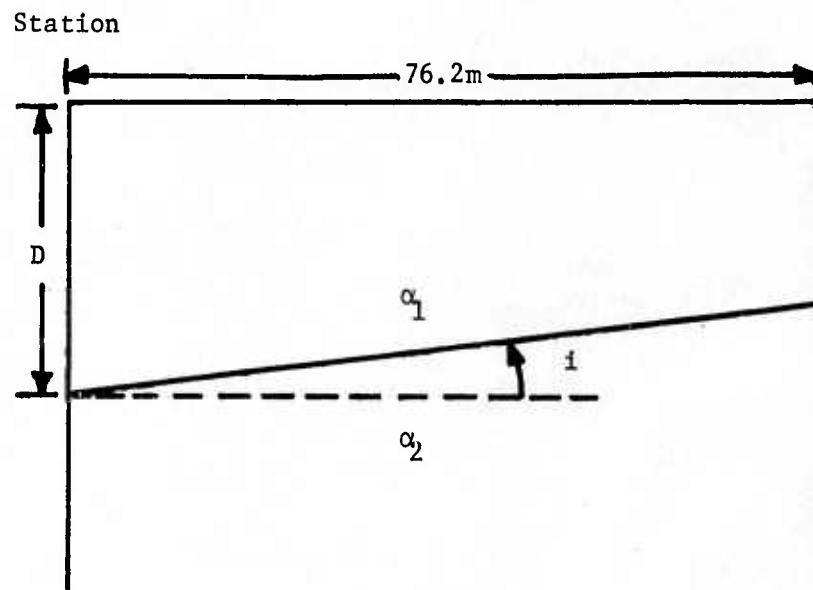


Figure 3. Summary of refraction survey results at the five closest sites occupied for the MIGHTY MITE series.

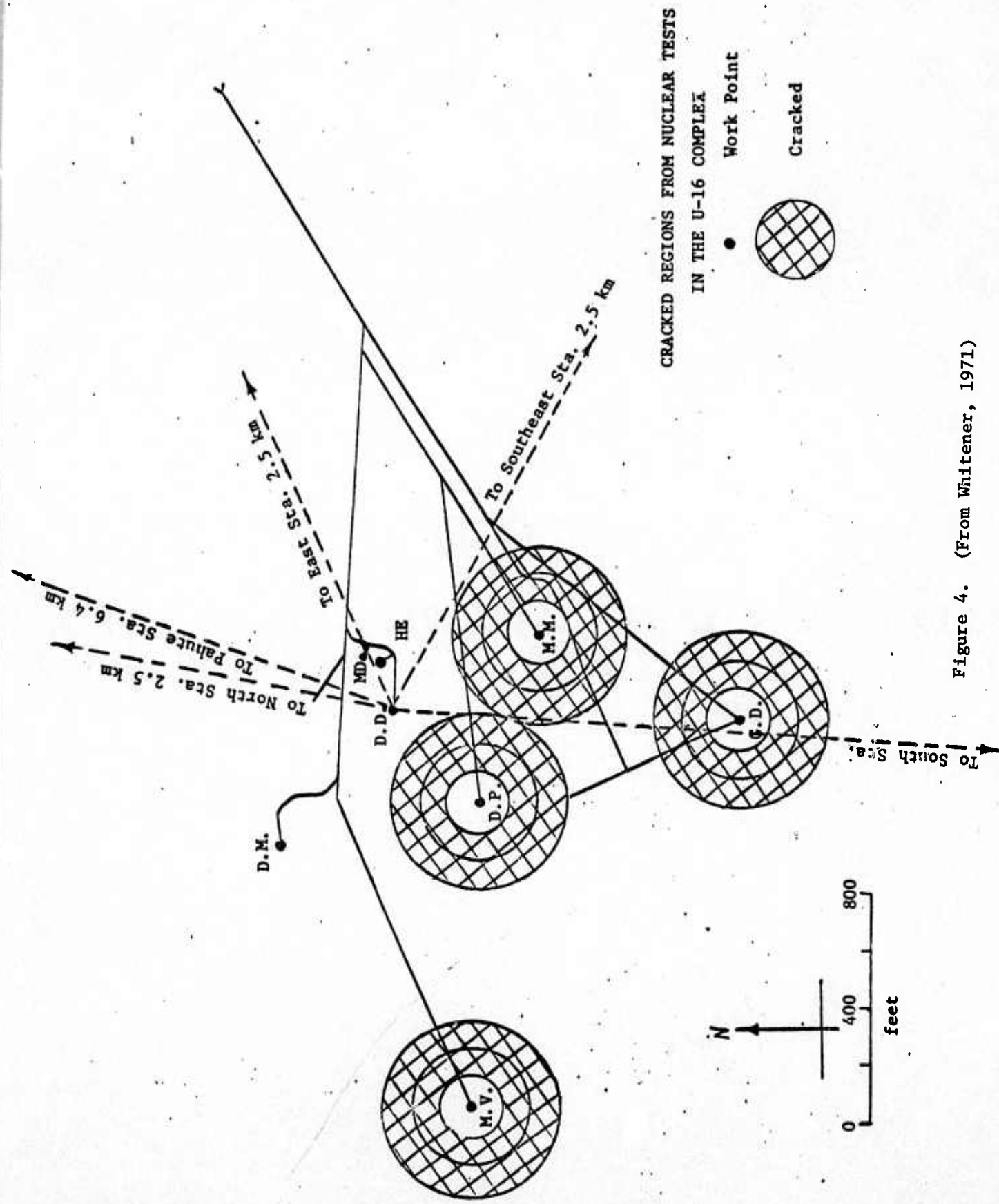


Figure 4. (From Whitener, 1971)

Pahute Mesa site, except for high frequencies for DIAMOND MINE, the signal levels were larger than expected on the same basis. Geological explanations have been given for these observations in the above mentioned reports.

Detailed spectral analyses of the MINE DUST HE data were made for the five close-in stations. Plots of these spectra appear in Appendix A. For comparison purposes with the earlier three events of this series composite plots of ground particle velocity vs. frequency were made for all four events. Figures B-1 through B-10 (Appendix B) contain the spectral analyses of the first compressional wave arrival recorded at each site on the vertical and longitudinal component seismometers. Particle velocity spectral ratios of MINE DUST HE/DIAMOND MINE HE as a function of site and wave type are given in Appendix C. Similar curves for DIAMOND DUST/DIAMOND MINE are shown in Appendix D. It can be seen (Appendix B) that the MINE DUST HE shot has signal levels slightly larger than the DIAMOND MINE HE shot at most frequencies but that the relationship is frequency dependent. In order to quantify this relationship, particle velocity ratios were computed for the first compressional (P) wave arrival and the maximum shear/surface wave ( $S_{max}$ ) recorded at each site. Geometric means for these ratios were computed using that portion of the spectrum which contained the predominant signal levels and which were well above background noise. These mean ratios are summarized in Table 2. The overall mean MINE DUST HE vs. DIAMOND MINE HE particle velocity ratio was 1.287. Also shown in this table are the means of the vertical and longitudinal components for first P from all stations and all three components for maximum S. The signal level associated with the latter is usually the largest signal on the seismogram.

TABLE 2.  
AVERAGE SPECTRAL RATIOS MINE DUST HE vs. DIAMOND MINE HE  
UNIVERSITY OF MICHIGAN STATIONS

Station/Component	First P		Maximum S		
	Vertical	Longitudinal	Vertical	Longitudinal	Transverse
Pahute Mesa	1.155	1.274	1.820	1.470	1.689
North	0.848	0.814	1.424	1.355	1.130
East	1.096	1.051	1.363	1.213	0.988
Southeast	1.862	1.616	1.470	1.267	1.514
South	1.197	0.814	1.972	1.129	1.585
Mean	1.191	1.075	1.592	1.281	1.352
Overall Mean:	1.287				

Another approach to the comparison of the ground motion generated by these two shots is to examine the ratio of the maximum signal level measured on the broadband seismograms. For the same component at the same site the time of the maximum signal will usually correlate between shots. However, the maximum signal on one component will not necessarily correlate in time with the maximum signal on the other two components for the same shot. The results of this analysis is shown in Table 3. T, L, and V are abbreviations for transverse longitudinal and vertical, respectively. It can be seen that the MINE DUST HE event was a factor of 1.32 larger than the DIAMOND MINE HE shot on the basis of these broadband signal level comparisons. This is very close to the overall spectral ratio amplitude of 1.287 shown in Table 2.

TABLE 3.  
MAXIMUM AMPLITUDE RATIOS MINE DUST HE vs. DIAMOND MINE HE  
UNIVERSITY OF MICHIGAN STATIONS

<u>Station</u>	<u>Component</u>	<u>Amplitude Ratio</u>
Pahute Mesa (20,016 ft)*	L	1.496
	T	1.413
	V	1.585
North (12,700 ft)*	L	1.259
	T	1.334
	V	1.334
East (7,698 ft)*	L	1.259
	T	.794
	V	1.259
Southeast (7,843 ft)*	L	1.496
	T	1.413
	V	1.334
South (8,443 ft)*	L	1.496
	T	1.496
	V	<u>1.059</u>

Mean = 1.32

Another measure of the relative sizes of the events is the energy spectrum as derived from theory. The theory and results of this analysis follow.

From Bullen (p. 268) we have the following:

$$E = 4\pi^3 \rho r_0 \sin \Delta \int H c C^2 \tau^{-2} dt.$$

The symbols and what each denotes are:

- E total source energy
- $\rho$  medium density
- $r_0$  Earth's radius
- $\Delta$  angle between source and sensor at the earth's center
- H medium depth
- c wave velocity
- C particle displacement amplitude
- $\tau$  period
- t time

The integral is taken over the signal of interest. This equation describes the total energy of the source if the assumptions are made that the energy is coupled spherically into the earth and that the energy is transmitted entirely by body waves. From the following:

$D \doteq r_0 \sin \Delta$ , distance from shot to sensor over the earth's surface

$f = 1/\tau$ , frequency

$\int V^2 dt \doteq \int (2\pi f C)^2 dt$ ,  $V$  = the particle velocity

we have

$$E = \pi \rho D H \int c V^2 dt.$$

For our purposes the integral is defined from the first arrival time to the time where the signal returns to background level. Based on an examination of the records the latter time is ten seconds after the former. We let  $t_0$  be the time of the first motion in seconds, with  $t = 0$  at the time of the shot.

With this definition of  $t$ ,  $c(t) = \frac{D}{t}$ , and the energy equation for a one-third-octave bandwidth about the frequency  $f$  becomes equivalent to

$$\frac{E(f)}{\pi \rho H D^2} = \int_{t_0}^{t_0+10} ((v_f(t))^2 / t) dt. \quad (1)$$

The actual calculation made in the energy program is a constant times the digital equivalent of the right-hand side of this equation. The assumption is then made that for a given site the transmitting medium does not change from shot to shot (i.e.,  $\rho$ ,  $D$  and  $H$  do not change).

Since the ground particle velocity is sensed in three mutually orthogonal directions (transverse, longitudinal, and vertical), it may be expressed as the square root of the sum of the squares of its components at any given time. Assuming this rule holds for the filtered particle velocity, Eq. 1 may be written:

$$\frac{E(f)}{\pi \rho H D^2} = \int_{t_0}^{t_0+10} (((v_{Tf}(t))^2 + (v_{Lf}(t))^2 + (v_{Zf}(t))^2) / t) dt$$

or as the sum of three integrals of the form

$$\int_{t_0}^{t_0+10} ((v_{if}(t))^2 / t) dt \quad (2)$$

where  $v_{if}(t)$  denotes the  $i^{\text{th}}$  component of the particle velocity filtered in the one-third-octave band about  $f$  at time  $t$ .

The discrete form of this integral is

$$\sum_{j=0}^m ((v_{if}(t_j))^2 / t_j) (\delta t)_j, \quad t_m = t_0 + 10 \quad (3)$$

Assuming the sample interval to be constant (i.e.,  $t_{j+1} - t_j = (\delta t)_j = \text{constant} = T$ ) it may be removed from the summation. At time  $t_j$  the actual value

digitized is

$$U_{if}(t_j) = kV_{if}(t_j) \quad (4a)$$

where

$$k = (512/3) (10)^{-a/20} \quad (4b)$$

and

$$\begin{aligned} a = & \text{geophone response in dB re } 10^{-2} \text{ cm/sec} \\ & + \text{spectrum level correction in dB} \\ & - \text{total system gain in dB.} \end{aligned} \quad (4c)$$

512/3 = 1024/6 is the digitizing scale: +3 volts to -3 volts (full record level from tape) is divided into 1024 levels (10 bits). Note that k is independent of time for a given frequency and component, and it may be removed from the summation. Thus (3) may be written

$$\frac{T}{k^2} \sum_{j=0}^m (U_{if}(t_j))^2 / t_j, \quad t_m = t_o + 10. \quad (5)$$

This final expression is the digital equivalent of (2) in terms of the digitized data and the explicitly defined parameters (4).

A program (Appendix E) was written to calculate these values. The square roots of the results are shown in Appendix F. The energy spectrum ratios as a function of site are displayed in Appendix G. These are simply point by point ratios of the values squared given in the previous appendix. Since the energy calculation requires good data from all three components and since timing is critical, those stations lacking one or the other have been excluded. However, the data are sufficiently redundant to enable quantitative comparisons to be made of the relative energy levels of the four shots.

A number of qualitative observations may be made at this point. At the North site the indication is that the source energy peaks at 10 Hz and at the Pahute Mesa site the peak has dropped to 4-5 Hz, at which frequency the North site contains a secondary peak. A partial explanation of this is that the energy calculation does not take the absorption of the medium into account. There is not enough information available to estimate an absorption coefficient, which would be needed to account entirely for the results. The apparent peaks also drop from 10 Hz to 3-4 Hz as seen by each station in turn, looking clockwise from the North site to the South site. This again may be due to the lack of the inclusion of absorption factors in the calculation. It is to be expected that the factors increase in this direction because the geology becomes more and more complex (faulted).

The Pahute Mesa site data indicate that the apparent energy of DIAMOND MINE has comparatively less high frequency content than the other three shots. This may be due in part to that shot's proximity to a fault along which the rock material (tuff) is likely to be considerably more fractured. High frequencies would be attenuated greater in this type of medium. In short, in this case our assumption that the medium through which the energy travels remains the same from shot to shot for a given site may be wrong. The azimuth from the DIAMOND MINE working point to the North site does not lie along the fault as does that from the working point to the Pahute Mesa site.

In order to get a measure of the relative size of the four events the geometric mean of the energy ratio values were calculated. The six numbers thus derived are redundant; for each of the three inequalities relating the sizes of the events, three values may be found. The three values were different, in general, because all questionable data were ignored. A weighted average (proportional to the amount of data used) of the values appears in Table 4 along with other shot size determinations which have been made. These latter are means and ratios of particle velocity measurements and in order to compare them with the energy values the square roots of the energy ratios have also been included.

TABLE 4. SUMMARY OF RELATIVE SHOT SIZES

$\frac{DD^*}{HE}$	$\frac{MD^*}{HE}$	$\frac{DD^*}{MD}$	$\frac{DM^*}{DD}$	Source
6.985	1.233	5.665	6.316	Energy ratio
2.642-	1.110-	2.380+	2.513-	Square root of energy ratio
-----	1.29	-----	-----	Geometric mean of spectrum ratios
-----	1.32	-----	-----	Geometric mean of maximal of broadband signals
2.5	-----	-----	1.6	Average broadband signal†
-----	-----	-----	2.6	Seismic station at Beatty†
-----	-----	-----	3.2-5.6	2 Hz spectrum ratio†
-----	-----	-----	2.2-2.5	10 Hz spectrum ratio†
-----	1.7	1.4	2.5	Coda length magnitude†

\*DD: DIAMOND DUST  
 MD: MINE DUST HE  
 DM: DIAMOND MINE  
 HE: DIAMOND MINE HE

† See references 3 and 4.

The energy equation which has been used is valid for only body waves. Using it on data including surface waves gives results which are too large, since the surface waves have a geometric spreading proportional to the inverse square root of distance whereas, body wave energy spreads as the inverse square of distance. The seismic motion generated by DIAMOND MINE HE was predominantly body waves. The duration of the surface waves for DIAMOND DUST, MINE DUST HE, and DIAMOND MINE increased respectively, the latter having a coda about equally divided between surface waves and body waves. Consequently, the energy ratio of DIAMOND MINE to DIAMOND DUST,

for example, is probably too large. This is indicated in Table 4 by the "-" sign following the ratio. For the worst case, DIAMOND MINE, the  $E(f)/(\pi\rho D^2 4)$  calculation may be off as much as fifteen percent for the lower frequencies. It is recommended that the energy calculation for surface waves be programmed and used for those parts of the data which are clearly surface motion phases.

Table 5 gives a breakdown of the energy ratios derived from the data recorded at the individual sites. For the MINE DUST HE/DIAMOND MINE HE, DIAMOND DUST/MINE DUST HE, and DIAMOND DUST/DIAMOND MINE HE--for those not involving DIAMOND MINE--the ratios agree among the sites. This would indicate that, even though the geology along the energy paths vary, the data from any of them give a good estimate of the energy ratios--when DIAMOND MINE is excluded. This is what should be expected if the assumptions made in the above calculations were true.

TABLE 5.  
ENERGY RATIO CALCULATIONS BASED ON THE  
DATA RECEIVED AT EACH SITE

Site	$\frac{MD^*}{HE}$	$\frac{DM^*}{MD}$	$\frac{DD^*}{MD}$	$\frac{DM^*}{HE}$	$\frac{DD^*}{HE}$	$\frac{DM^*}{DD}$
Pahute Mesa	1.463	-----	5.139	-----	7.517	-----
North	1.196	37.93	-----	45.35	-----	-----
East	-----	48.05	-----	-----	-----	-----
Southeast	1.587	19.82	4.507	31.46	7.152	4.399
South	1.042	51.42	6.516	49.35	6.254	7.891
Mean	1.287	36.92	5.324	41.29	6.953	5.892

\*DM: DIAMOND MINE  
DD: DIAMOND DUST  
MD: MINE DUST HE  
HE: DIAMOND MINE HE

For those ratios involving DIAMOND MINE, however, the variance from site to site is quite large, but consistent. With respect to the mean of the ratios, the Southeast site data indicates an average of 49 percent less than the mean energy from DIAMOND MINE and the South site data indicates 31 percent more. The data from East and North sites indicate DIAMOND MINE to be a little larger than the means. The Pahute Mesa data estimates were lower as was mentioned previously. One way to account for this azimuthal variation is to hypothesize that energy was released in the fault next to which the DIAMOND MINE working point was located. The P wave radiation pattern generated by slippage along the fault nearest the working point is shown in figure 5. The observed energy ratios agree with the hypothesis as can be seen. The fact that more surface wave energy was generated during this event also supports the hypothesis.

The site occupied for the MINE DUST HE event at a distance of 225 km did not receive adequate signal levels to confidently identify the signal arrival. This site was carefully selected for very low background levels in anticipation of the very small signal levels. The average background level during the time of the event was approximately  $5 \times 10^{-7}$  cm/sec as measured over the data band from 2 Hz to 15 Hz. This level of signal is well within the capabilities of the instrumentation used at that site. To overcome this ambient seismic background would require a seismometer array which could be processed to allow the enhancement of signals from a particular direction.

## 2.2. U. S. GEOLOGICAL SURVEY

Four special seismograph stations were established to record this shot in addition to the regular stations operated by the U.S.G.S. Of the latter approximately 15 stations were recalibrated and gains adjusted for this shot. The locations of these stations are listed in Table 6a. The data discussed in this section were supplied by Mr. Fred Fischer, U.S.G.S., National Center for Earthquake Research, Menlo Park, California.

The stations designed India, Tango, Juliet, and Quebec were special portable stations that were equipped with magnetic tape recorders and employed three-component short-period seismometers and linear arrays of vertical seismometers. The two most distant stations (Juliet,  $\Delta = 86$  km, and Quebec,  $\Delta = 238$  km) received no detectable signals from the shot.

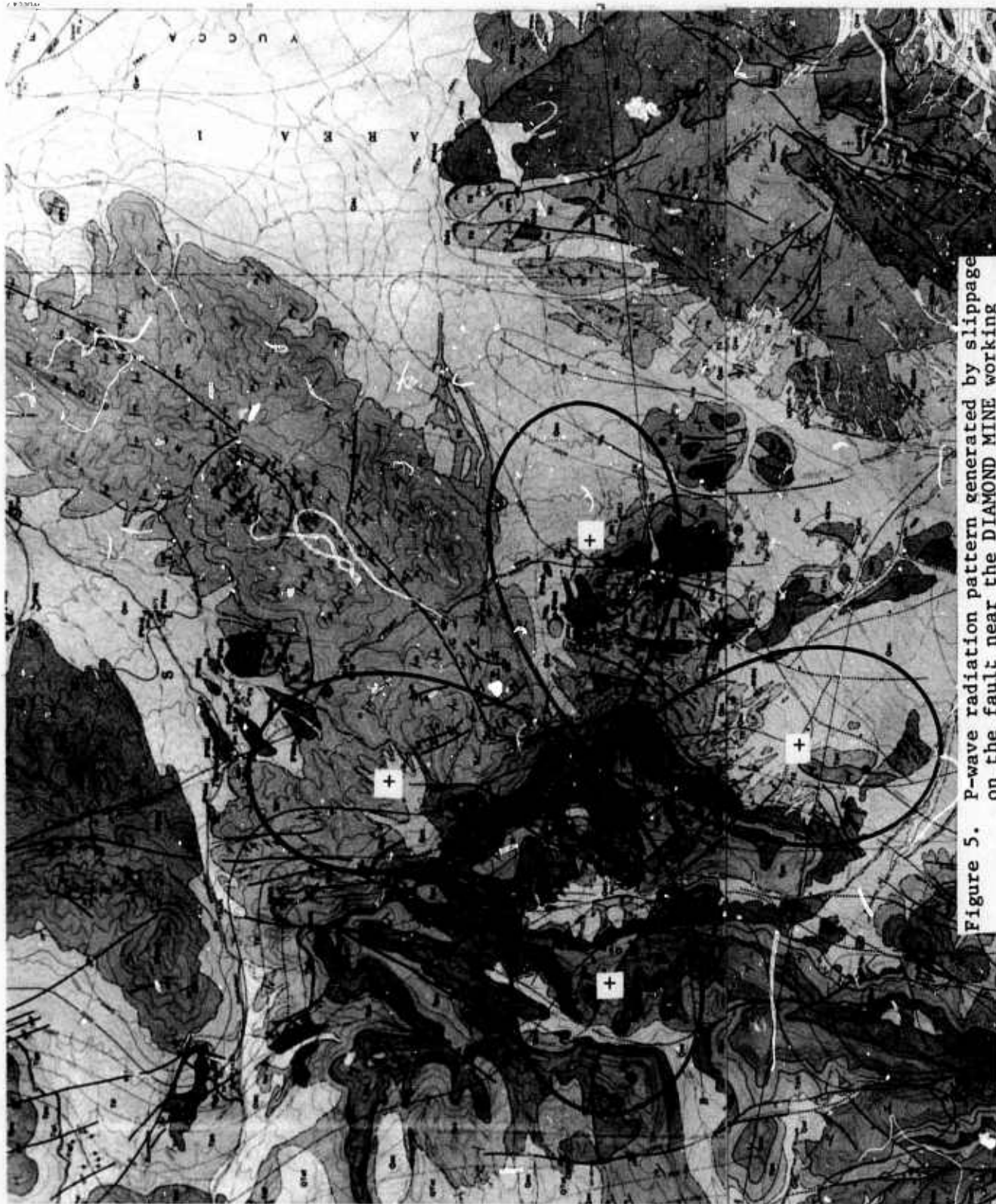


Figure 5. P-wave radiation pattern generated by slippage on the fault near the DIAMOND MINE working point.

TABLE 6a Station Locations

L	STN	LAT N	LONG W	ELV	DELAY
1	11	37 6.05	11618.46	0	0.0
2	12	37 5.82	11618.69	0	0.0
3	13	37 5.55	11618.96	0	0.0
4	14	37 5.55	11618.83	0	0.0
5	15	37 5.32	11618.60	0	0.0
6	16	37 5.11	11618.39	0	0.0
7	17N	37 5.55	11618.63	0	0.0
8	18E	37 5.55	11618.83	0	0.0
9	13	3722.53	11626.03	0	0.0
10	14	3722.53	11626.07	0	0.0
11	17N	3722.53	11626.03	0	0.0
12	18E	3722.53	11626.03	0	0.0
13	NT123713.78		11626.81	1990	0.10
14	NT1337 9.42		11640.04	1628	-0.07
15	NT1437 8.66		11615.79	1737	-0.10
16	NT153713.58		11630.40	1891	0.14
17	NT1637 5.55		11618.96	1637	-0.05
18	NYND37 7.96		116 5.88	1094	-0.19
19	NT183725.76		11623.52	1649	-0.03
20	NT193717.00		11618.30	2135	0.07
21	N2223712.81		11618.94	2198	0.18
22	NYCH37 9.30		116 9.32	1695	-0.03
23	NY3737 0.48		11558.48	1286	-0.35
24	NYMC3713.88		116 3.14	1603	-0.53
25	NYRS37 3.32		116 5.50	1279	-0.15
26	NYSR37 1.95		11610.13	1509	0.0
27	CPX 3655.92		116 3.33	1285	-0.26

Recording Truck INDIA

Recording Truck TANGO

Recording Truck JULIET

Recording Truck QUEBEC

37° 37' 116° 35'  
38° 55' 115° 0'

Received no energy from the blast

TABLE 6b Velocity model

CRUSTAL VELOCITY	MODEL 1 DEPTH
2.700	0.0
3.400	0.963
3.800	1.327
4.400	2.140
5.100	2.500
6.100	5.000
7.000	25.000
8.000	35.000

Reproduced from best available copy.

The U.S.G.S. data are summarized in Tables 7 and 8. The velocity model for travel time correction is shown in Table 3b. It is interesting to note that at station NT18 ( $\Delta = 49.4$  km, azimuth =  $340.3^\circ$ ) the observed ground displacement and particle velocity is the same as recorded at Beatty ( $\Delta = 51.8$  km, azimuth =  $254.4^\circ$ ).

### 2.3. NOAA/ESL

The Nevada Special Projects Party of the Earth Sciences Laboratories, National Oceanic and Atmospheric Administration operated 10 seismic stations to record this shot. These stations were equipped as shown in Table 9. (Mr. K.W. King, personal communication). All stations used at least one vertical short-period seismometer and four stations had horizontal seismometers. Eight of the 10 stations used magnetic tape recorders. The shot was well recorded at three stations, weakly recorded at a fourth station, and not detected on the remaining six.

The fact that the shot was not recorded at ETS-1, RHN, and SMN would indicate that there were either strong azimuthal variations, local background noise masked the signal, or the original record gains were too low. As mentioned in the previous section, the signal level recorded at approximately 50 km to the north and to the west was equal. As a distance of approximately 31 km the signal level at station LSM (azimuth  $\approx 191.7^\circ$ ) was a factor of two or more lower than stations N119 (azimuth  $\approx 343.3^\circ$ ) and NT12 (azimuth  $\approx 291.7^\circ$ ) thus indicating that there was an azimuthal effect with lower signals recorded to the south. Comparing stations CPX and NT16 shows that this asymmetry extends to the southeast. This azimuthal asymmetry was also observed in the previous shots from Area 16 (Ref.3).

### 2.4. MAGNITUDE CALCULATIONS

The MINE DUST HE shot did not generate large enough signals to be detected at 200 km so a body wave magnitude ( $m_b$ ) could not be determined directly. An XMAG was computed by the USGS from their local seismic network (see Table 7). This XMAG is approximately equivalent to Richter's  $M_L$  local magnitude. Using the  $M_L$  to  $m_b$  conversion discussed in our earlier report (Ref.3) gives an  $m_b$  magnitude of 2.2

TABLE 7

DATE	ORIGIN	LAT N	LONG W	DEPTH	MAG	NU	DM	GAP	M	RMS	ERH	ERZ	Q	SGD	ADJ	IN	NR	AV	
720510	12 0	0.10	37-	0.65	116-12.08	0.0	0.48	16	4	187	1	0.13	0.6	0.6	0.0	9	23	0.0	
STN	DIST	AZM	AIN	PRMK	HRMN	P-SEC	TPOBS	TPCAL	DLY/HI	P-RES	P-WT	AMX	PRX	CALX	K	XMAG	RMK	FMP	FMAG
NYSR	3.8	50	90	IPU	12 0	1.50	1.40	1.39	0.0	0.01	1.20	50	10	5.30	5-0.5*	0.9	CLIPPED	14	0.5
NYSR	10.9	63	32	IPU	12 0	3.16	3.06	3.28	-0.15	-0.07	1.20	11	25	0.0	5			7-0.1*	
16	12.5	311	32	IPU	12 0	3.78	3.68	3.58	0.0	0.10	1.19	16	40	3.80	1	0.9			
15	13.0	312	32	IPU	12 0	3.90	3.80	3.68	0.0	0.12	1.19	15	40	3.80	1	0.9			
18E	13.5	312	32	EPW	12 0	3.90	3.80	3.78	0.0	0.02	1.20	0	0	4.00	1				
17N	13.5	312	32	IPN	12 0	3.90	3.80	3.78	0.0	0.02	1.20	0	0	4.00	1				
14	13.5	312	32	EPU	12 0	3.92	3.82	3.78	0.0	0.04	1.20	13	40	3.80	1	0.9			
13	13.6	312	32	IPU	12 0	3.97	3.87	3.81	0.0	0.06	1.20	27	11	3.80	1	0.7			
NT16-	13.6	312	32	IPU	12 0	3.98	3.88	3.81	-0.05	0.12	1.19	36	15	22.00	1	0.2			27 1.1*
12	13.7	314	32	IPU	12 0	3.98	3.88	3.82	0.0	0.06	1.20	18	11	3.90	1	0.5			
11	13.8	317	32	EP 4	12 0	4.05	3.95	3.83	0.0	0.12	0.0	13	10	1.80	1	0.7			
CPX	15.7	124	32	IPU	12 0	3.98	3.88	4.20	-0.26	-0.06	1.20	11	10	0.0	1				9 0.2
NT14	15.8	340	32	EP 3	12 0	4.34	4.24	4.23	-0.10	0.11	0.30	0	0	11.00	1				27 1.1*
NYND	16.3	34	32	EP 2	12 0	4.10	4.00	4.34	-0.19	-0.15	0.59	0	0	0.0	1				
NYCH	16.5	14	32	IPU	12 0	3.93	3.83	4.37	-0.03	-0.51	0.29	32	10	12.00	5-0.1*				13 0.5
NYJT	20.2	91	32	EP 4	12 0	4.45	4.35	5.09	-0.35	-0.39	0.0	9	15	0.50	5 1.0*				
N222	24.7	336	26	IPU	12 0	5.90	5.80	5.85	0.18	-0.23	1.15	14	10	14.00	1	0.2			
NYMC	27.8	28	26	EP 4	12 0	5.70	5.60	6.37	-0.53	-0.24	0.0	9	10	0.0	5				7-0.0*
NT19-	31.6	343	26	EP 4	12 0	0.0	***	5.99	0.07		0.0	13	15	20.00	1	0.4			
NT12	32.7	318	26	EP 4	12 0	0.0	*****	7.16	0.10		0.0	11	20	20.00	1	0.4			18 0.8
NT13	44.5	291	26	EP 4	12 0	9.55	9.45	9.10	-0.07	0.42	0.0	16	15	20.00	1	0.7			10 0.3
T3	45.4	333	26	EP 4	12 0	9.60	9.50	9.25	0.0	0.25	0.0	12	20	23.00	1	0.6			
T4	45.5	333	26	EP 2	12 0	9.65	9.55	9.26	0.0	0.29	0.51	13	40	23.70	1	0.9			
NT18	49.4	340	26	EP 4	12 0	0.0	*****	9.91	-0.03		0.0	10	10	40.00	1	0.1			10 0.3

$\overline{M}_D = 0.66$   
 $\approx M_L$

$\overline{X}_{MAG} = 0.61$   
 $\approx M_L$

TABLE 7 - EXPLANATION

*The listing of the solution for the blast gives first the parameters for the blast itself, and then the data and parameters from each seismograph station. The following symbols are used:*

DATE: Year month day  
ORIGIN: hour (GMT) minute second  
LAT N: in degrees and minutes  
LONG W: in degrees and minutes  
DEPTH: in kilometers  
MAG: duration magnitude, approximately equal to Richter  $M_L$ .  
NO: number of first-arrival times actually used in the location.  
DM: epicentral distance, in kilometers, to the nearest station.  
GAP: largest azimuthal separation, in degrees, between stations.  
RMS: root mean square error of time residuals in seconds.  
ERH: standard error of the epicenter in kilometers.  
ERZ: standard error of the focal depth, in kilometers.  
Q: solution quality of the hypocenter; A = excellent, B = good, C = fair, D = poor.

For the individual station parameters the following symbols are used:

STN: station code name  
DIST: epicentral distance to the station, in kilometers.  
AZM: azimuthal angle to the station, from 0° north.  
AIN: angle of inclination at which the first-arrival ray leaves the earthquake focus.

Table 7 Explanation (cont)

- PRMK: I = impulsive first arrival; E = emergent; P = phase remark;  
U = compressional first motion; D = dilatational first  
motion.
- HRMN: hour minute (GMT).
- P-SEC: first-arrival time.
- TPOBS: observed P-wave travel time.
- TPCAL: calculated P-wave travel time.
- DELAY: station delay, introduced at the beginning of the program  
to compensate for local variations in the velocity model.
- P-RES: travel time residual, in seconds;  $(TPOBS)-(TPCAL)-(DELAY) =$   
P-RES.
- P-WT: weight assigned to station reading in the location; a  
decreasing function of distance.

TABLE 8

GROUND MOTION CALCULATIONS.

NCER standard system magnification =  $M = MF1 \times C_{10}$   
 where  $MF1 =$  frequency dependent system magnification  
 $C_{10} =$  system calibration factor

PERIOD	$\rightarrow$ MF1
0.20	$5.48 \times 10^4$
0.15	$6.80 \times 10^4$
0.10	$9.44 \times 10^4$

STANDARD NCER STATION	DISTANCE TO BLAST (km)	MAX. VIEWER AMPLITUDE (mm)	PERIOD (SEC) PRX	$C_{10}$	M	GROUND DISPLACEMENT (cm)	GROUND VELOCITY (cm/sec) $V = 2\pi d / PRX$
	$\Delta$	AMX				d	
NT16	13.6	36	0.15	22	$1.5 \times 10^6$	$2.4 \times 10^{-6}$	$1.0 \times 10^{-4}$
N119	31.7	13	0.15	20	$1.4 \times 10^6$	$9.3 \times 10^{-7}$	$3.9 \times 10^{-5}$
NT12	32.7	11	0.20	20	$1.1 \times 10^6$	$1.0 \times 10^{-6}$	$3.1 \times 10^{-5}$
NT13	44.5	16	0.15	20	$1.4 \times 10^6$	$1.1 \times 10^{-6}$	$4.6 \times 10^{-5}$
NT18	49.4	10	0.10	40	$3.8 \times 10^6$	$2.6 \times 10^{-7}$	$1.6 \times 10^{-5}$

\* assuming simple harmonic motion

TABLE 9  
PRE-MINE DUST SEISMIC MEASUREMENTS  
10 May 1972

I. NOAA/ECL Stations

Station	Distance	Type of Record	Arrival Time *		Component	Ground Motion (P-P)			Remarks
			Phase	GMT		Velocity cm/sec	Period sec	Displacement cm	
CPX	15.59	Helicorder, magnetic tape & 16 mm film	IP	120003.6	Z	$4.7 \times 10^{-5}$	0.08	$6.0 \times 10^{-7}$	Displacement derived assuming simple harmonic motion
ETS-1	21.94	Magnetic tape	-	-	Z, EW, & NS	-	-	-	No amplitude detected
RHN	26.6	Magnetic tape	-	-	Z, EW, & NS	-	-	-	No amplitude detected
LSM	30.81	Helicorder, magnetic tape & 16 mm film	E(P)	120006.4	Z	$1.5 \times 10^{-5}$	0.1	$2.4 \times 10^{-7}$	
SMN	45	Helicorder, magnetic tape & 16 mm film	-	-	Z	-	-	-	No amplitude detected
MCV	46.17	Helicorder & 16 mm film	E(P)	-	Z	-	-	-	Very small amplitude
BTY	51.81	Helicorder, magnetic tape & 16 mm film	E(P)	120009.9	Z	$1.6 \times 10^{-5}$	0.1	$2.6 \times 10^{-7}$	
ALA	101.14	Helicorder	-	-	Z	-	-	-	No amplitude detected
LVW	138	Magnetic tape & brush recorder	-	-	Z, EW, & NS	-	-	-	No amplitude detected
LVN	138.5	Magnetic tape	-	-	Z, EW, & NS	-	-	-	No amplitude detected

\* = Preliminary

which is obviously too high. Table 10 summarizes the coda length magnitudes ( $M_D$  computed from the USGS network (Mr. Fred Fischer, personal communication) for the four events of this series. The MINE DUST HE shot is 0.23 magnitude units larger than the earlier HE shot and 0.15 magnitude units lower than DIAMOND DUST. These  $M_D$  values are believed to be significant insofar as their relationship to each other. However, the dilemma of computing an accurate body wave magnitude for these small events has still not been resolved. The body wave magnitude is important since that is the basis on which seismological decoupling estimates have been made.

TABLE 10  
CODA MAGNITUDE DETERMINATIONS

EVENT	DATE	STN	AMX(mm)	PRX(sec)	CODA(sec)	MD
DD	5/12/70 1400	NT14	80	.10	37	1.75
		NT16	30	.10	25	
		N122	39	.10	37	
H.E.	2/4/71 1838	NT14	19	.11	14	1.37
		NT16	24	.10	26	
DM	7/1/71 1400	NT14	Clip	----	53	2.20
		NT16	Clip	----	61	
		N222	19	.11		
MD	5/10/72 1200	NT14	32	.12	27	1.60
		NT16	35	.15	28	

3

CONCLUSIONS AND RECOMMENDATIONS

This POR complements the previously issued technical report (ref. 5) for the MINE DUST HE event and contains the final results of the analyses which have been performed on all of the MIGHTY MITE events but which have not been reported previously (refs. 3, 4, 5). It was originally planned to instrument the same sites in the same way for the MINE DUST nuclear event. Construction difficulties have postponed this event indefinitely. The following conclusions are a summary of the results reported herein.

1. The geometric mean of the spectral ratios for the first compressional wave arrival and the maximum shear wave recorded at the five close-in stations indicate that the MINE DUST HE shot was a factor of 1.287 larger than the DIAMOND MINE HE shot.
2. The ground velocity amplitudes measured from the broadband seismograms indicate that the MINE DUST HE shot was, at the mean, a factor of 1.32 larger than the DIAMOND MINE HE shot.
3. Coda length magnitudes calculated for MINE DUST HE and DIAMOND MINE HE indicate that the MINE DUST HE shot was 0.23 magnitude units larger.
4. The MINE DUST HE shot did not generate large enough signals to determine body wave magnitude directly.
5. The geometric mean of an energy ratio measure indicated that MINE DUST HE was 1.23 times larger than DIAMOND MINE HE; that DIAMOND DUST was 5.67 times larger than MINE DUST HE; that DIAMOND MINE was 6.32 times larger than DIAMOND DUST. These values are energy ratio values, so they are comparable to the squares of the velocity ratio values given above.
6. There is evidence that tectonic strain release may have occurred at the time of DIAMOND MINE.

The following recommendations are made based on these conditions.

1. Body wave magnitude measurements have not been possible because sufficient data have not been gathered at a distance of 200 km or more. An alternative to having a shot in the same area which would be large enough to record at that distance--this not being feasible--is having a smaller shot


and deploying a sensor array at the appropriate distance. Summing the sensor outputs or other array processing techniques could then be employed to distinguish the signal of interest from the background.

2. An analytic approach to measuring the body wave magnitude differences between the shots may be possible by extrapolating on the data already recorded. This will require: a) the preshaping of the P-wave train data with a filter matched to the response of the World-Wide Standard Seismograph Network short-period instruments, and b) computing the square root of the P-wave energy for each component taken separately and in combination. The results can then be compared with existing data on the  $P_n$  branch of the travel time curve.

3. As mentioned in Section 2.1, the energy ratio calculations can be made more accurate by using a separate equation for the surface-wave phases of the coda. This will require: a) writing another program comparable to the one in Appendix E for the body wave energy calculations, b) obtaining parameters from the records which would define a partition of the data into surface and body phases, and c) rerunning the programs using the data which has already been digitized.

4. Tectonic strain release apparently occurred at the time of DIAMOND MINE, which further confuses the determination of its relative energy. If there were strain release the total energy radiated would be the sum of the energy from both sources less the amount of energy from DIAMOND MINE which was transformed to the mechanical work needed to trigger the strain release. The data and theory are sufficient to get a first order estimate of the proportion of the energy due to tectonic strain release. This could be accomplished by fitting the observed data to the theoretically derived radiation patterns generated by the mechanism hypothesized in Section 2.1.

REFERENCES

1. Bullen, K. E., An Introduction to the Theory of Seismology, Cambridge, The University Press, 1963.
2. Dobrin, Milton B., Introduction to Geophysical Prospecting, New York, McGraw Hill Book Co., 1960.
3. McLaughlin, R. and D. E. Willis, Interpretation of Seismic Measurements Taken in the DIAMOND MINE SERIES, University of Michigan, Geophysics Group, Technical Report 37180-4-T/POR 6574, May 1972.
4. 
5. Willis, D. E. and R. McLaughlin, Summary of the Seismic Measurements Taken in the MINE DUST HE Event, University of Michigan, Geophysics Group, Technical Report 37180-8-T, August 1972.

APPENDIX A  
MINE DUST HE Spectral Analyses

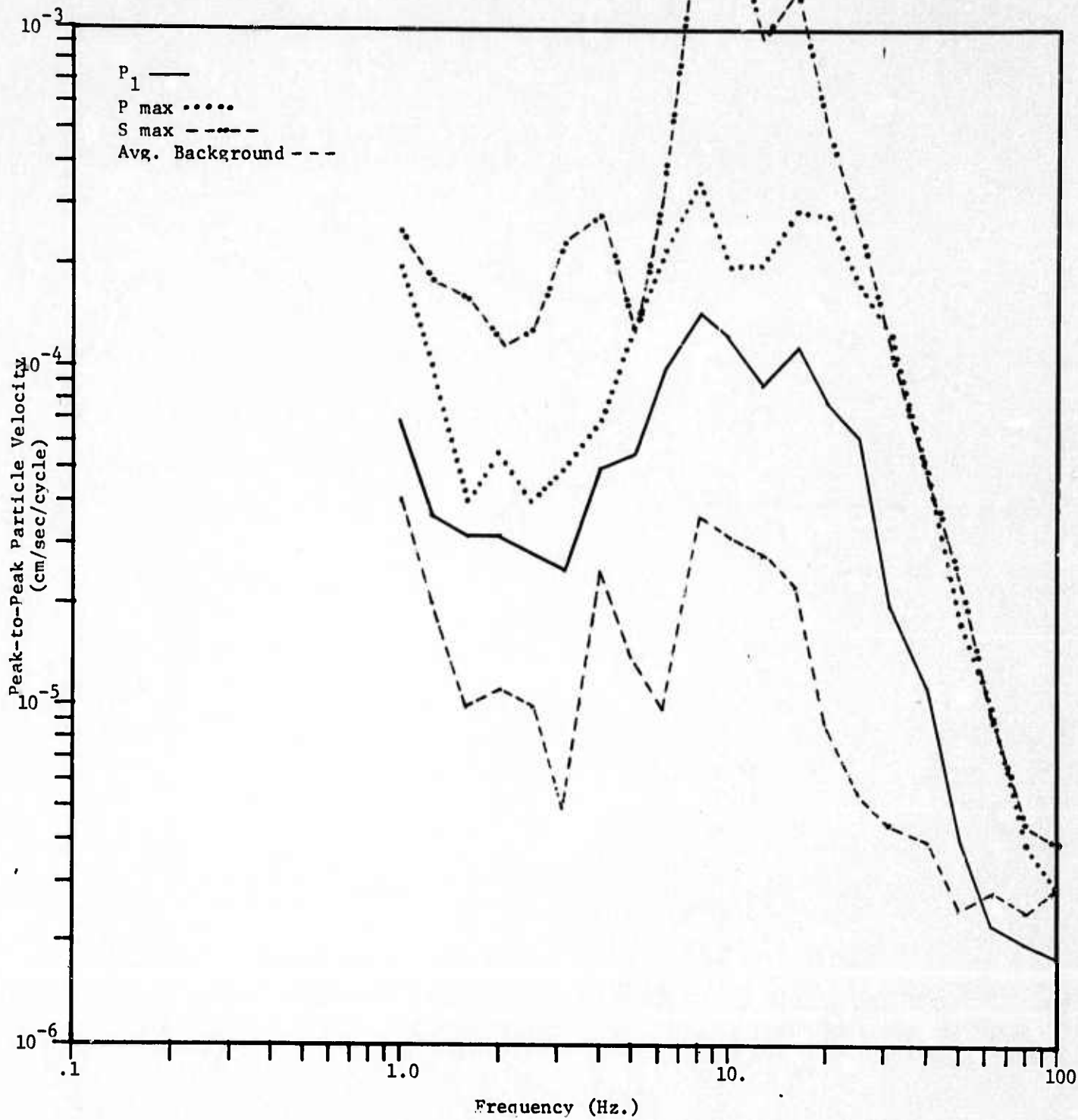


Figure A-1. MINE DUST HE, NTS, North Site (Longitudinal)

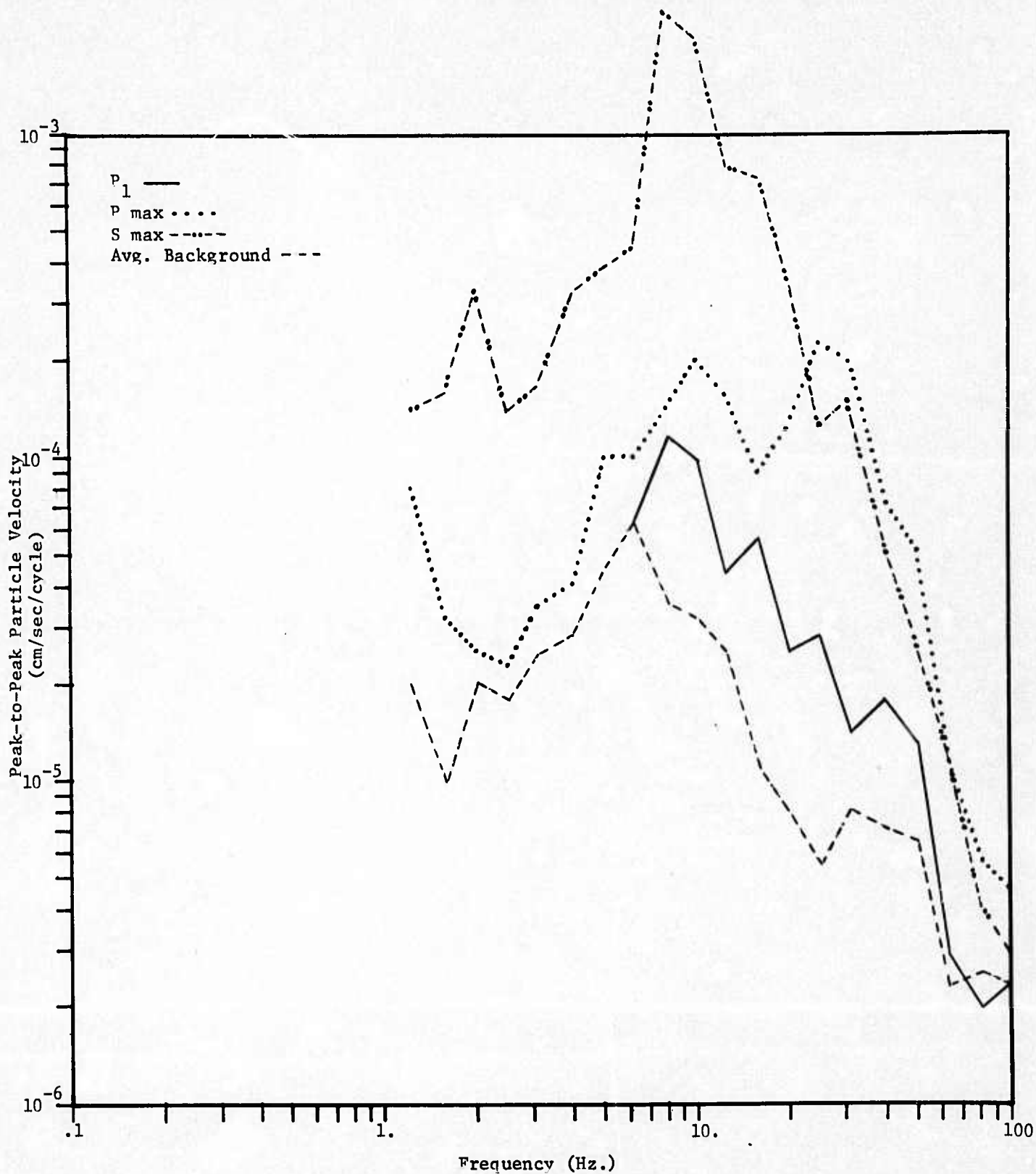


Figure A-2. MINE DUST HE, NTS, North Site (Transverse)

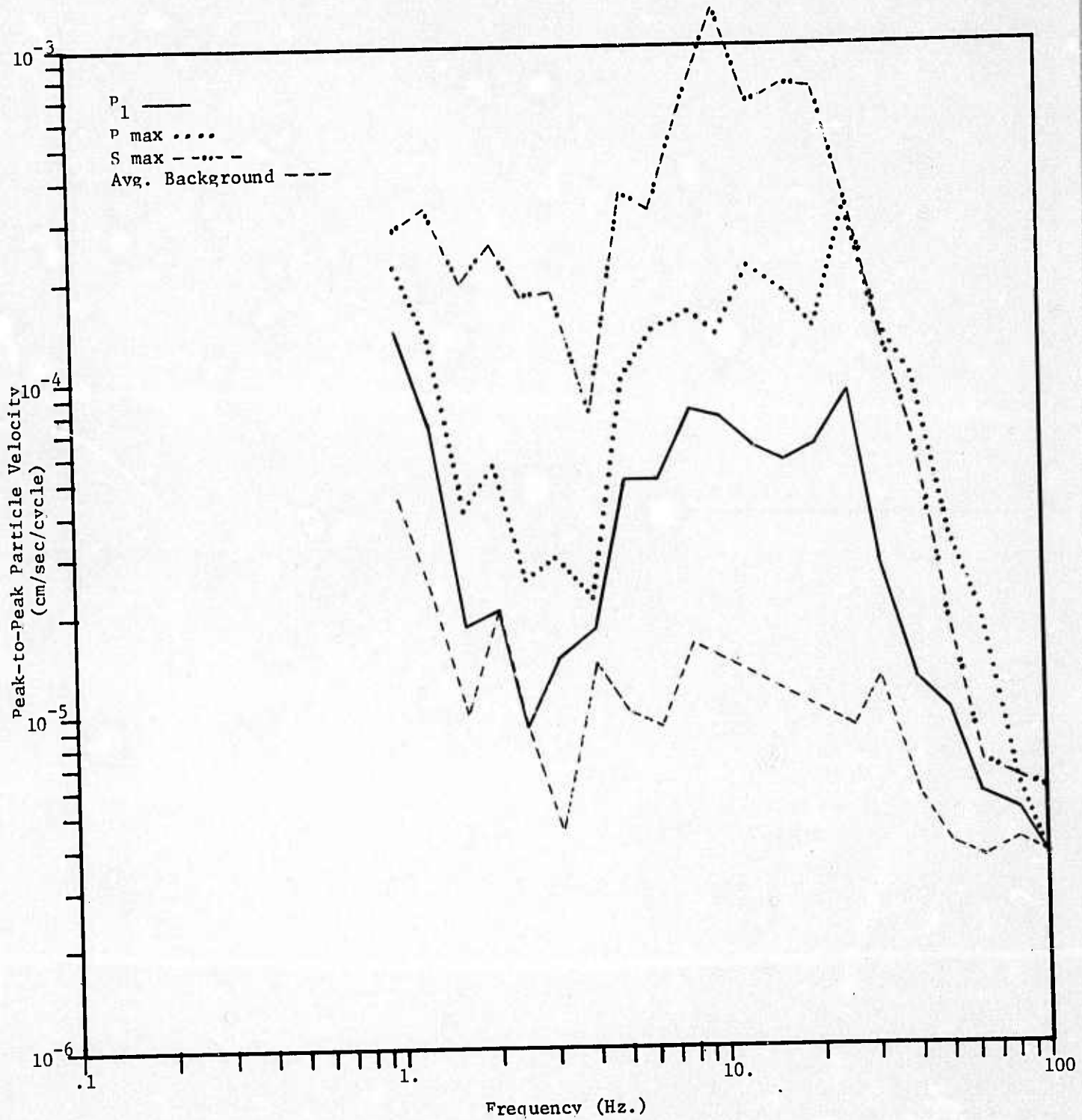


Figure A-3. MINE DUST HE, NTS, North Site (Vertical)

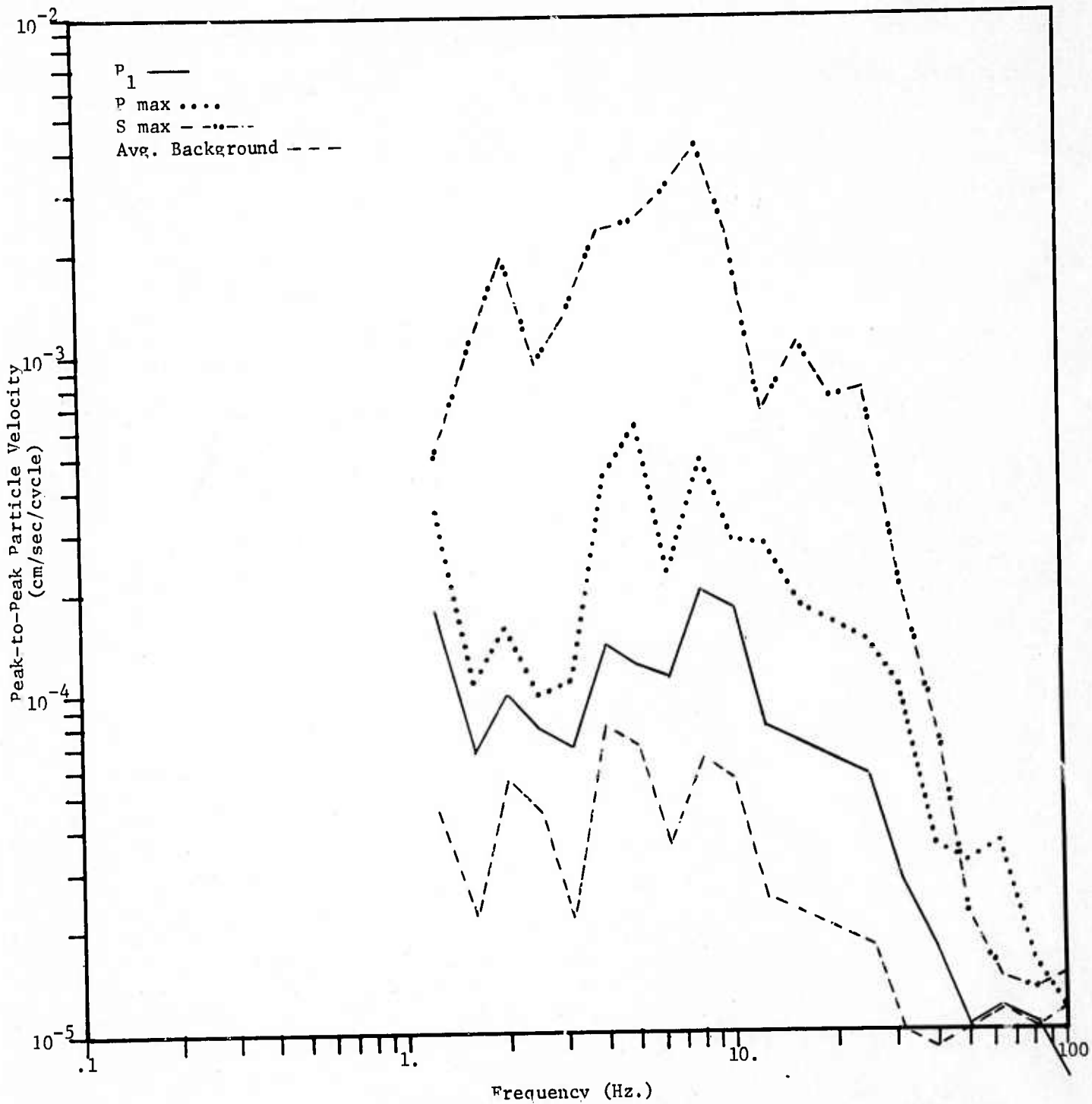


Figure A-4. MINE DUST HE, NTS, East Site (Pole Line Road)  
(Longitudinal)

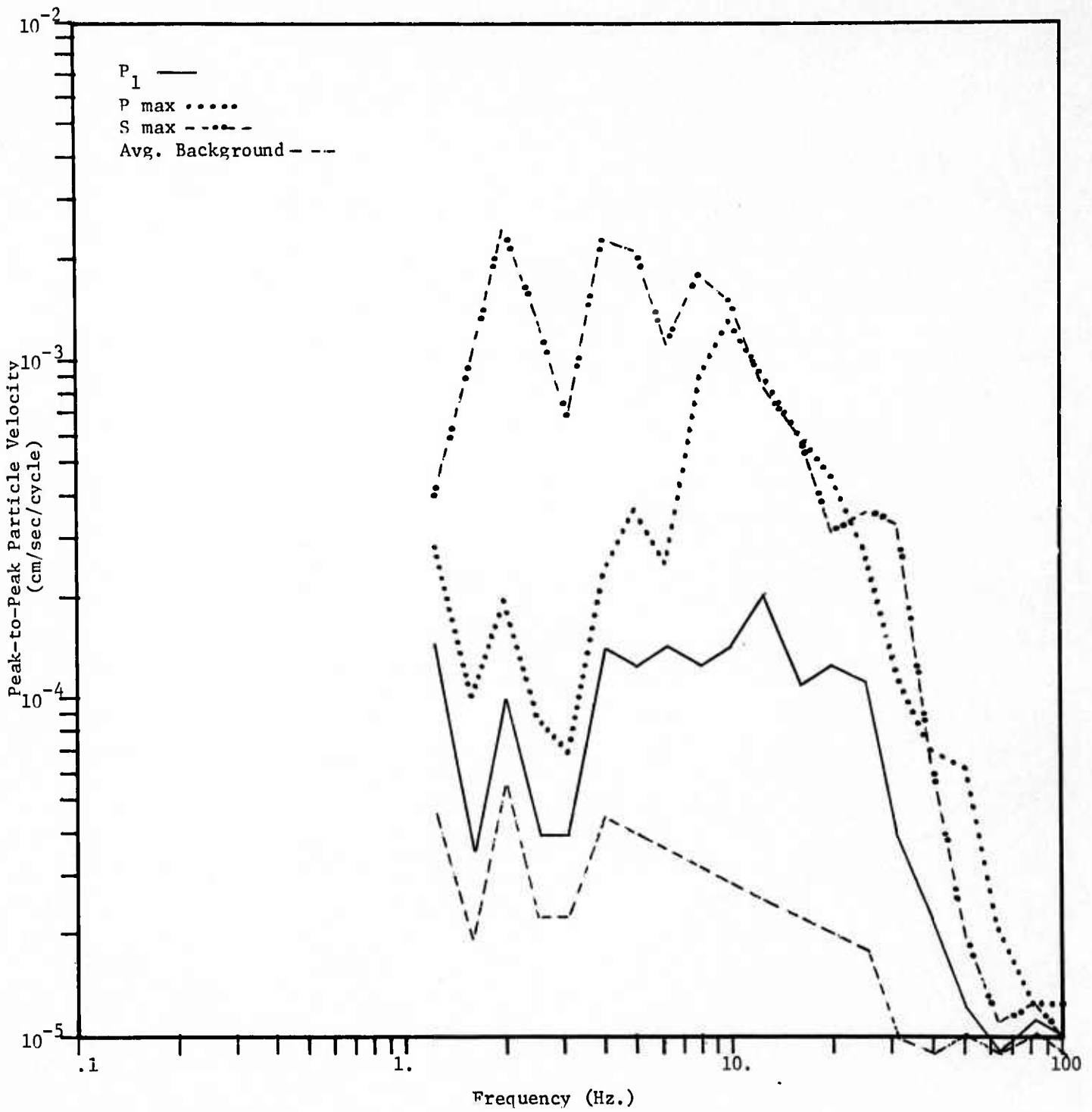


Figure A-5. MINE DUST HE, NTS, East Site (Pole Line Road)  
(Transverse)

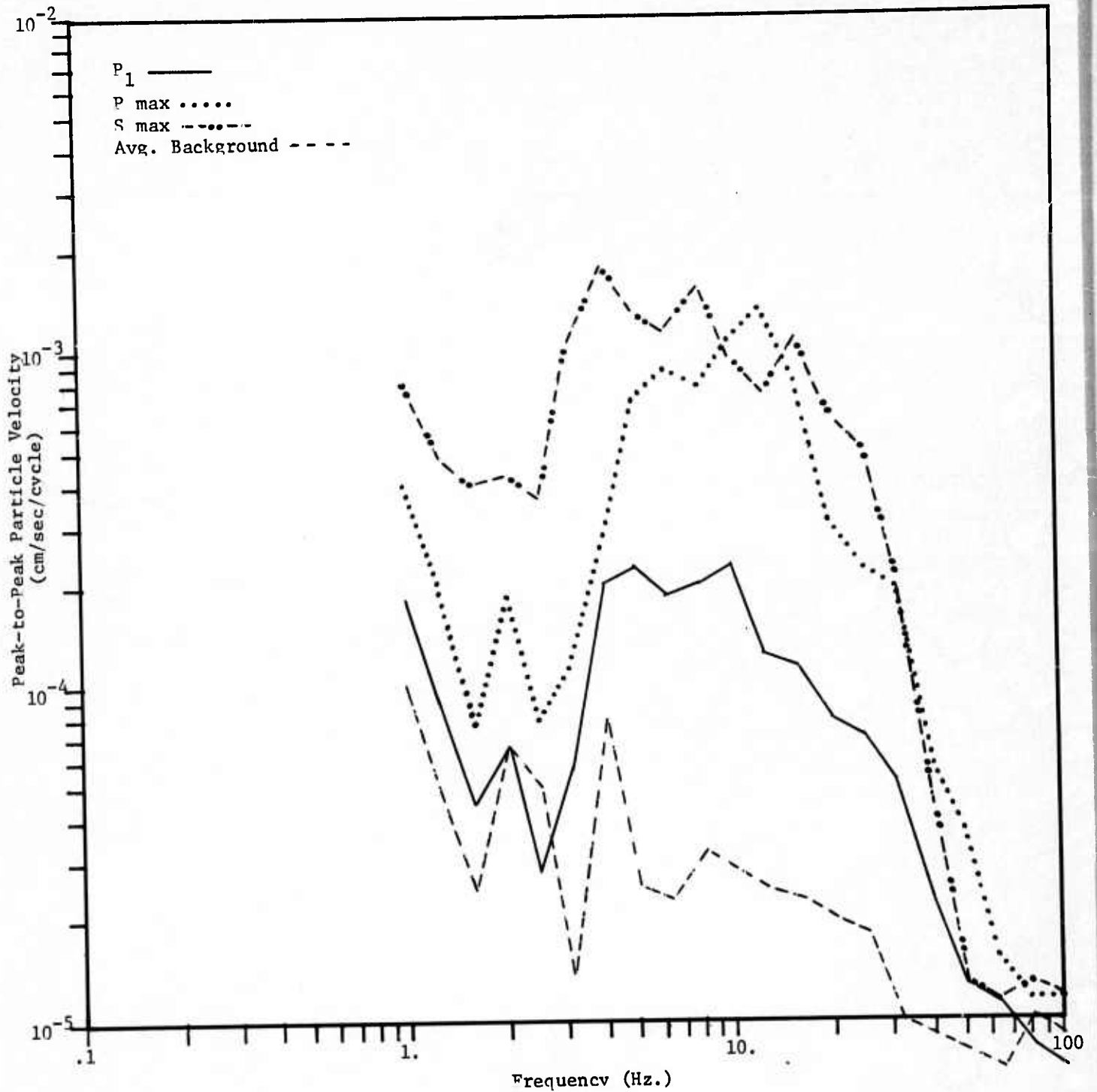


Figure A-6. MINE DUST HE, NTS, East Site (Pole Line Road)  
(Vertical)

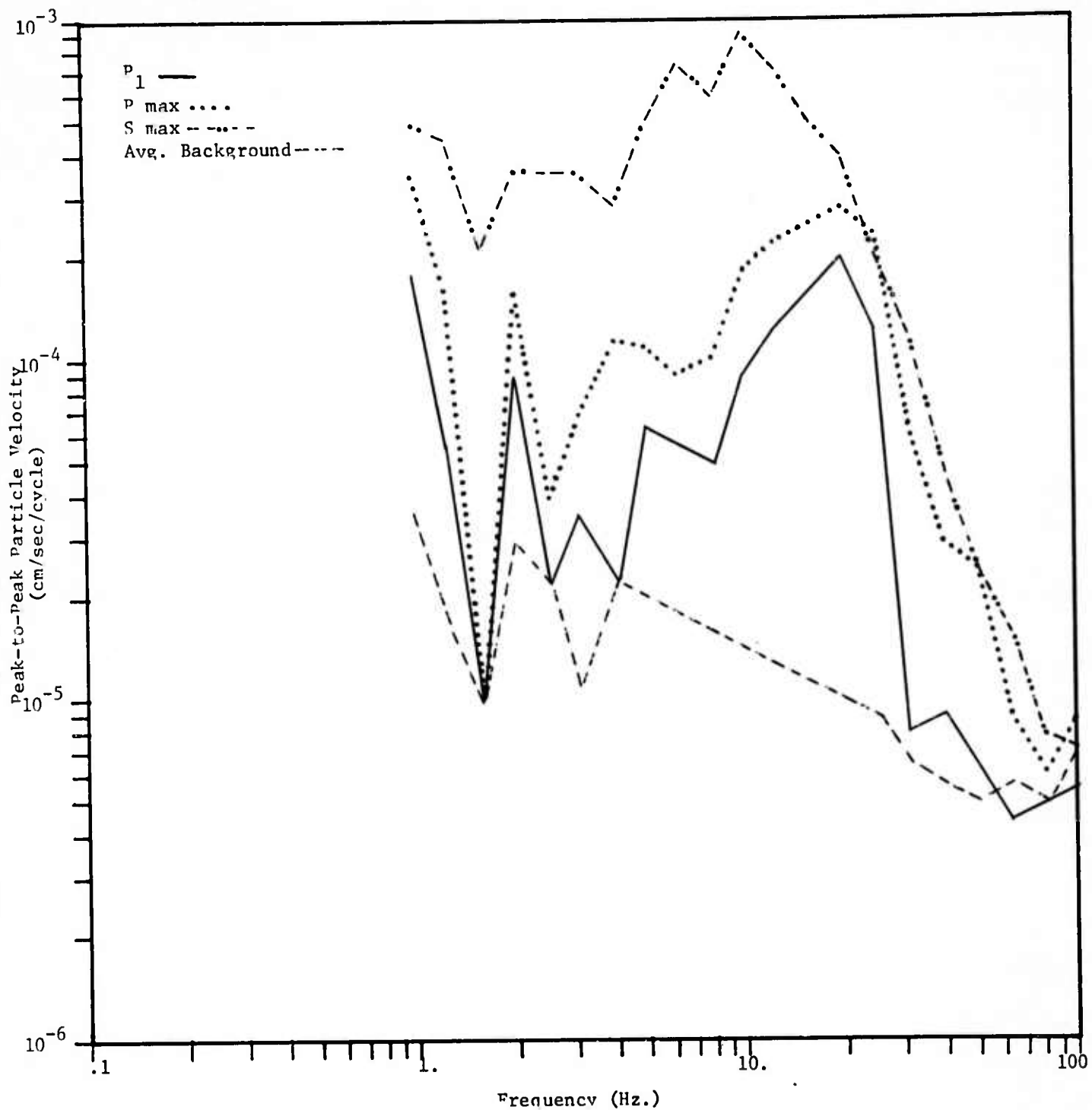


Figure A-7. MINE DUST HE, NTS, Southeast Site (Longitudinal)

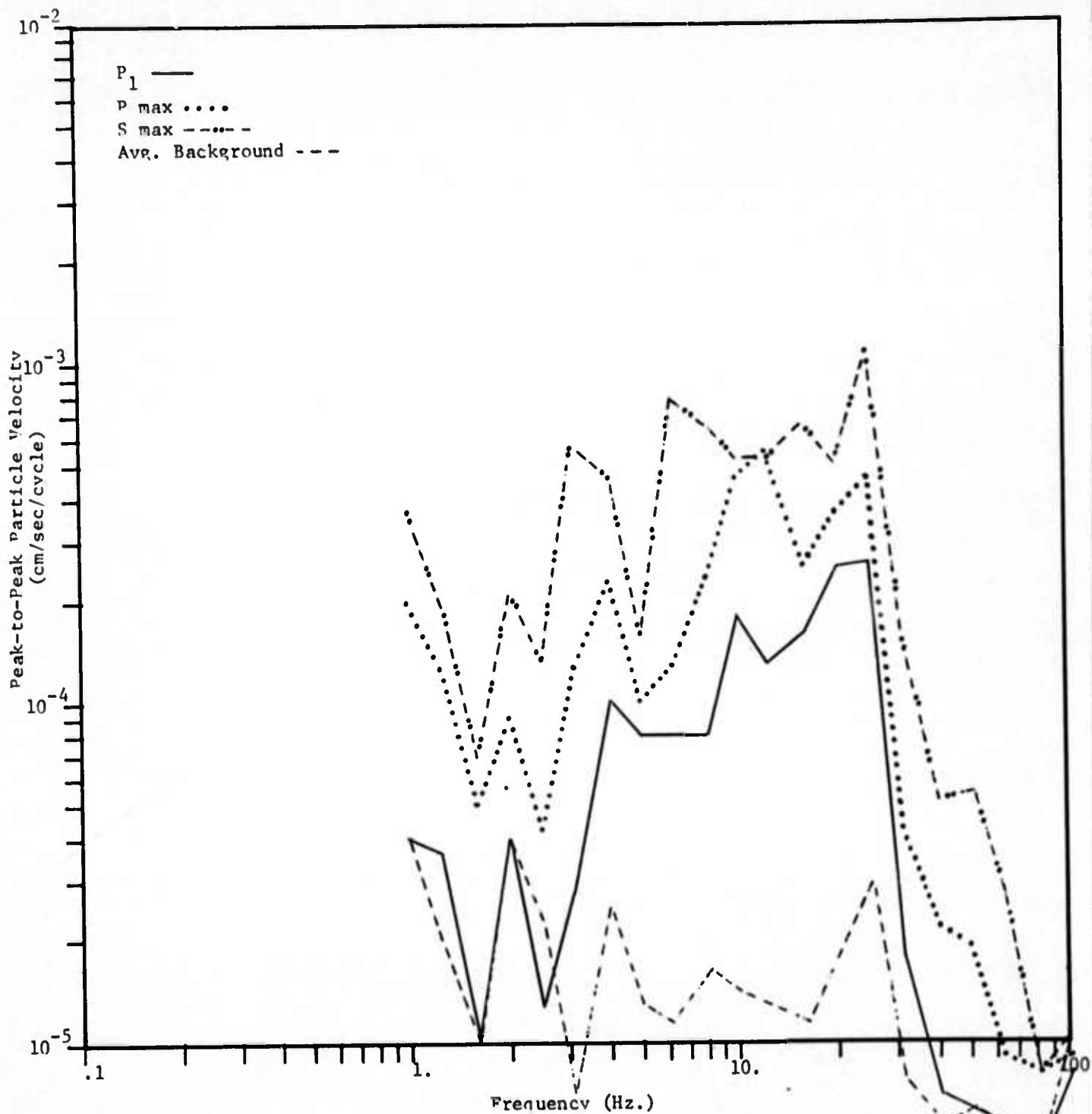


Figure A-8. MINE DUST HE, NTS, Southeast Site (Transverse)

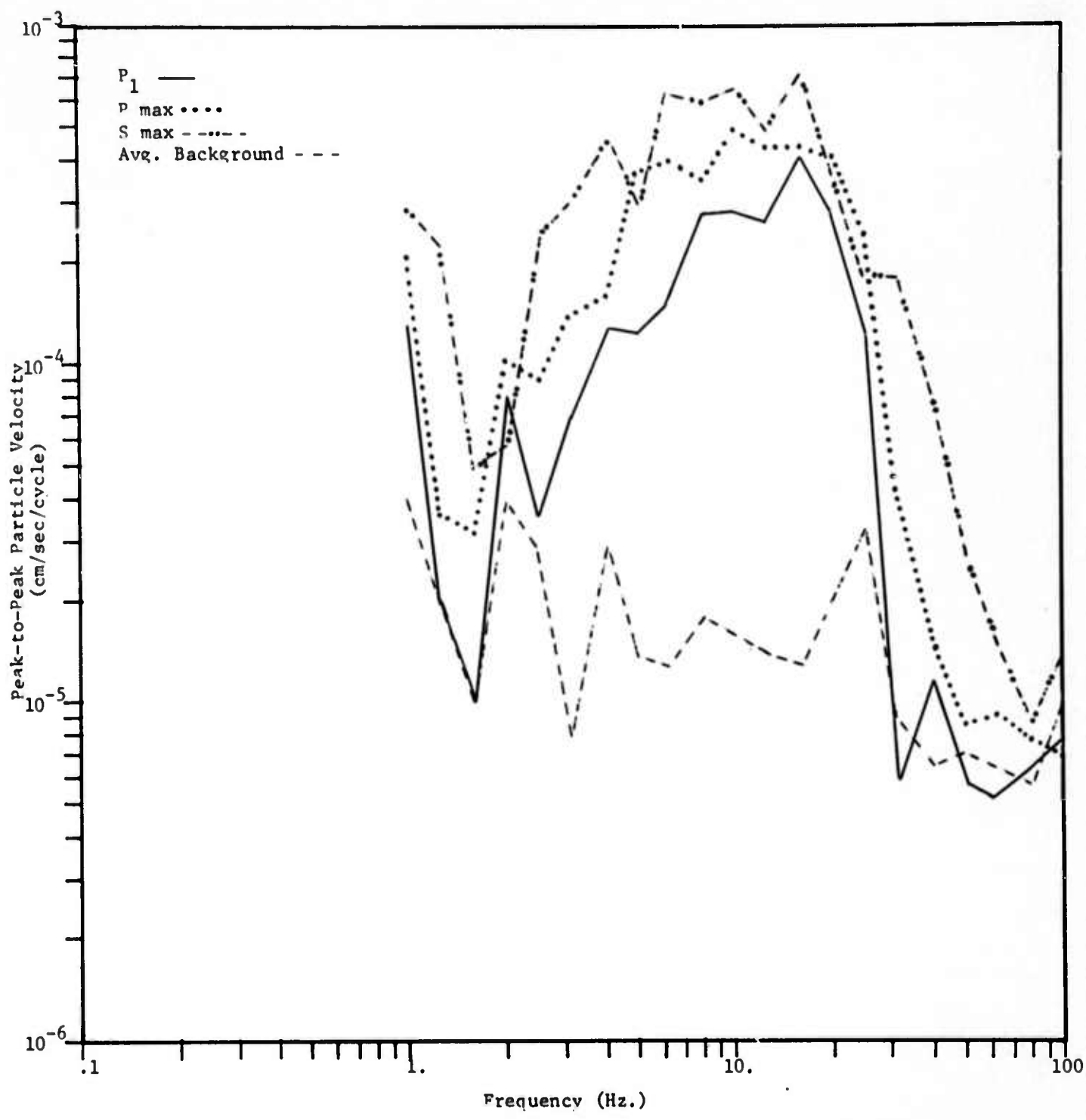


Figure A-9. MINE DUST HE, NTS, Southeast Site (Vertical)

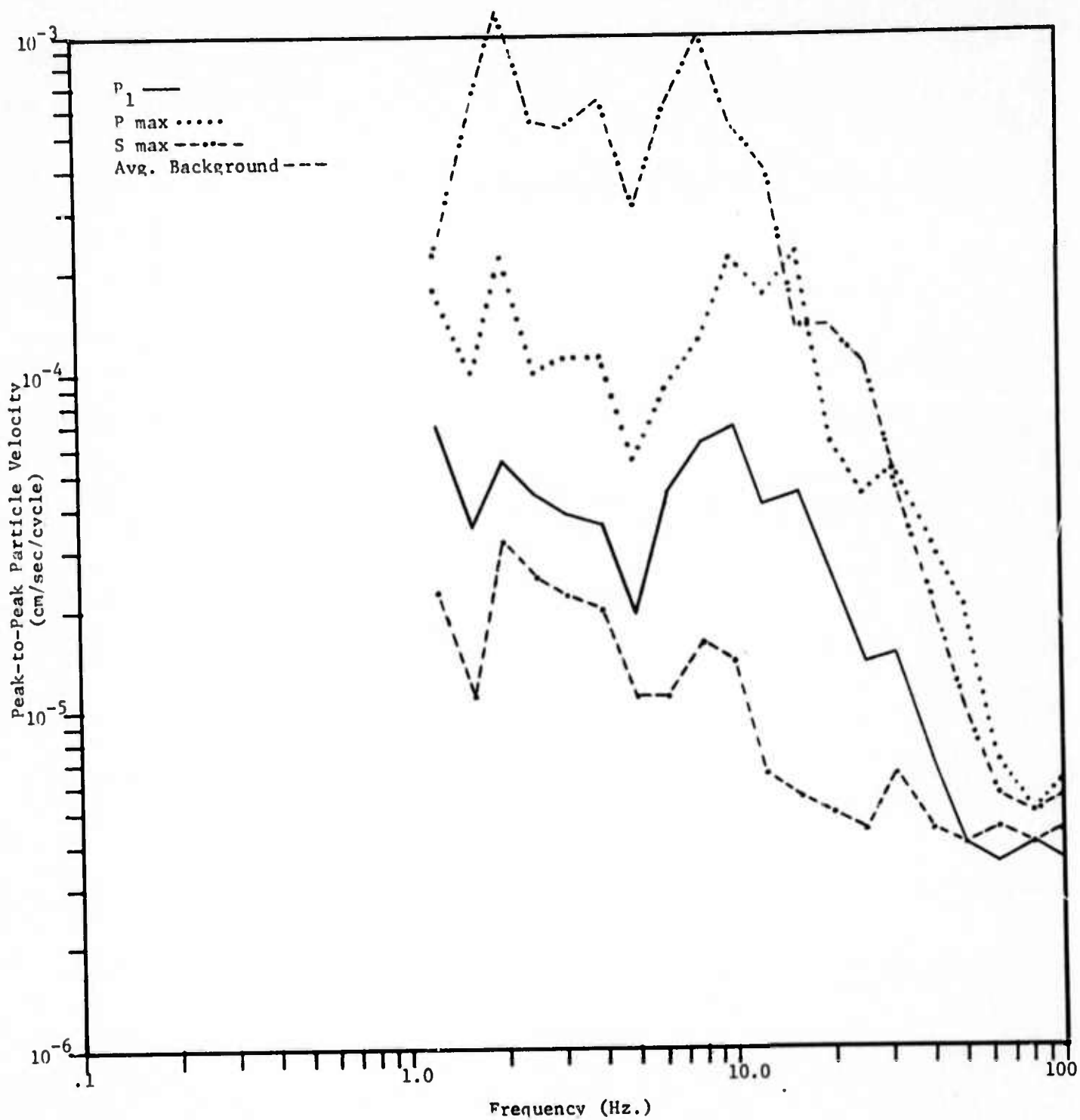


Figure A-10. MINE DUST HE, NTS, South Site (Longitudinal)

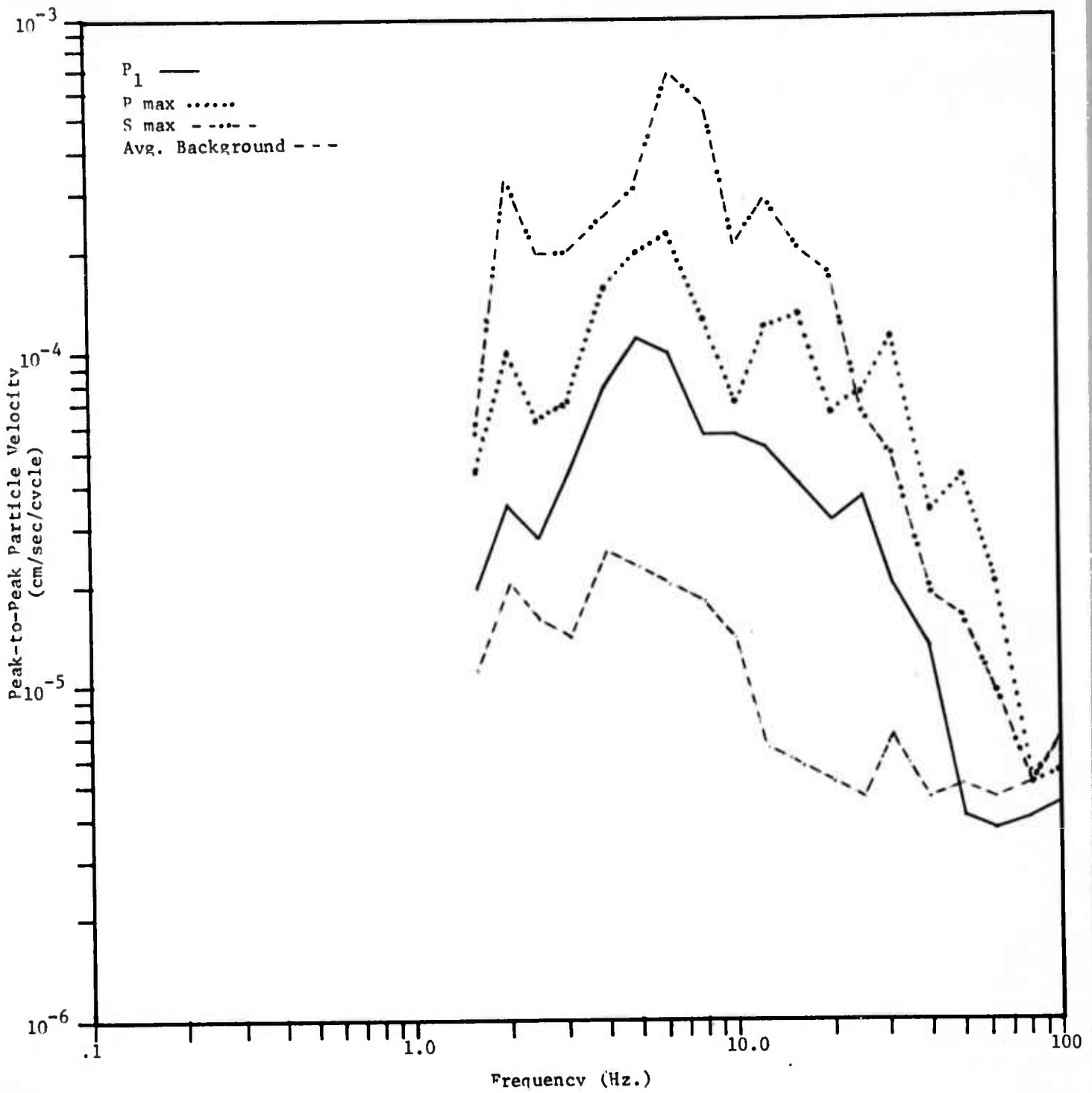


Figure A-11. MINE DUST HE, NTS, South Site (Transverse)

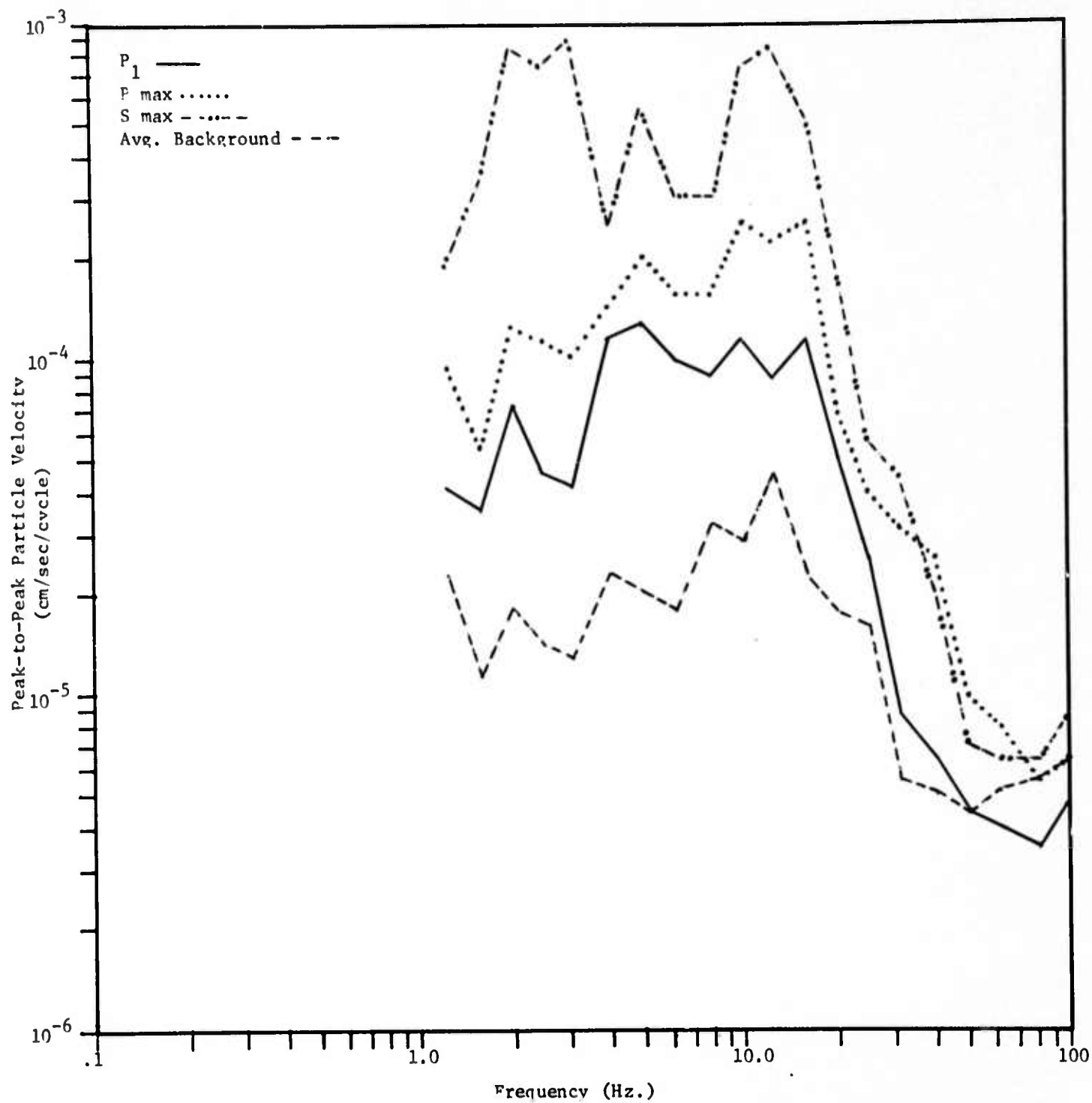


Figure A-12. MINE DUST HE, NTS, South Site (Vertical)

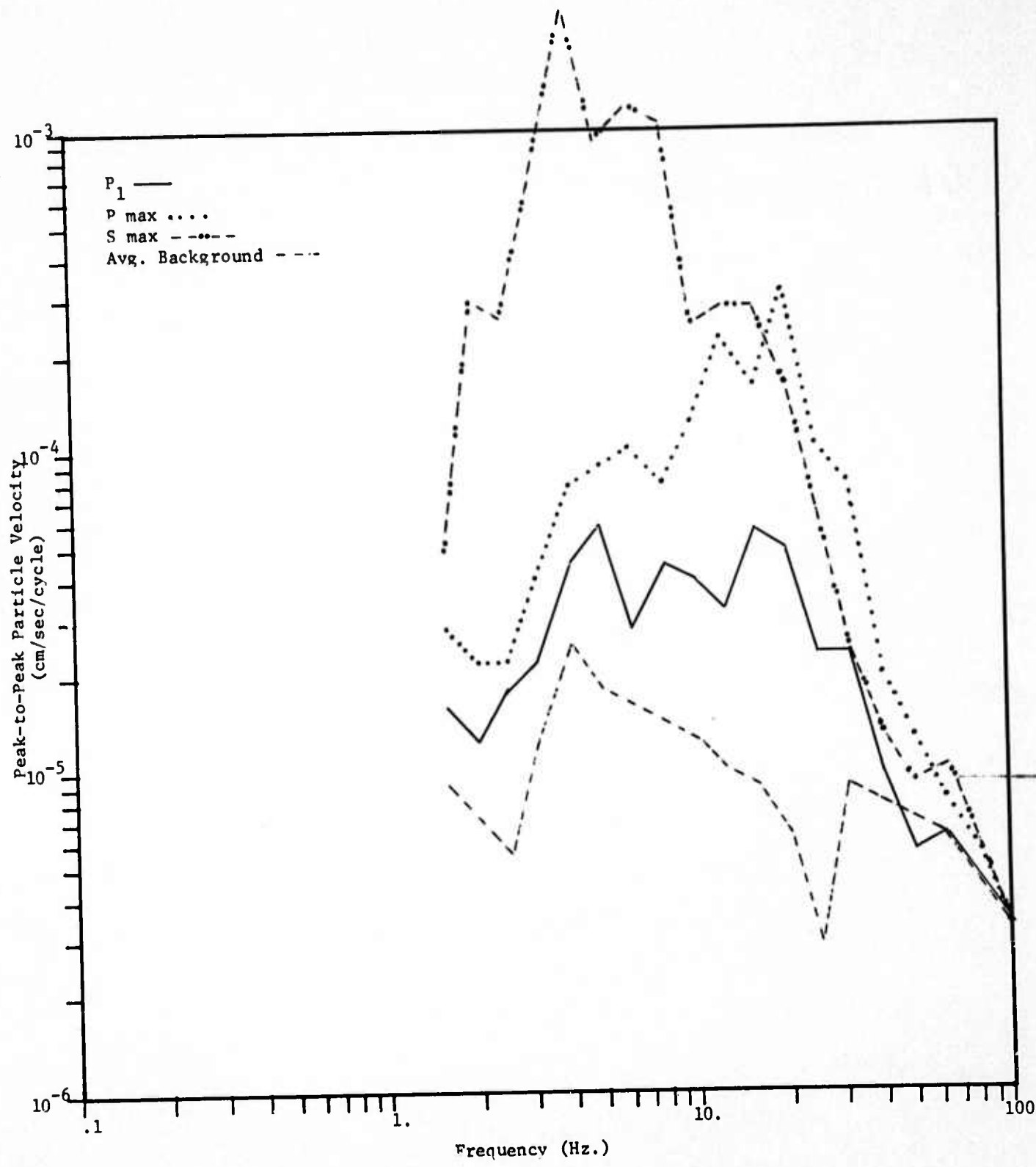


Figure A-13. MINE DUST HE, NTS, Pahute Mesa Site (Longitudinal)

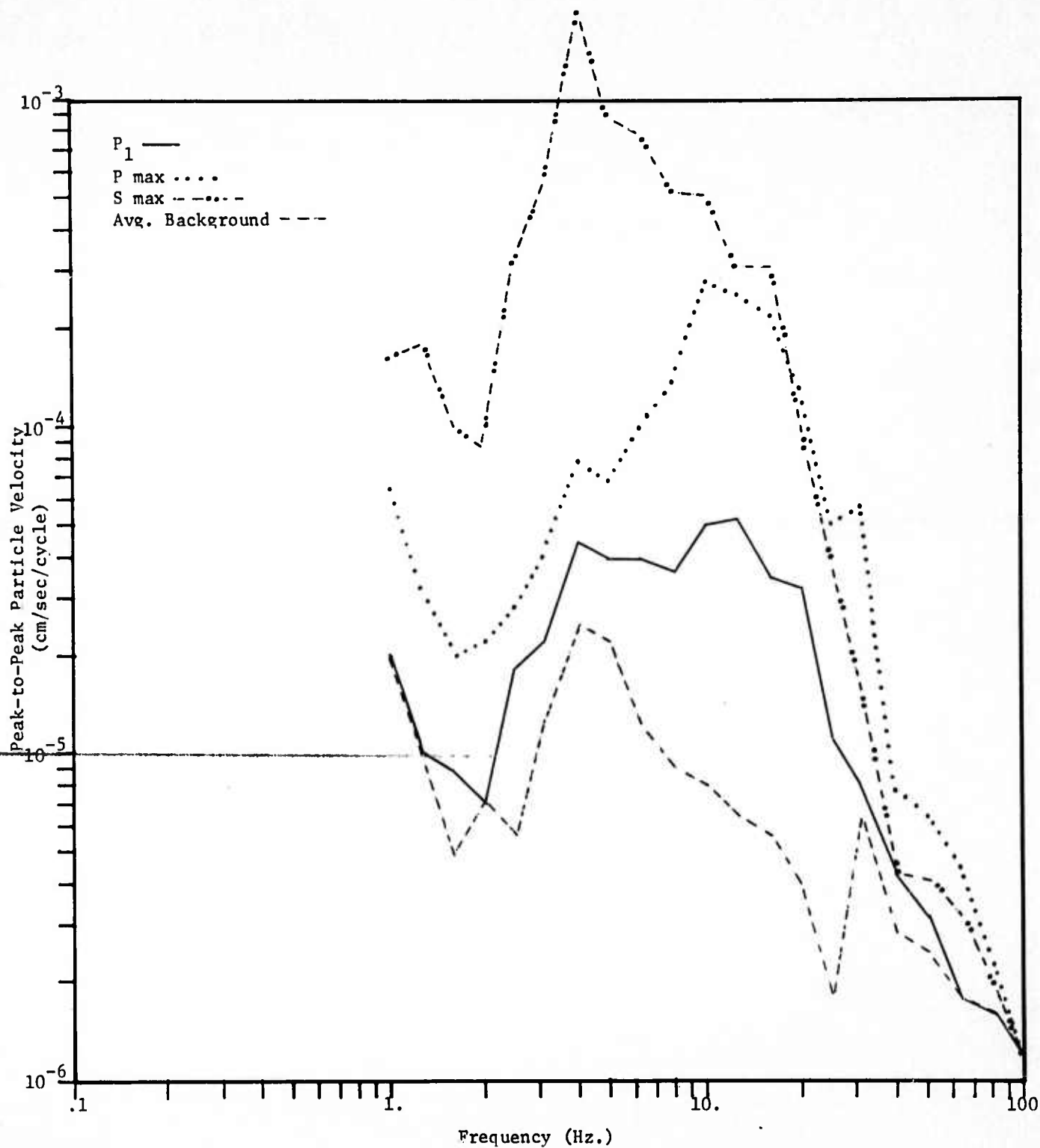


Figure A-14. MINE DUST HE, NTS, Pahute Mesa Site (Transverse)

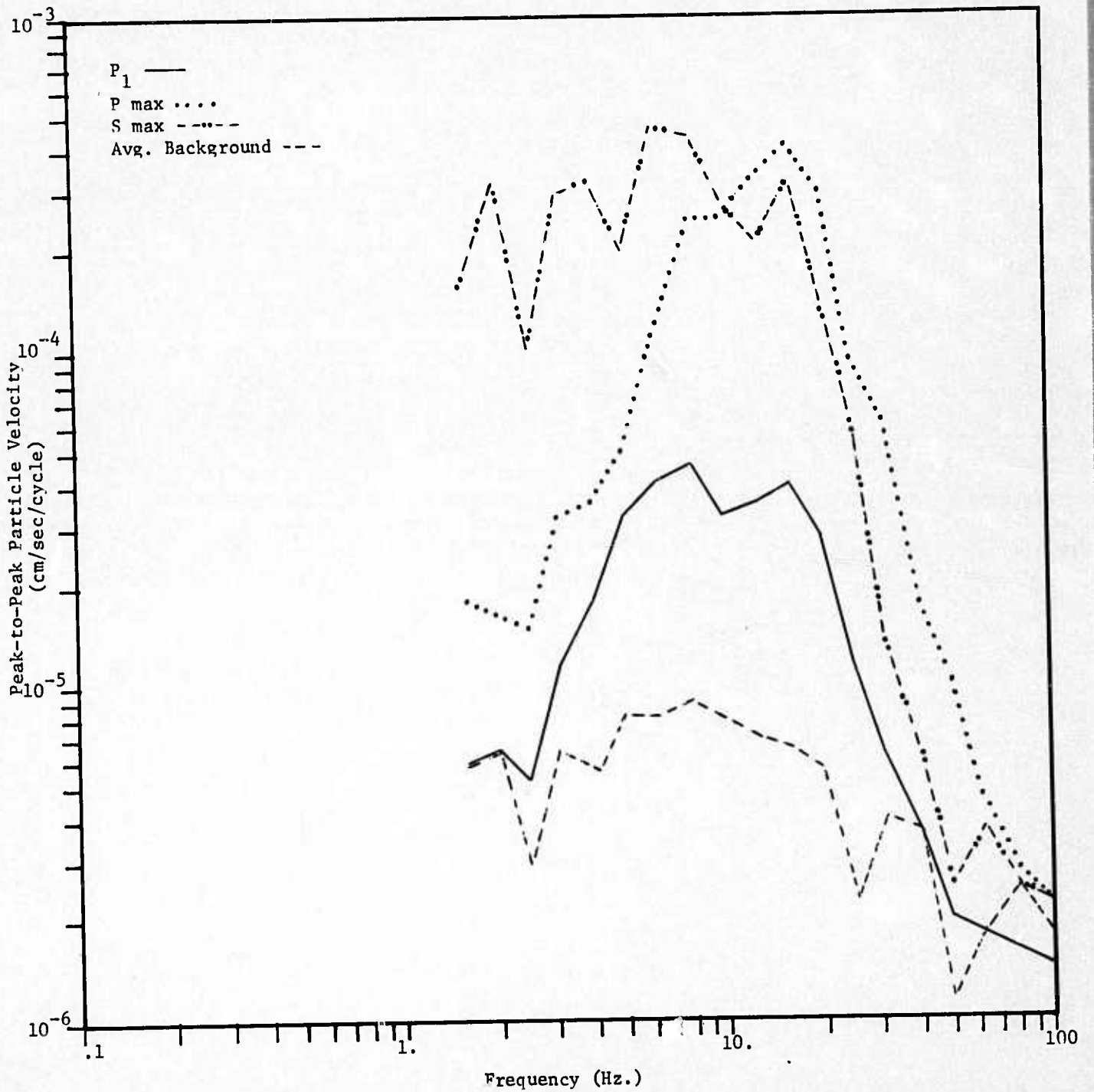


Figure A-15. MINE DUST HE, NTS, Pahute Mesa Site (Vertical)

APPENDIX B

Composite Spectral Curves as a Function of  
Event, Site, and Wave Type



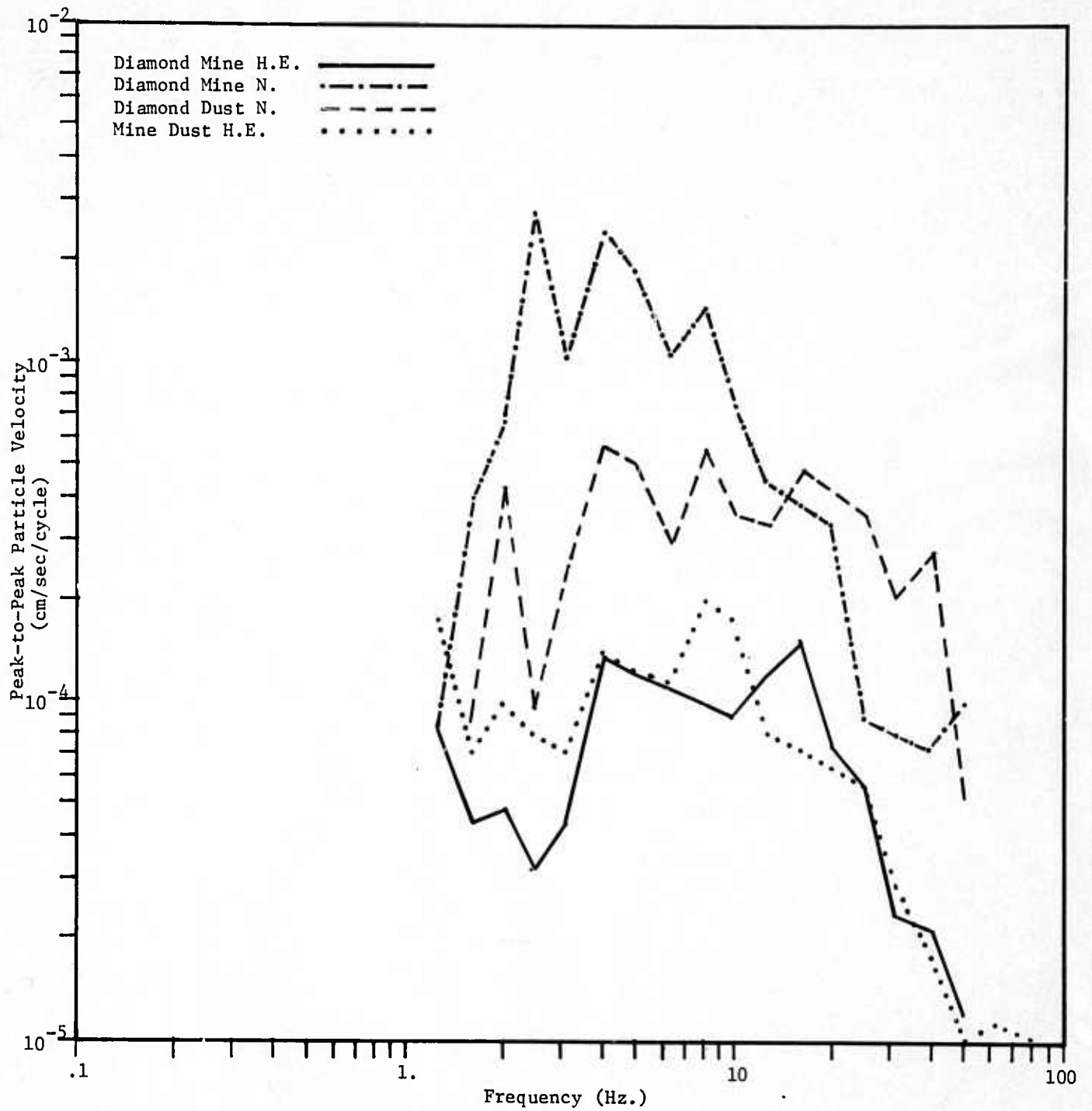


Figure B-2. East Site (Pole Line Road), NTS, First P  
(Longitudinal)

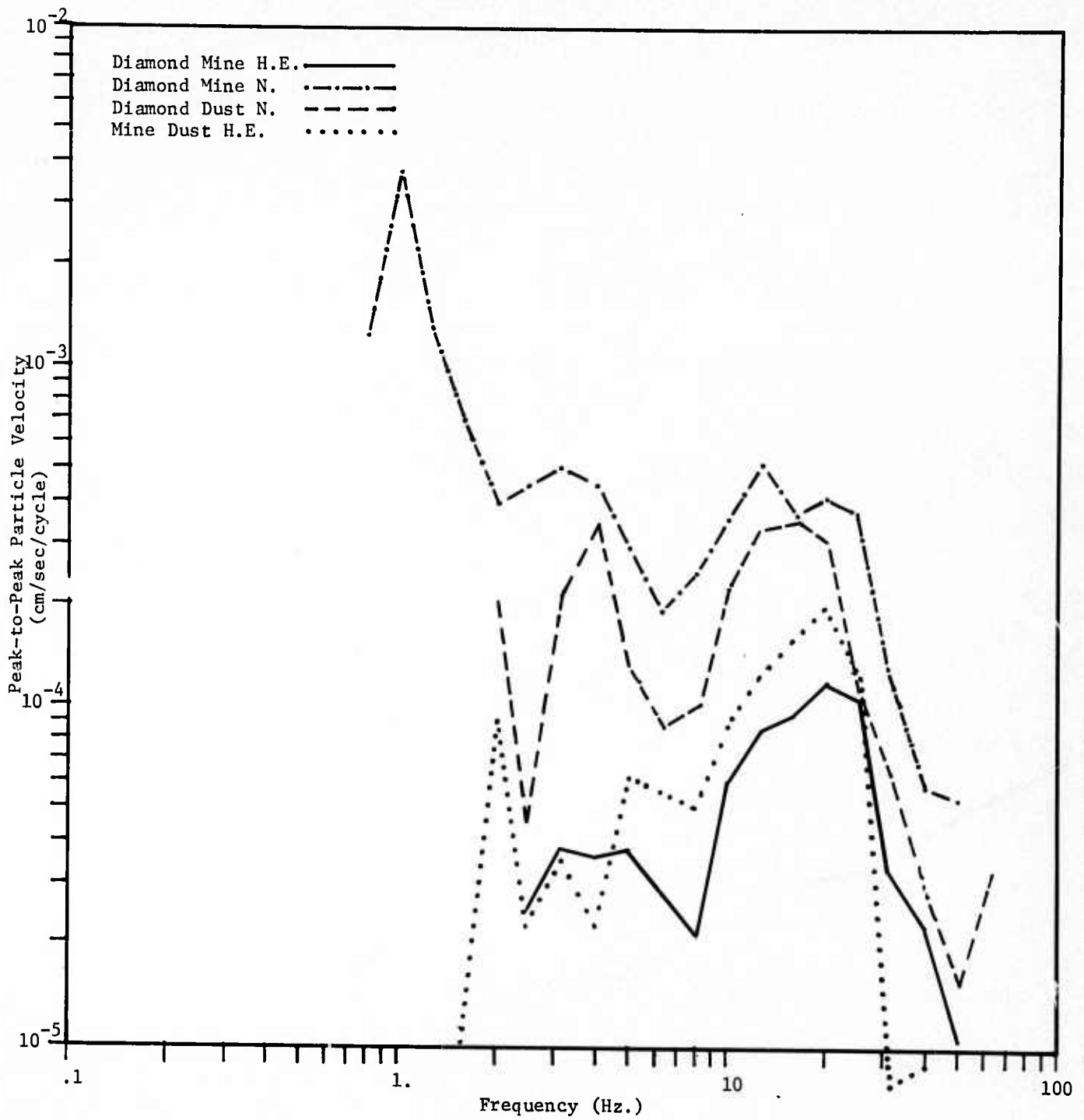


Figure B-3. Southeast Site, NTS, First P (Longitudinal)

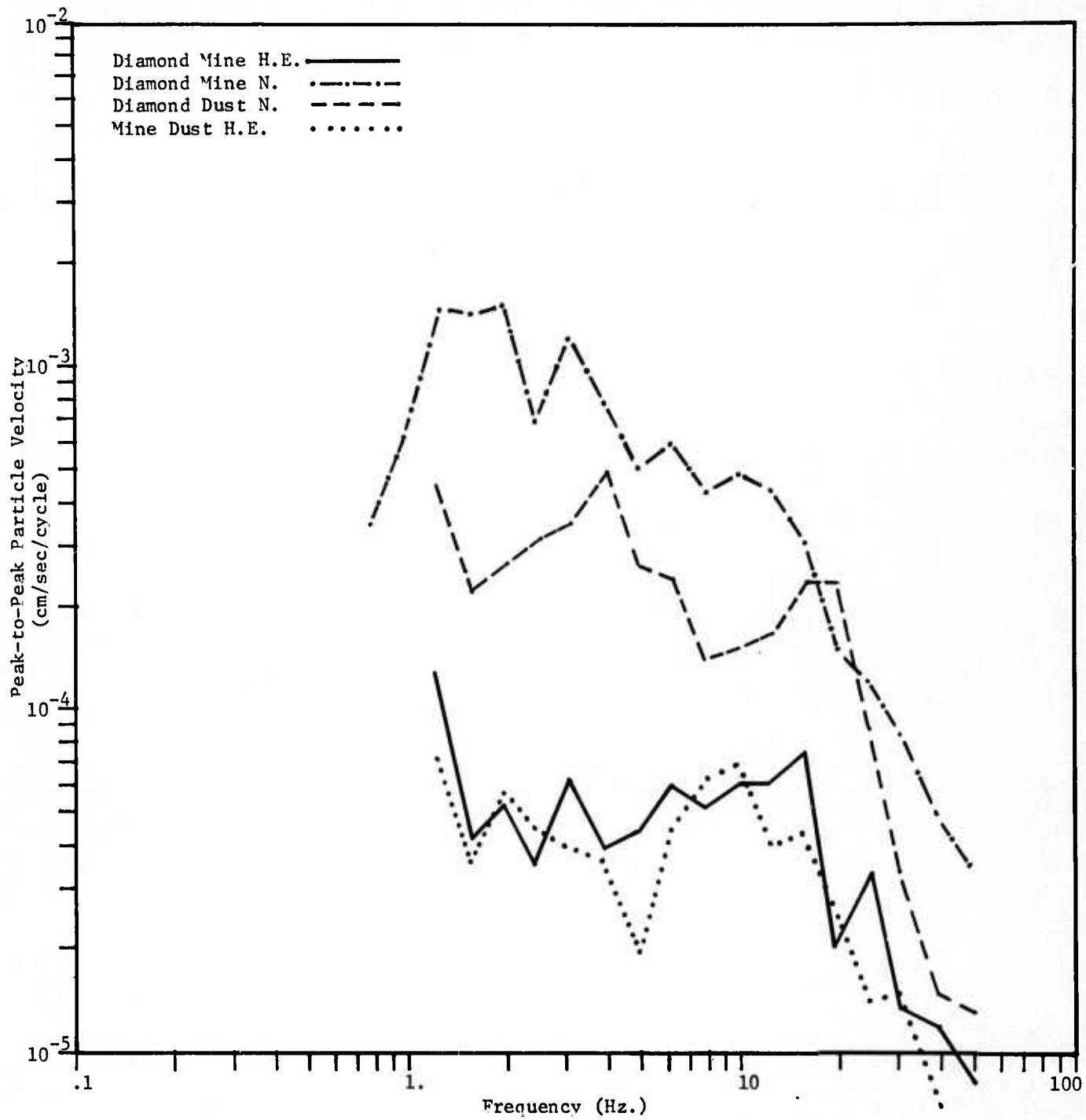


Figure B-4. South Site, NTS, First P (Longitudinal)

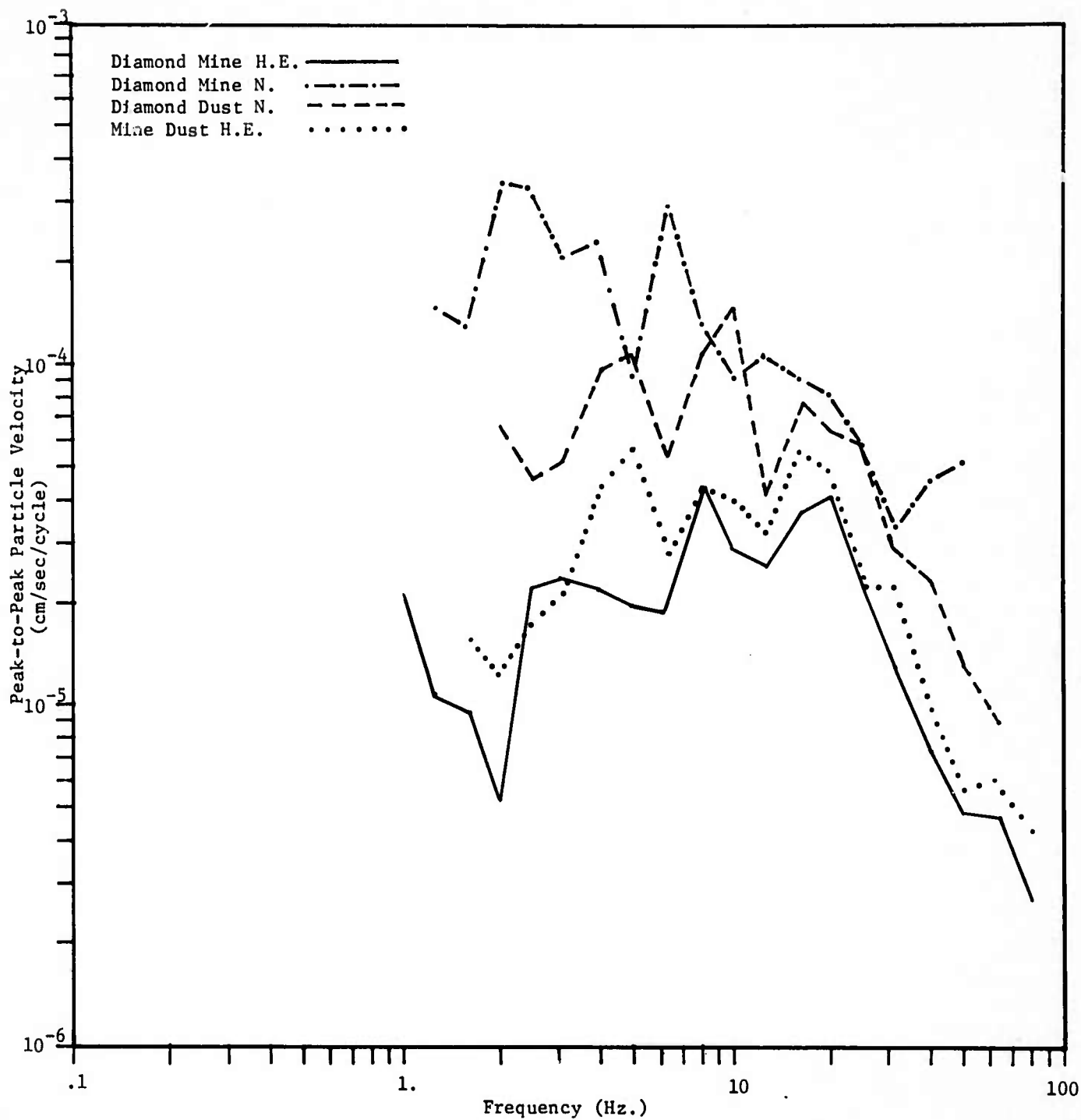


Figure B-5. Pahute Mesa Site, NTS, First P (Longitudinal)

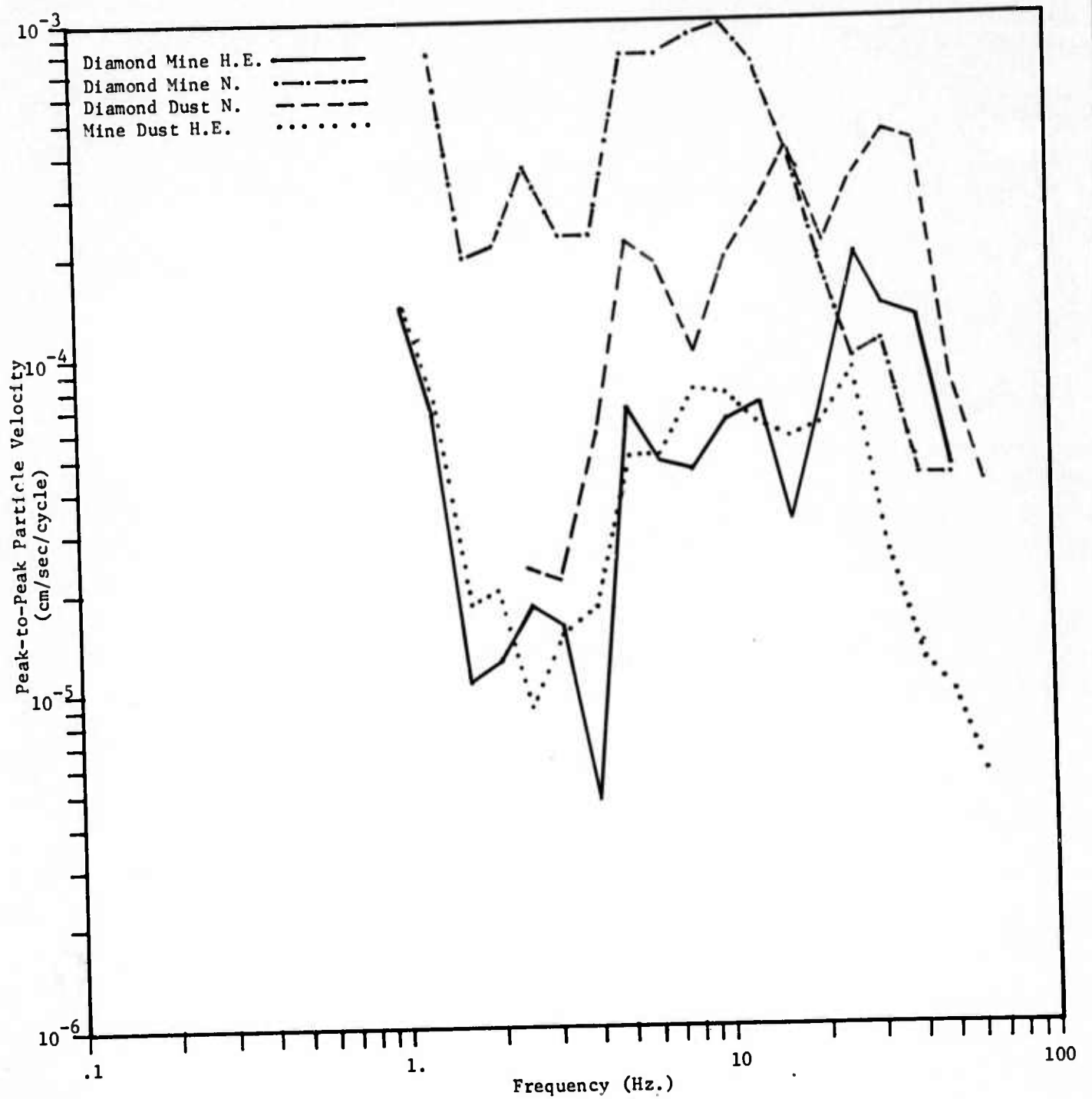


Figure B-6. North Site, NTS, First P (Vertical)

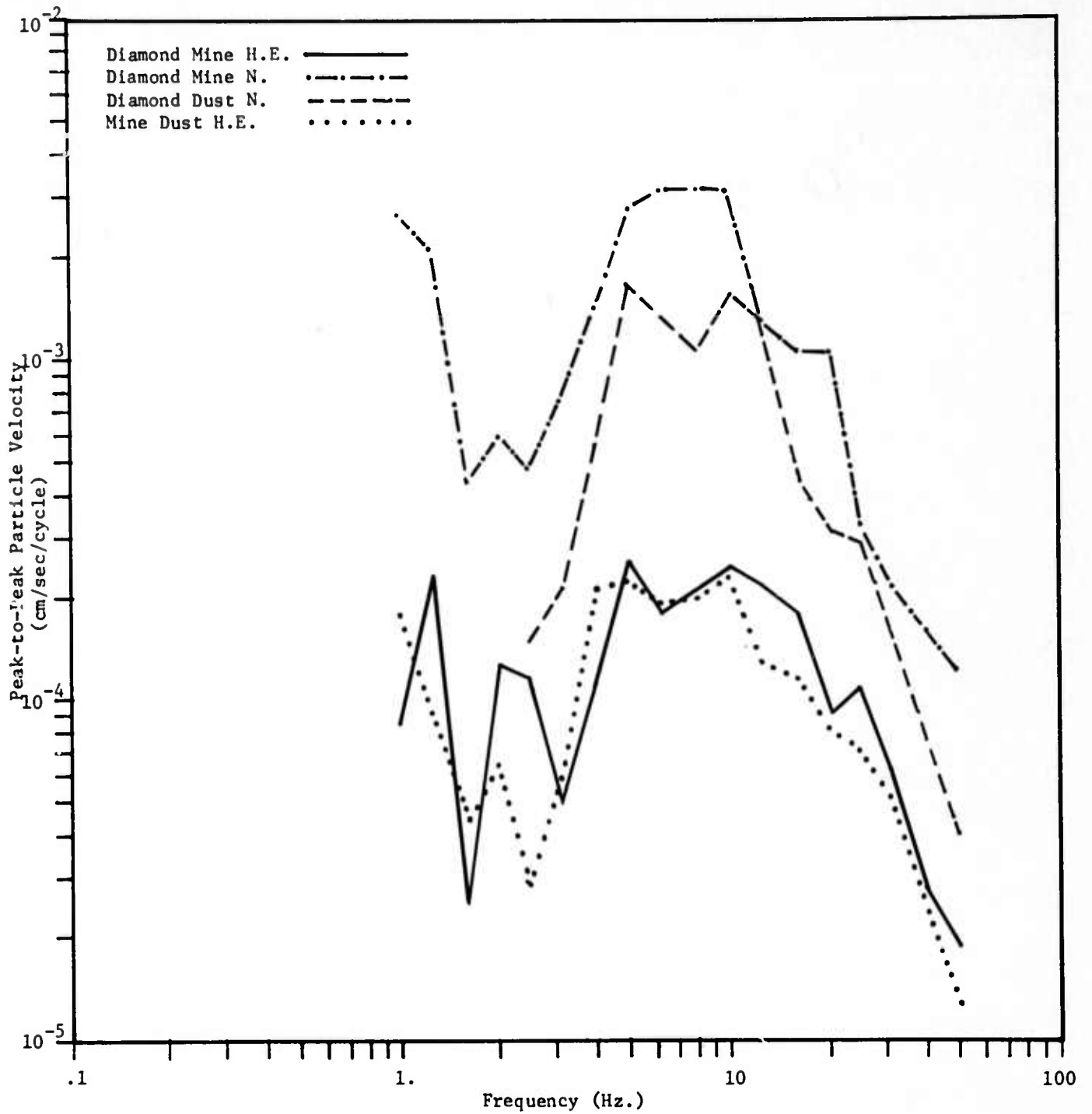


Figure B-7. East Site (Pole Line Road), NTS, First P (Vertical)



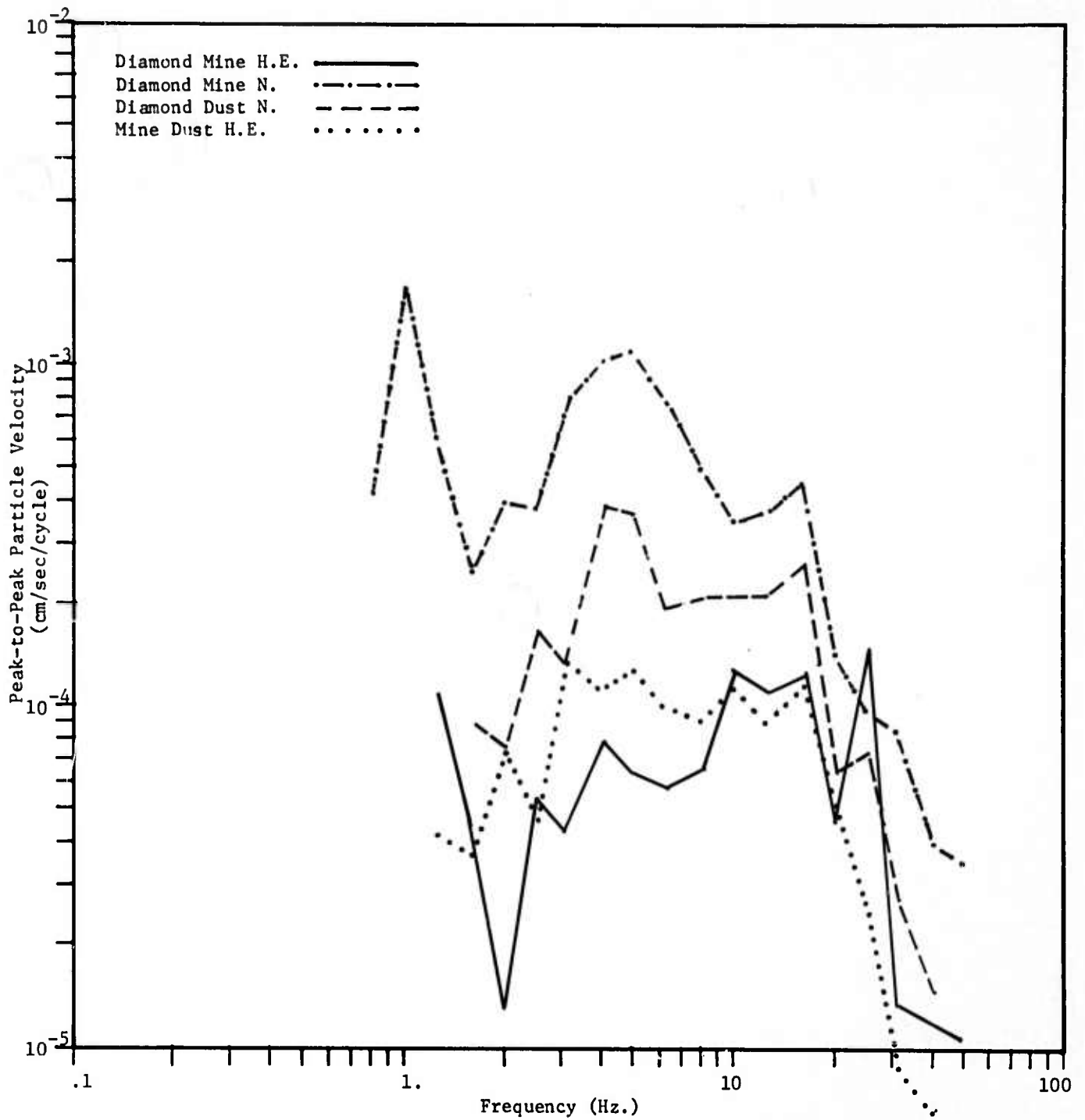


Figure B-9. South Site, NTS, First P (Vertical)

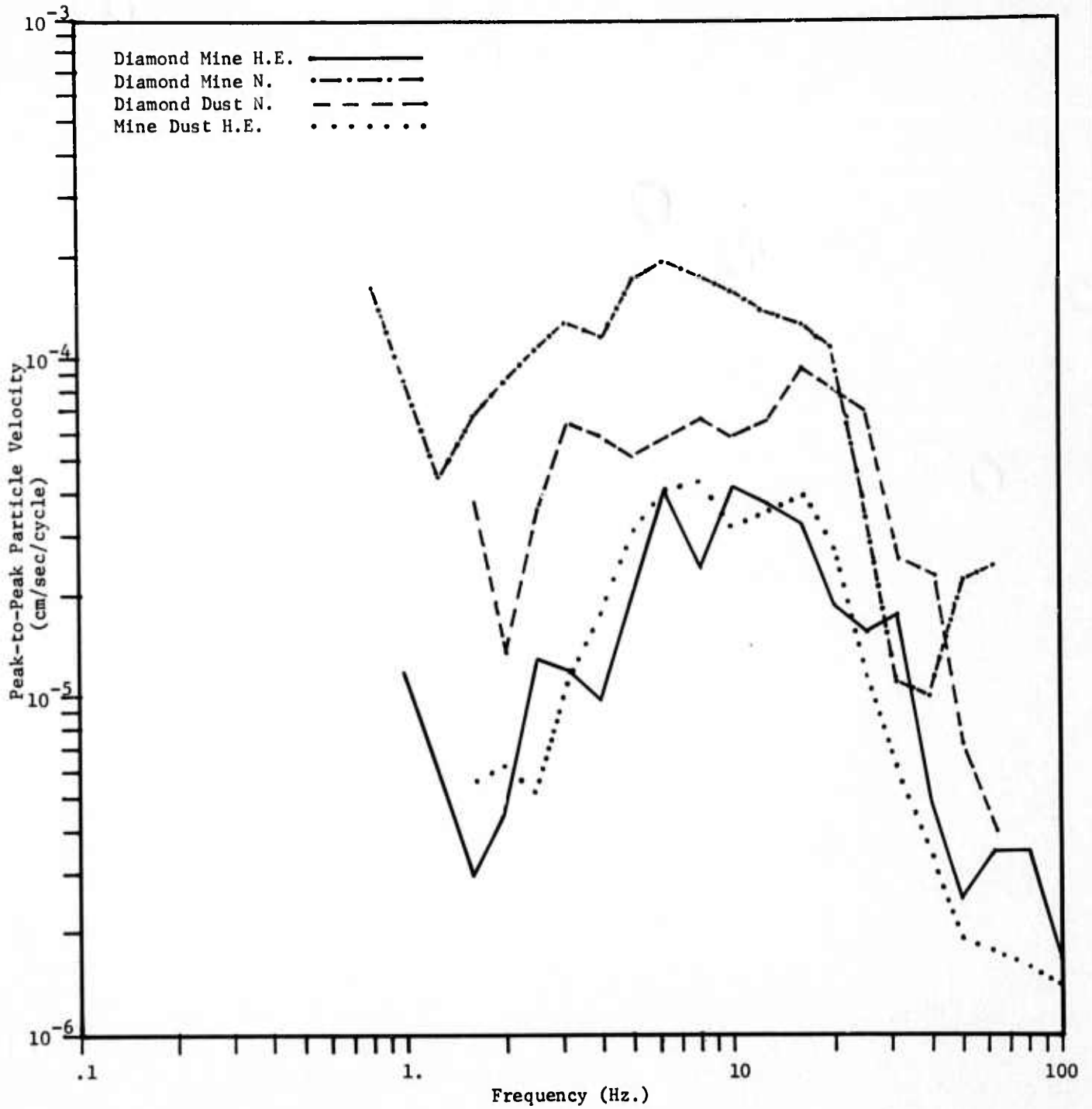


Figure B-10. Pahute Mesa Site, NTS, First P (Vertical)

APPENDIX C

Spectral Ratios of MINE DUST HE/DIAMOND MINE HE  
as a Function of Site and Wave Type

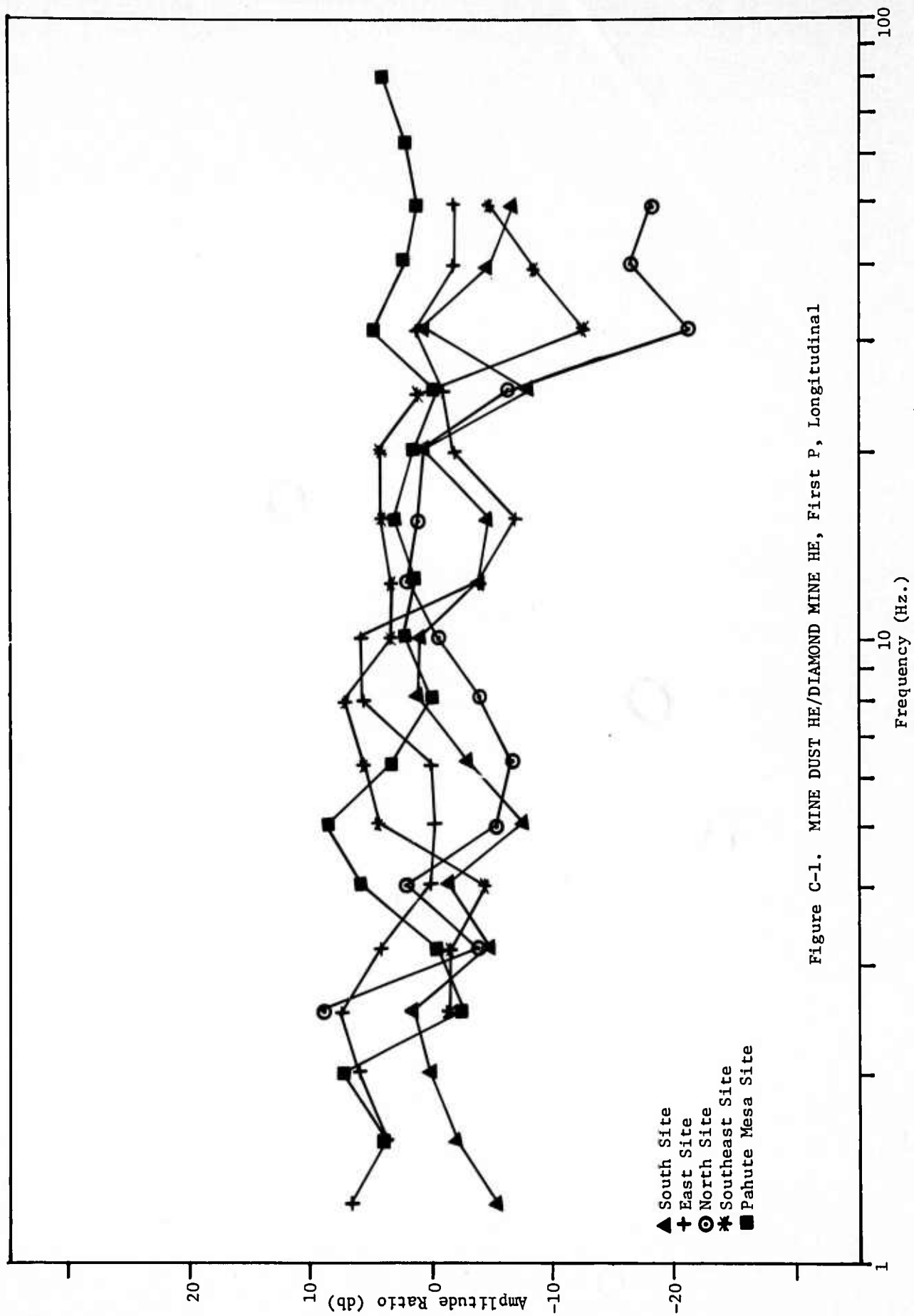


Figure C-1. MINE DUST HE/DIAMOND MINE HE, First P, Longitudinal

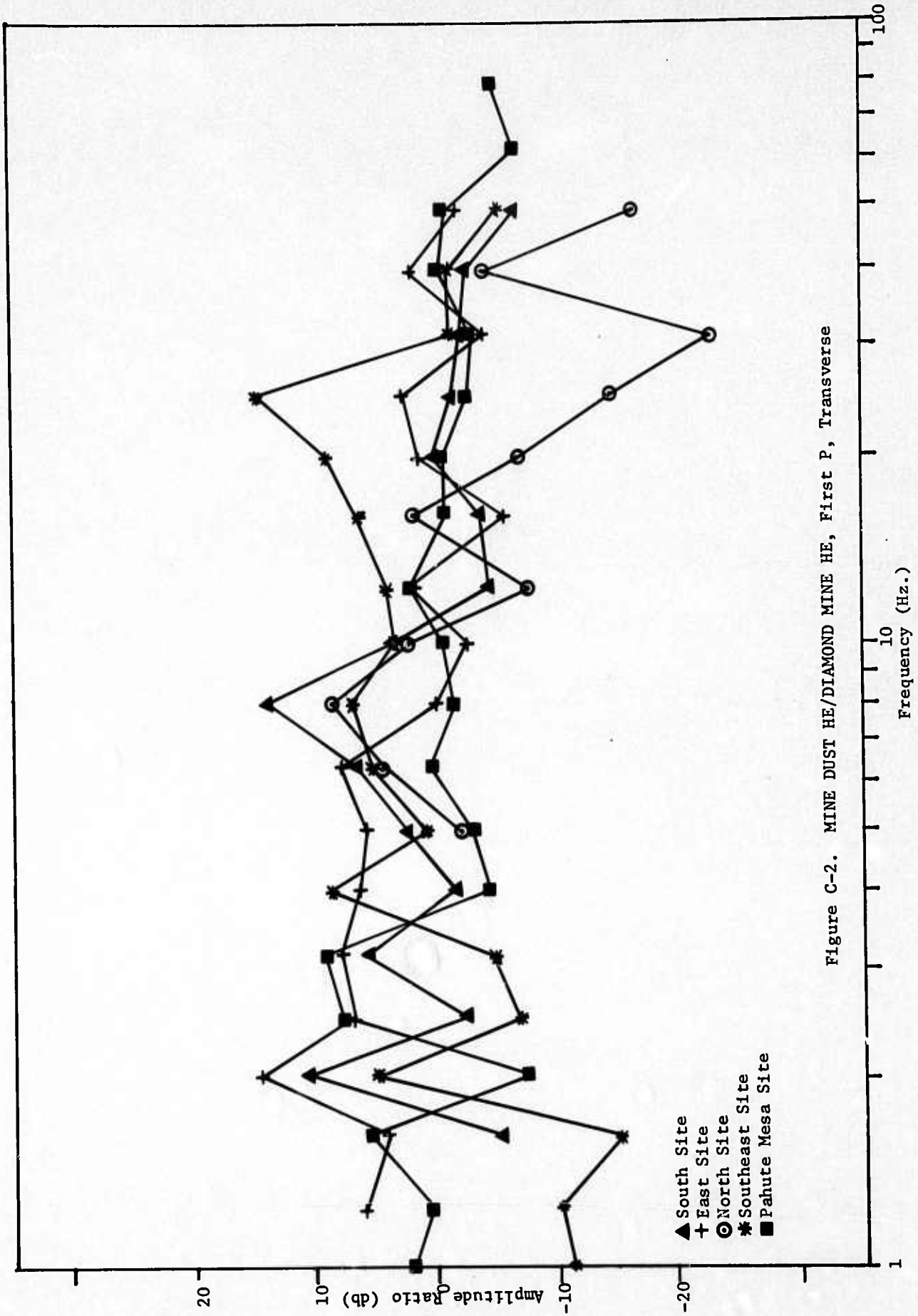


Figure C-2. MINE DUST HE/DIAMOND MINE HE, First P, Transverse

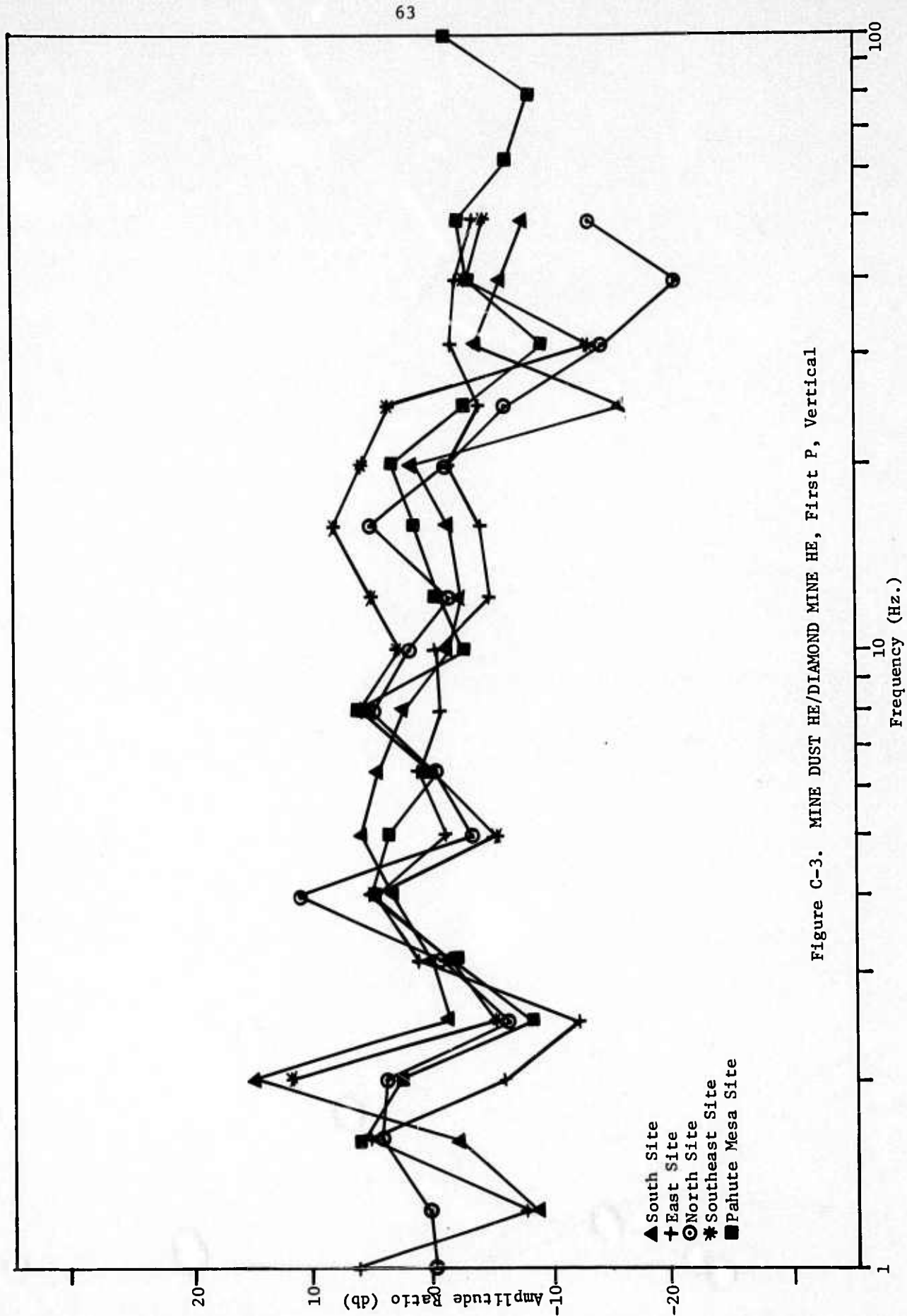


Figure C-3. MINE DUST HE/DIAMOND MINE HE, First P, Vertical

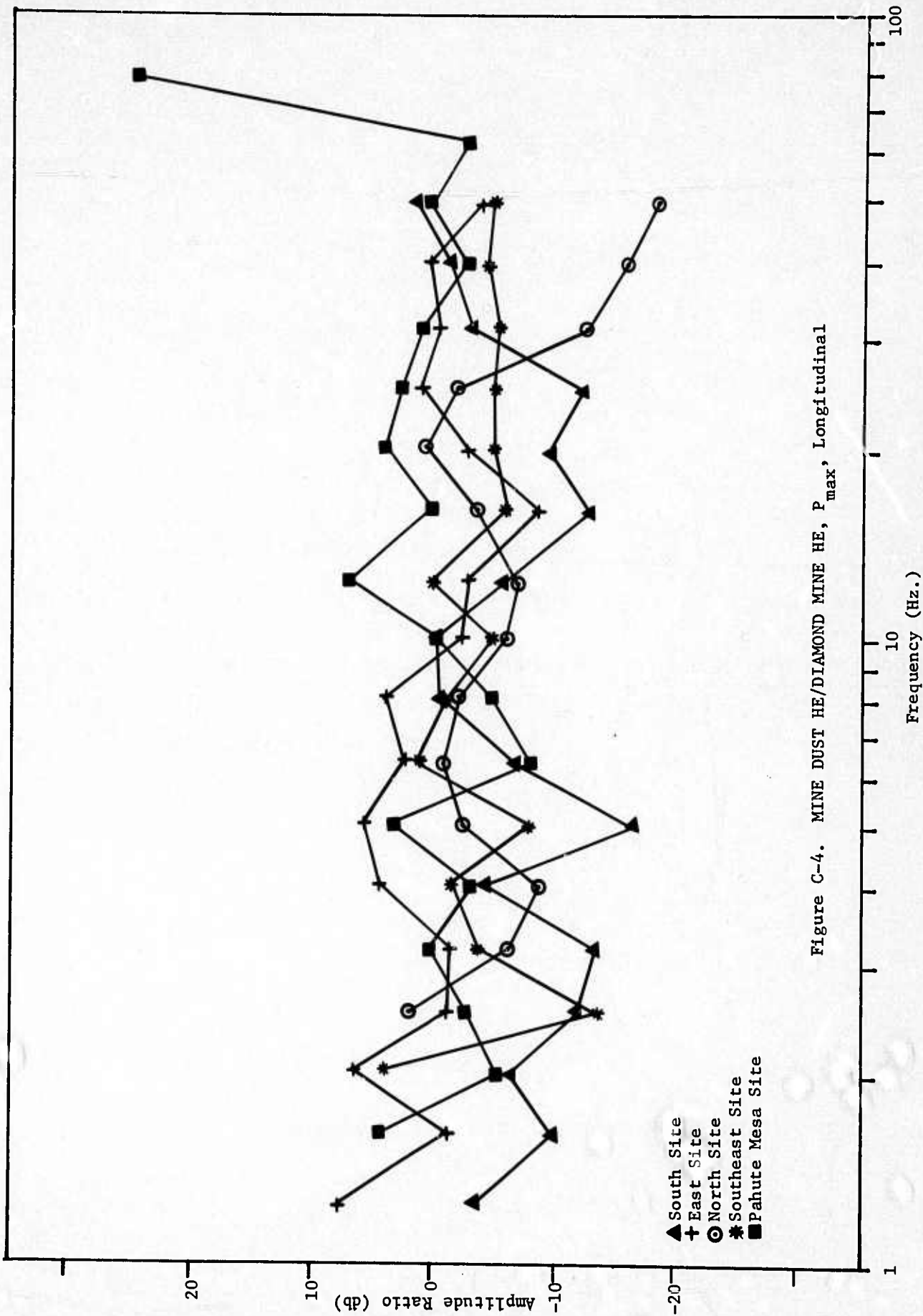


Figure C-4. MINE DUST HE/DIAMOND MINE HE, P<sub>max</sub>, Longitudinal

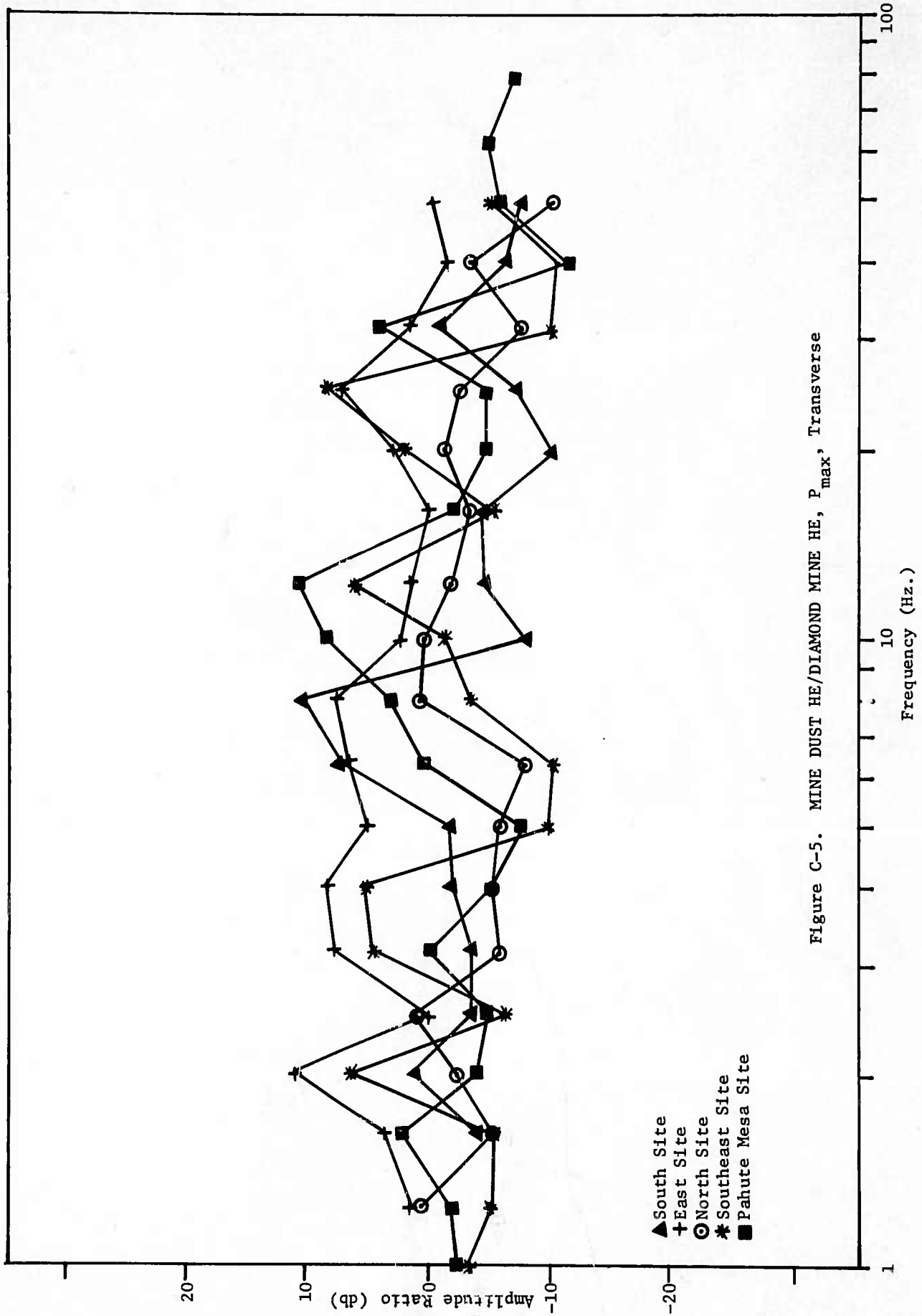


Figure C-5. MINE DUST HE/DIAMOND MINE HE, P<sub>max</sub>, Transverse

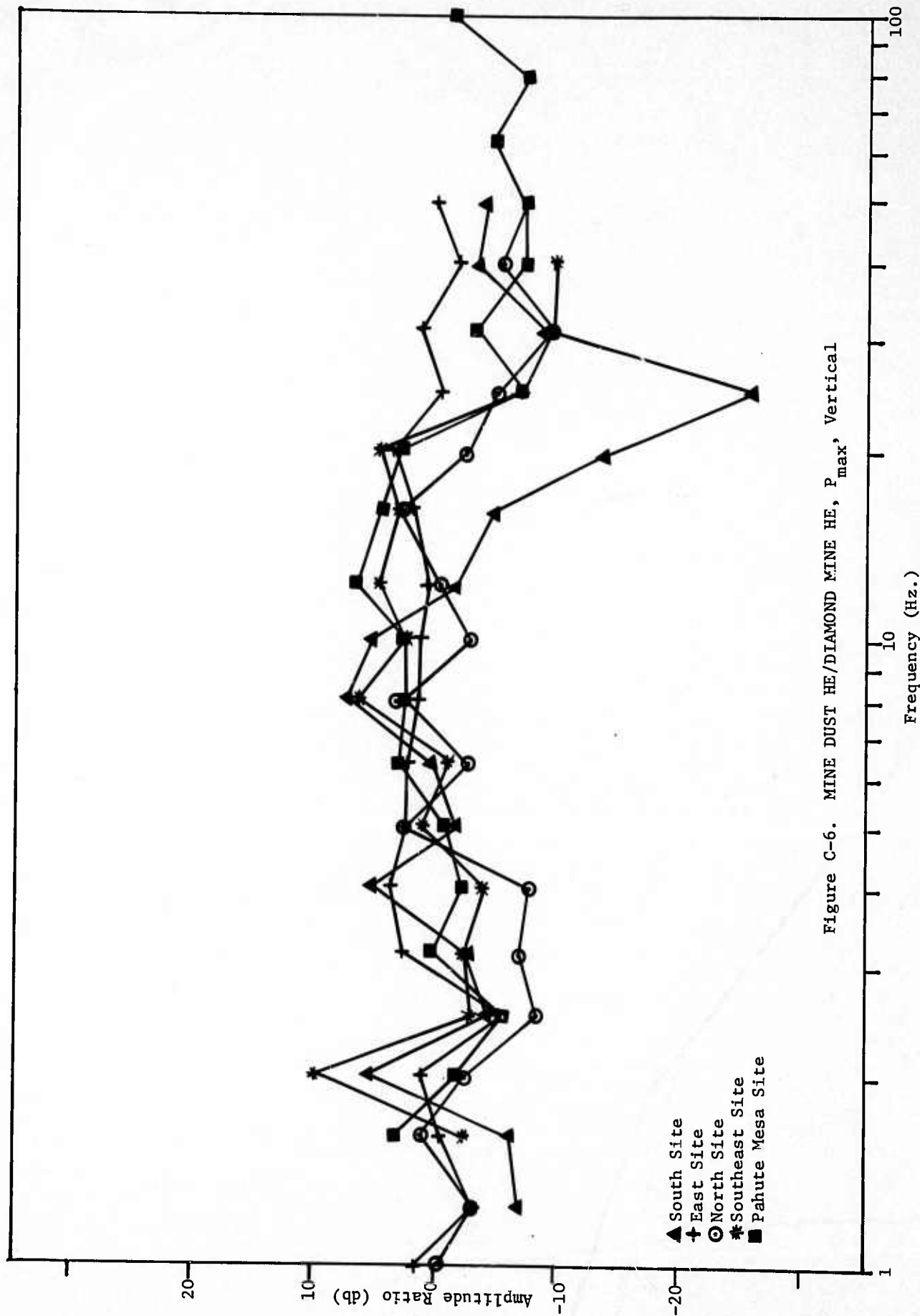


Figure C-6. MINE DUST HE/DIAMOND MINE HE, P<sub>max</sub>, Vertical

- ▲ South Site
- + East Site
- ⊙ North Site
- \* Southeast Site
- Pahute Mesa Site

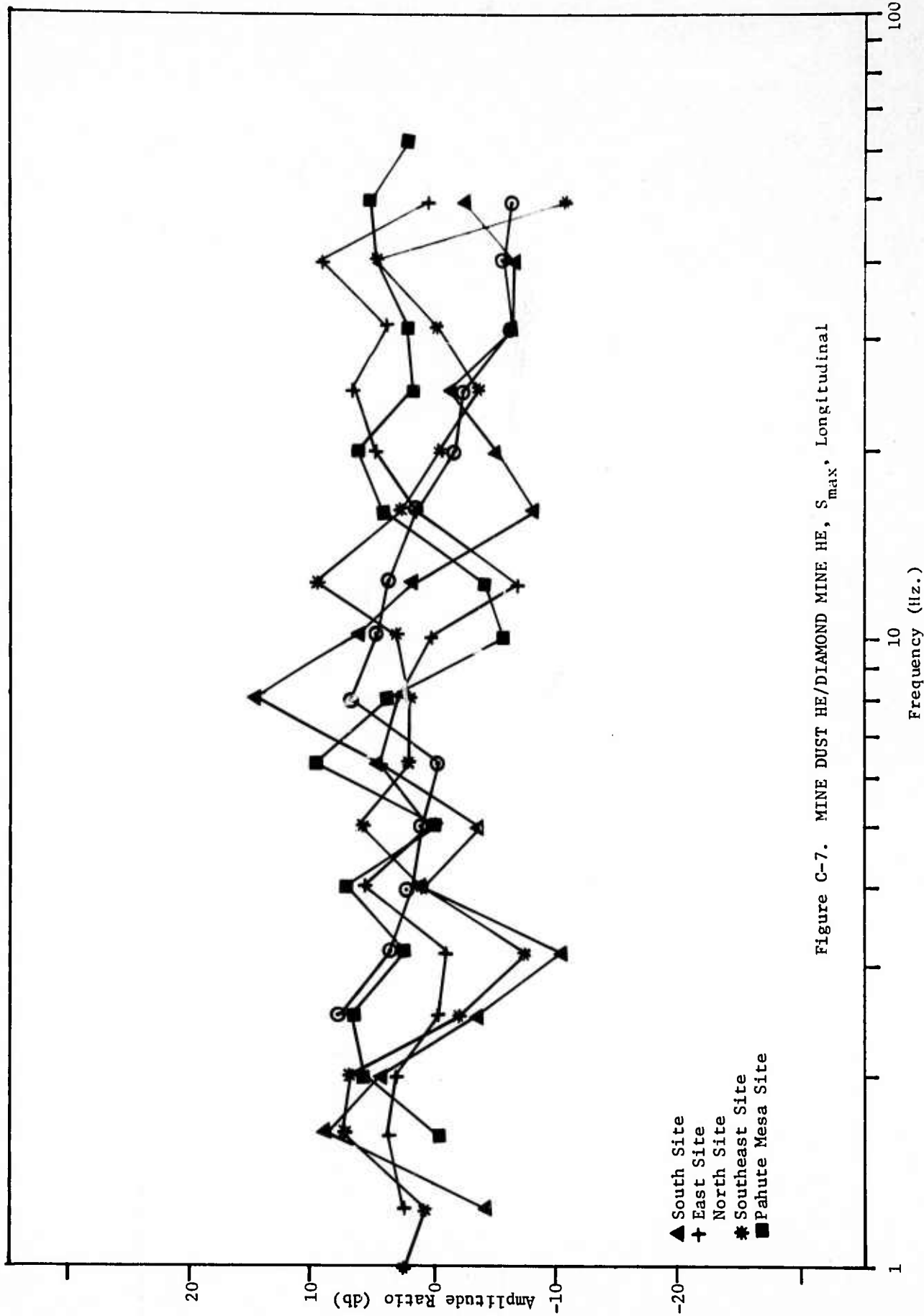


Figure C-7. MINE DUST HE/DIAMOND MINE HE, S<sub>max</sub>, Longitudinal

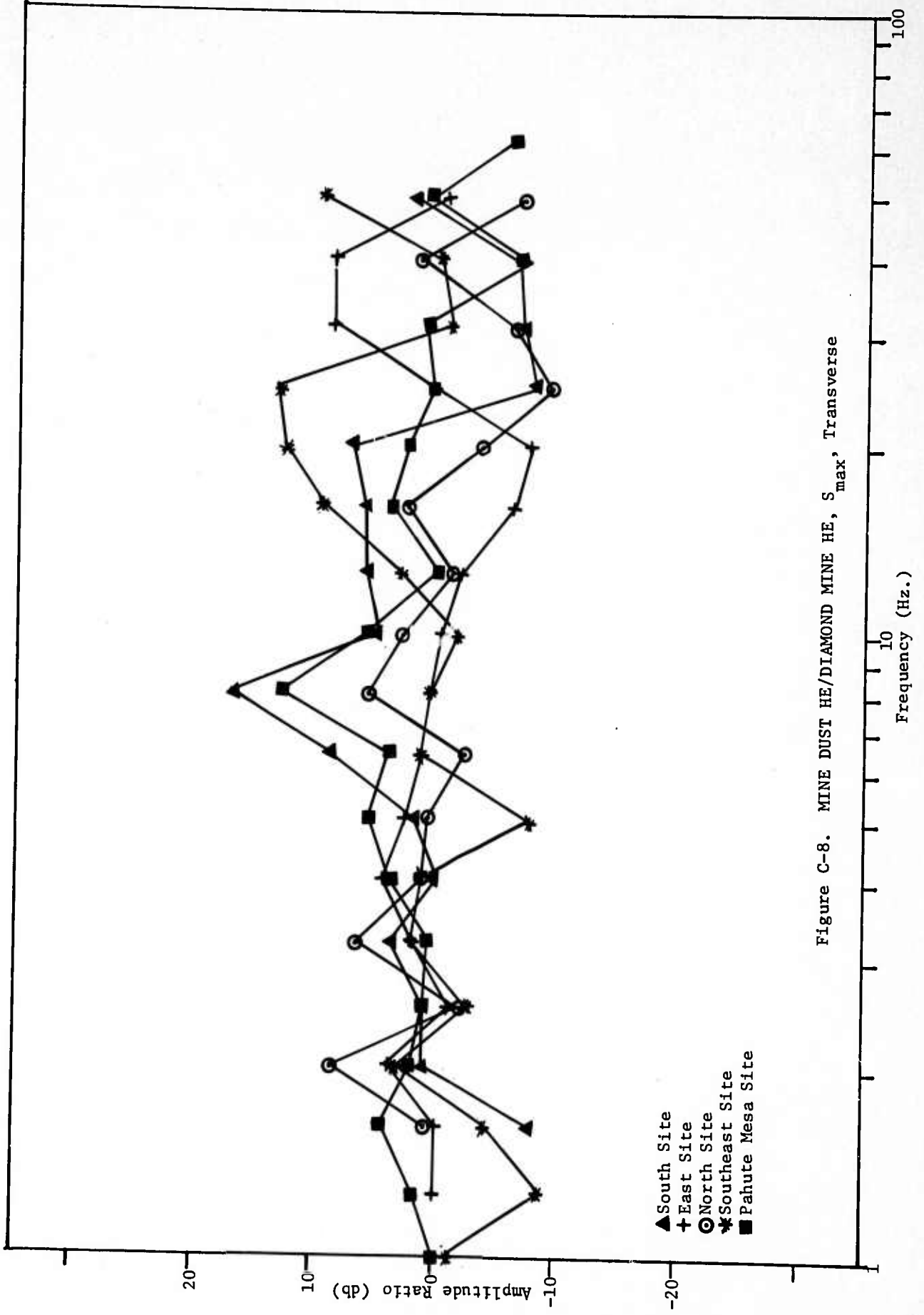


Figure C-8. MINE DUST HE/DIAMOND MINE HE,  $S_{max}$ , Transverse

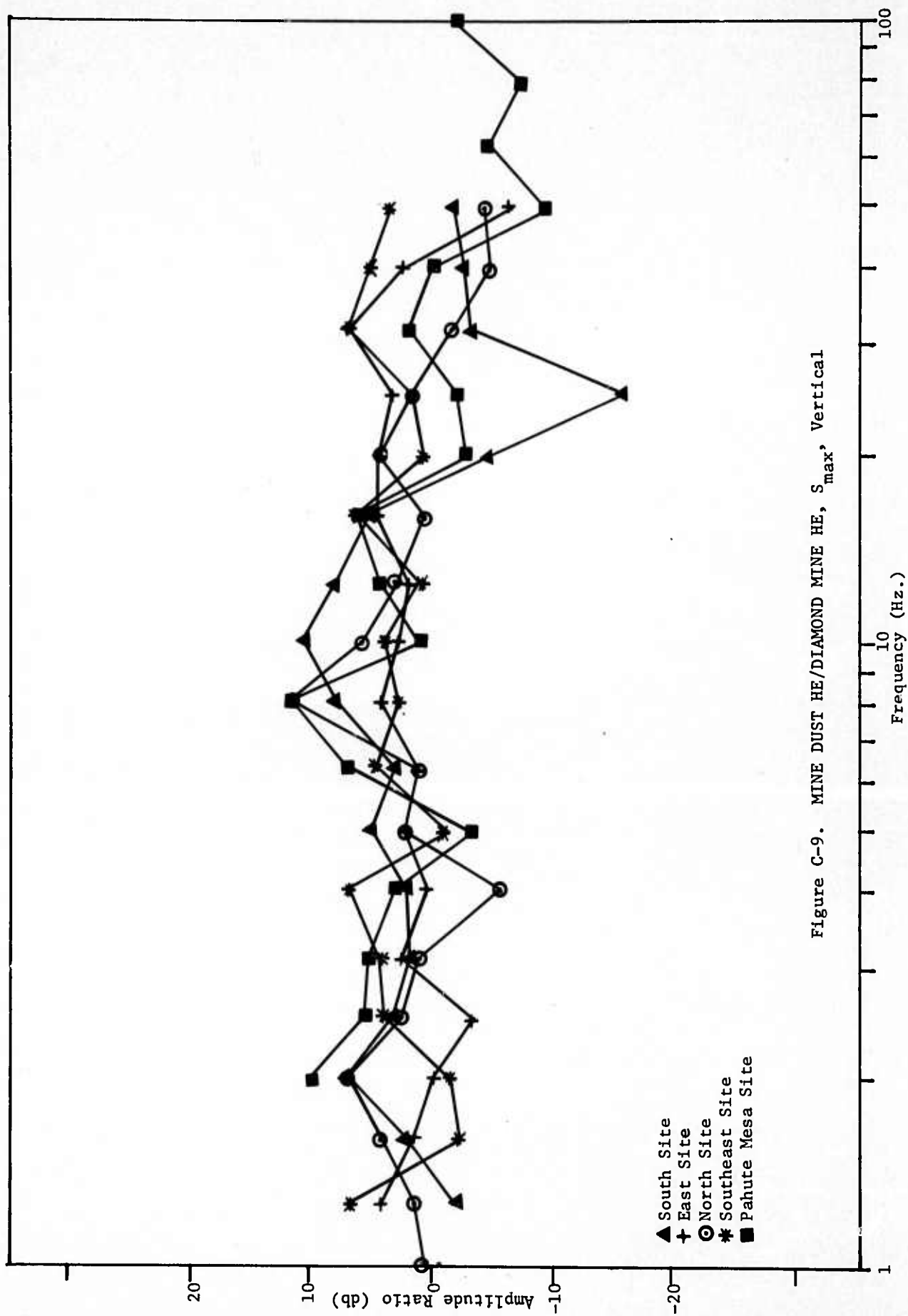


Figure C-9. MINE DUST HE/DIAMOND MINE HE, S<sub>max</sub>, Vertical

APPENDIX D

Spectral Ratios of DIAMOND MINE/DIAMOND DUST  
as a Function of Site and Wave Type

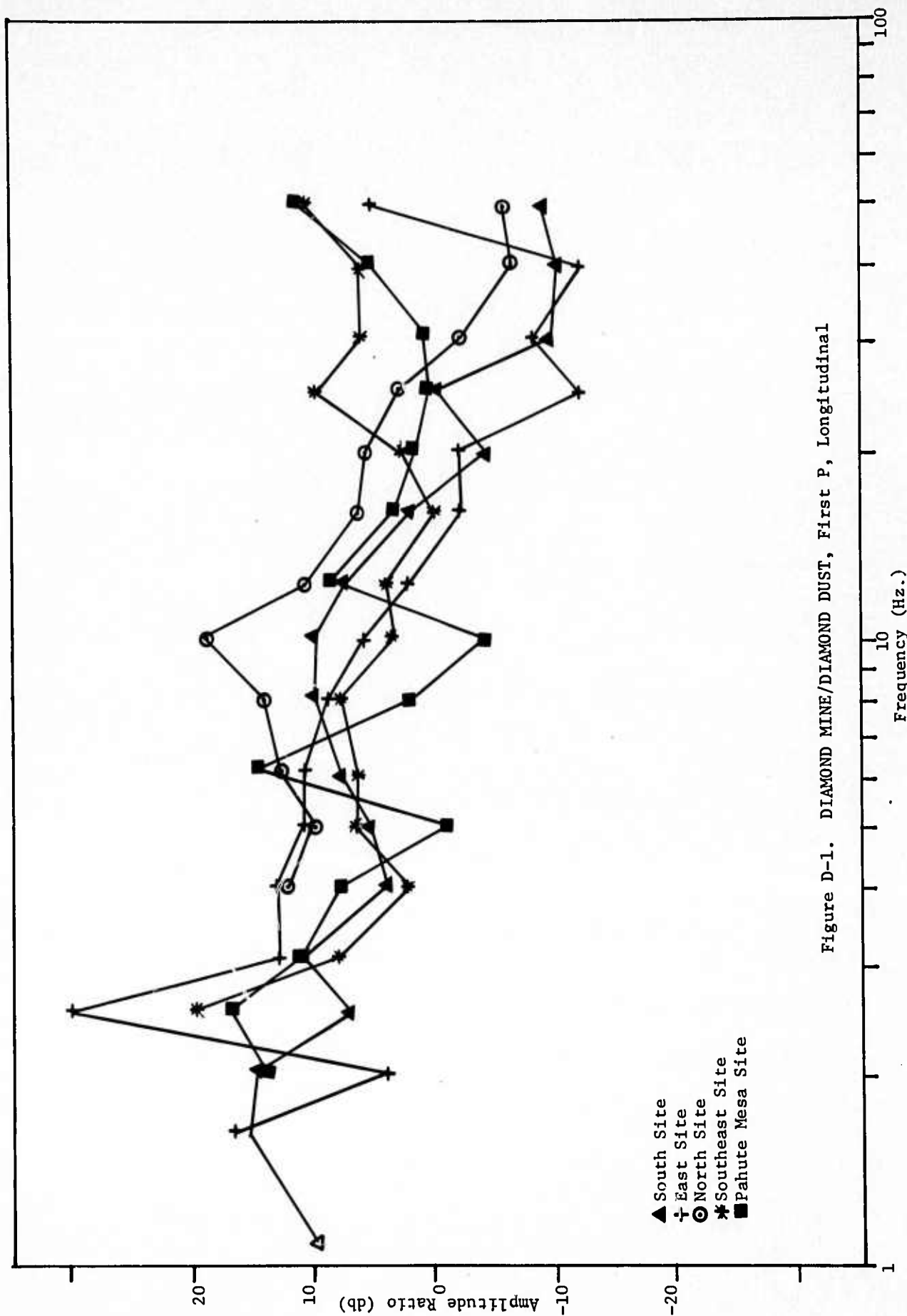


Figure D-1. DIAMOND MINE/DIAMOND DUST, First P, Longitudinal

- ▲ South Site
- + East Site
- ⊙ North Site
- \* Southeast Site
- Pahute Mesa Site

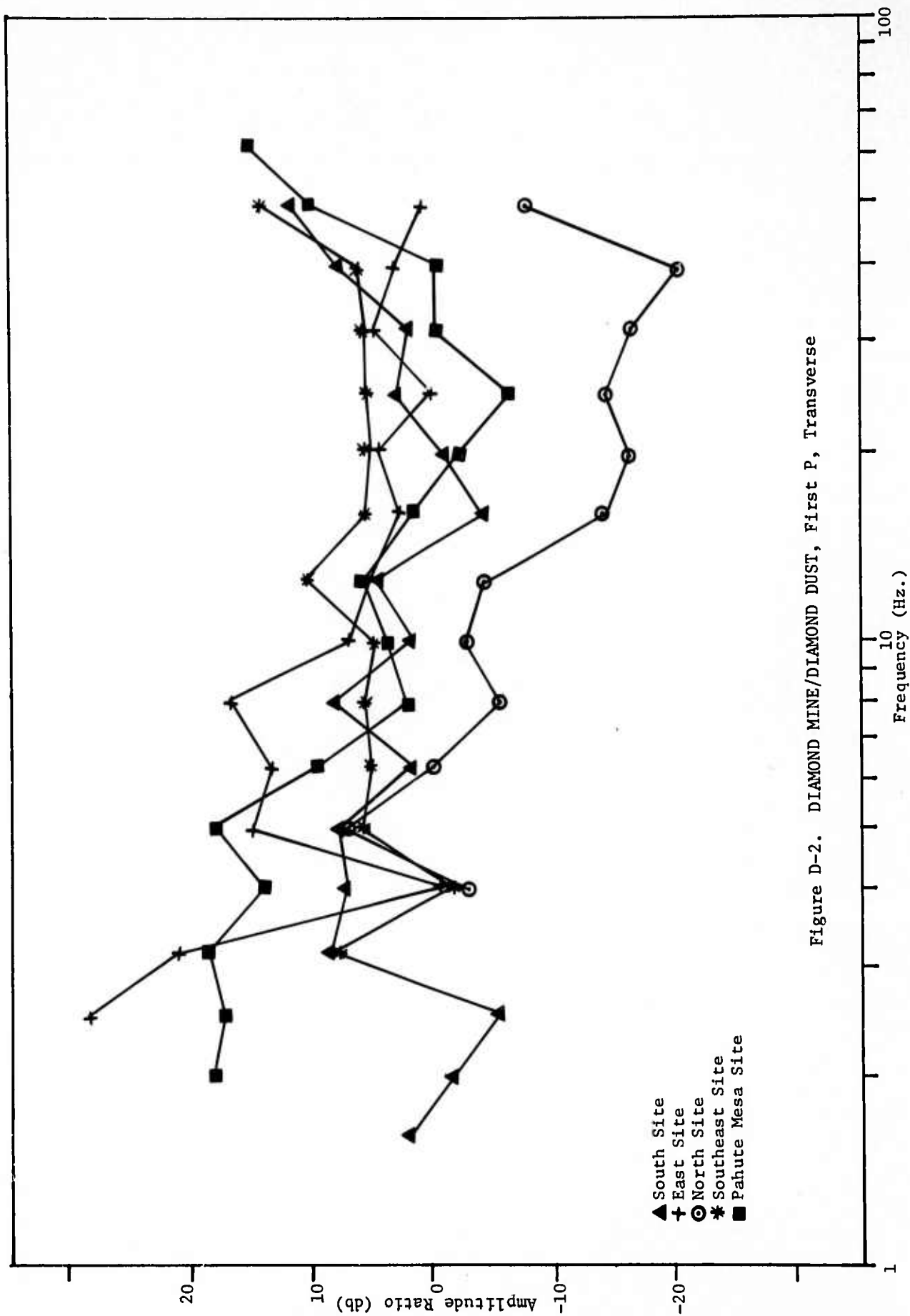


Figure D-2. DIAMOND MINE/DIAMOND DUST, First P, Transverse

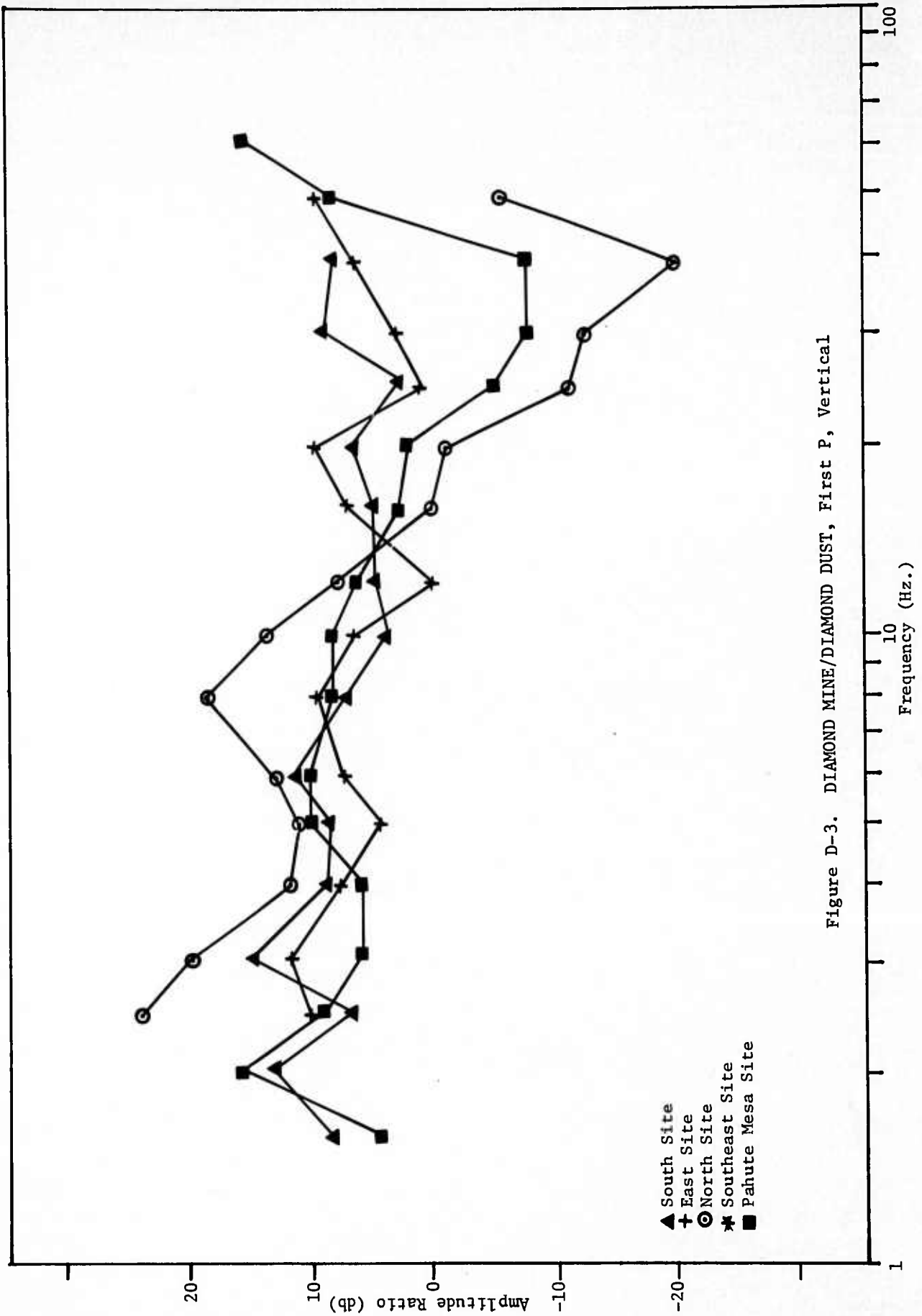


Figure D-3. DIAMOND MINE/DIAMOND DUST, First P, Vertical

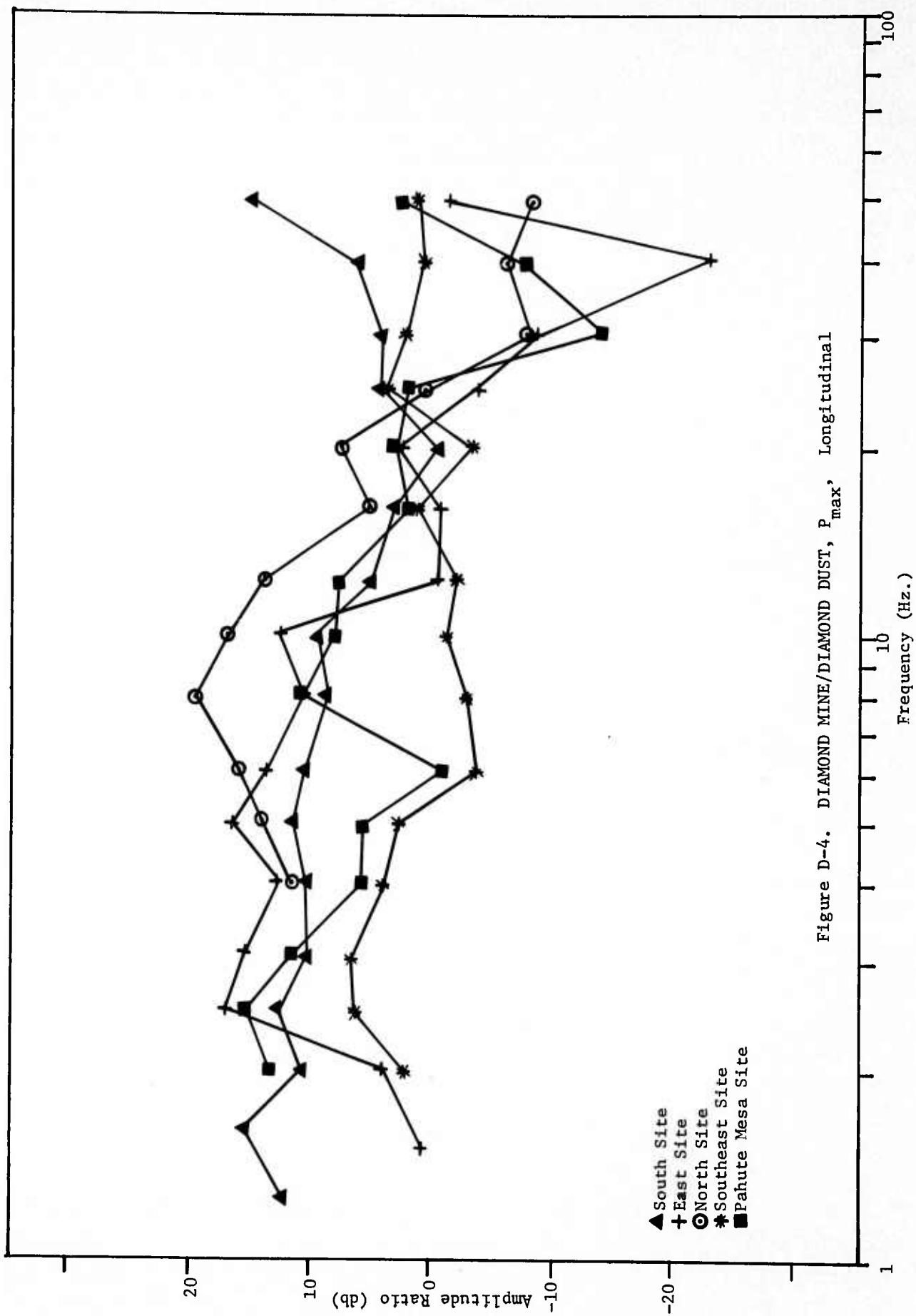


Figure D-4. DIAMOND MINE/DIAMOND DUST,  $P_{max}$ , Longitudinal

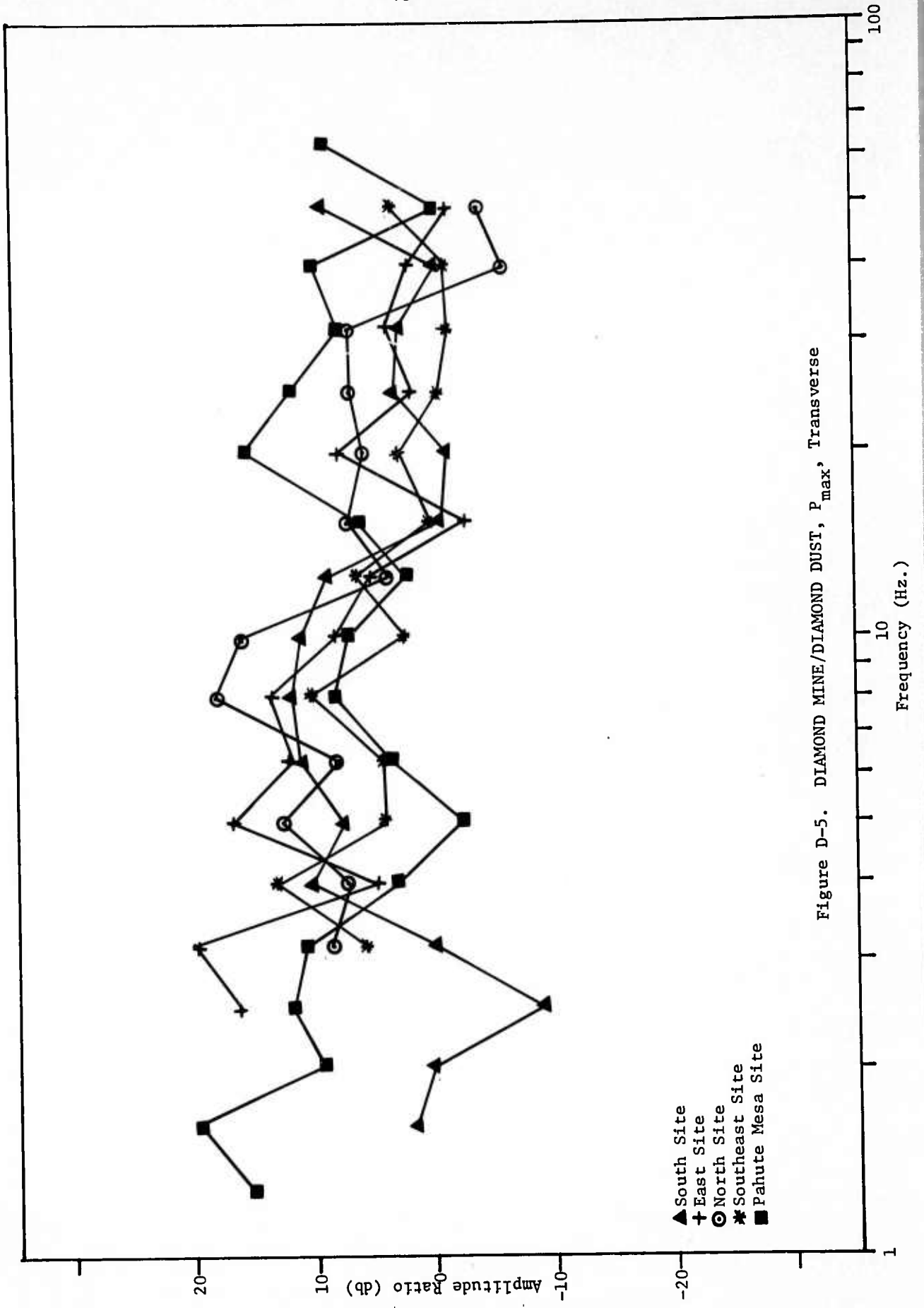


Figure D-5. DIAMOND MINE/DIAMOND DUST, P<sub>max</sub>, Transverse

- ▲ South Site
- + East Site
- ⊙ North Site
- \* Southeast Site
- Pahute Mesa Site

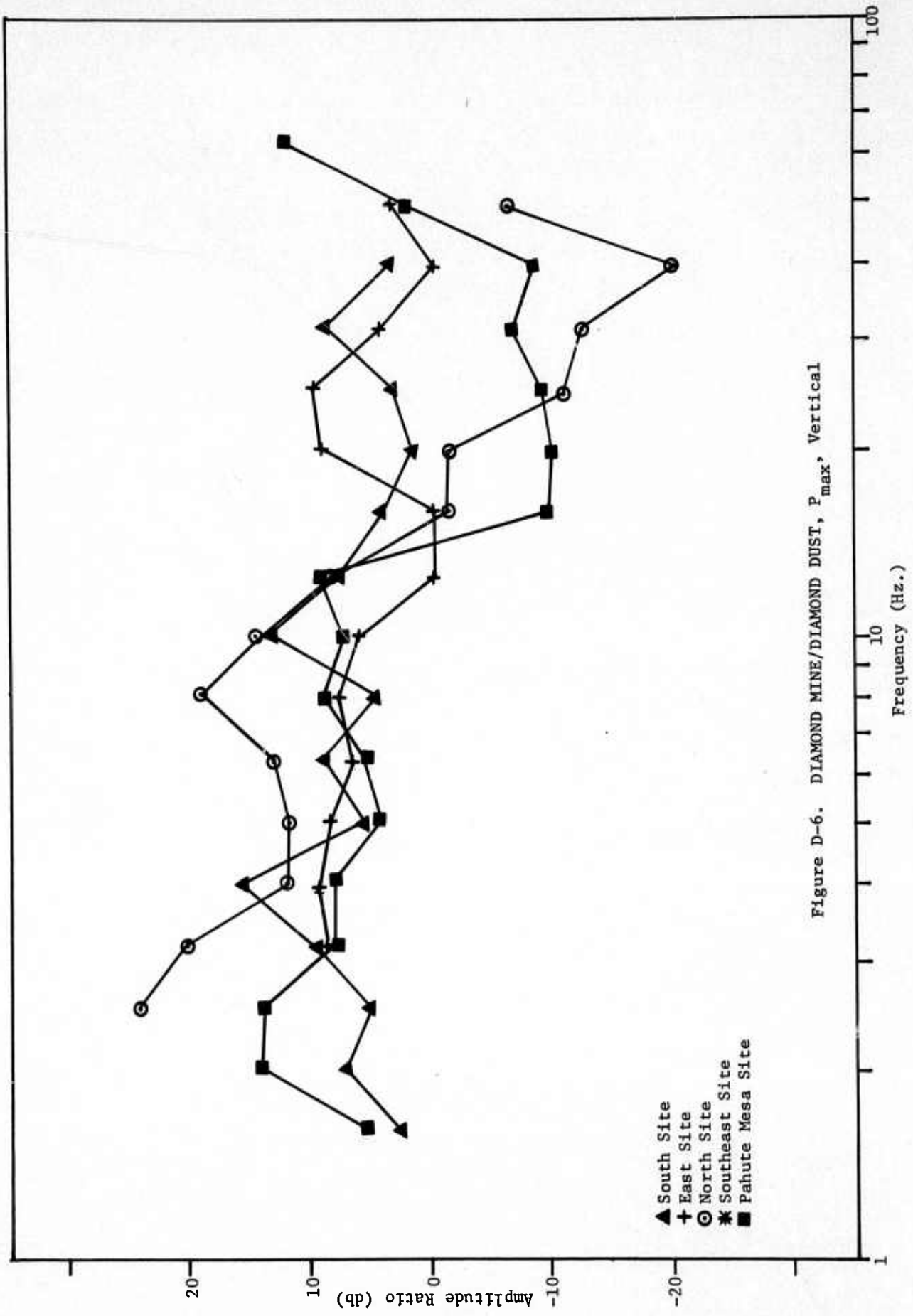


Figure D-6. DIAMOND MINE/DIAMOND DUST, P<sub>max</sub>, Vertical

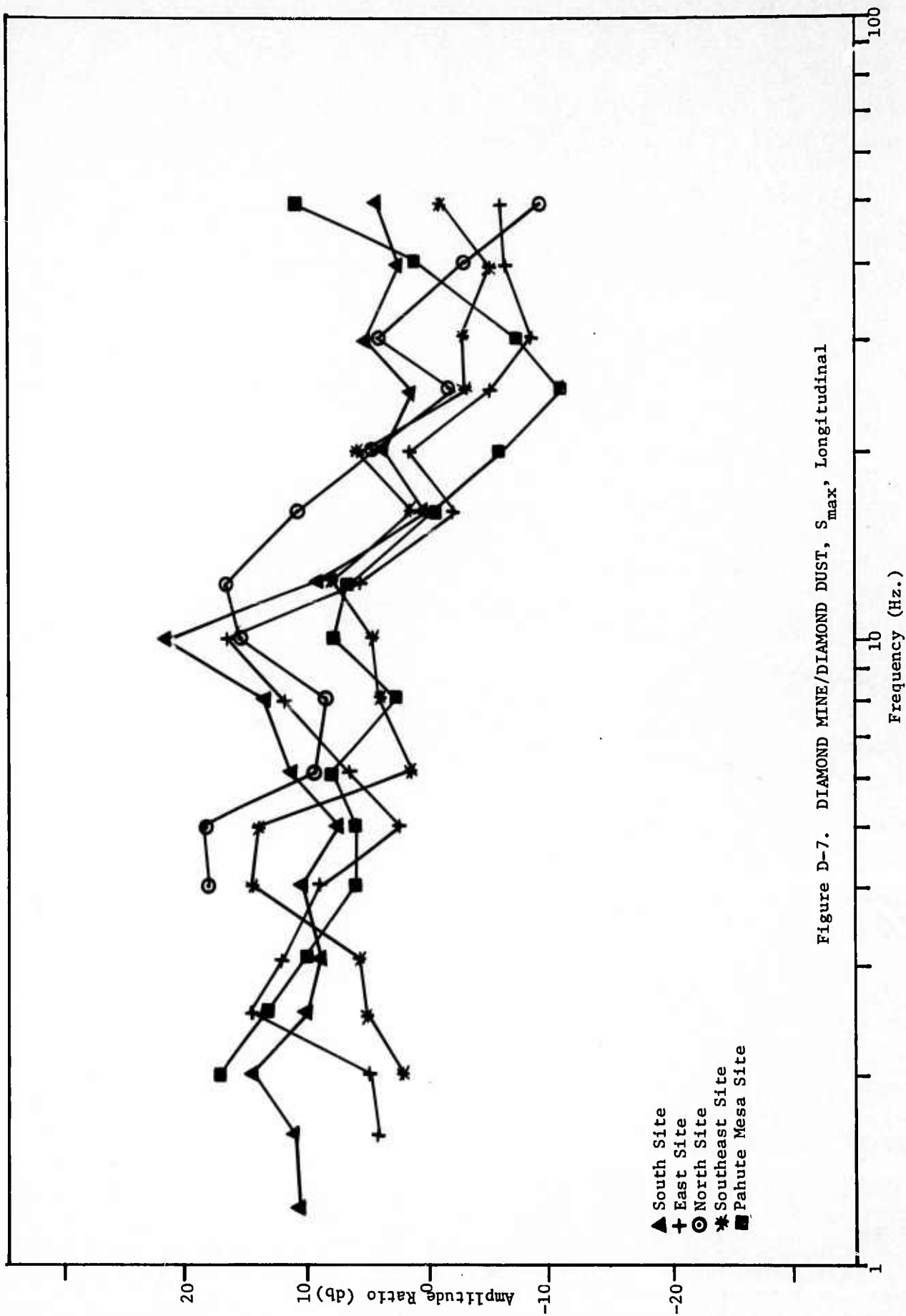


Figure D-7. DIAMOND MINE/DIAMOND DUST, S<sub>max</sub>, Longitudinal

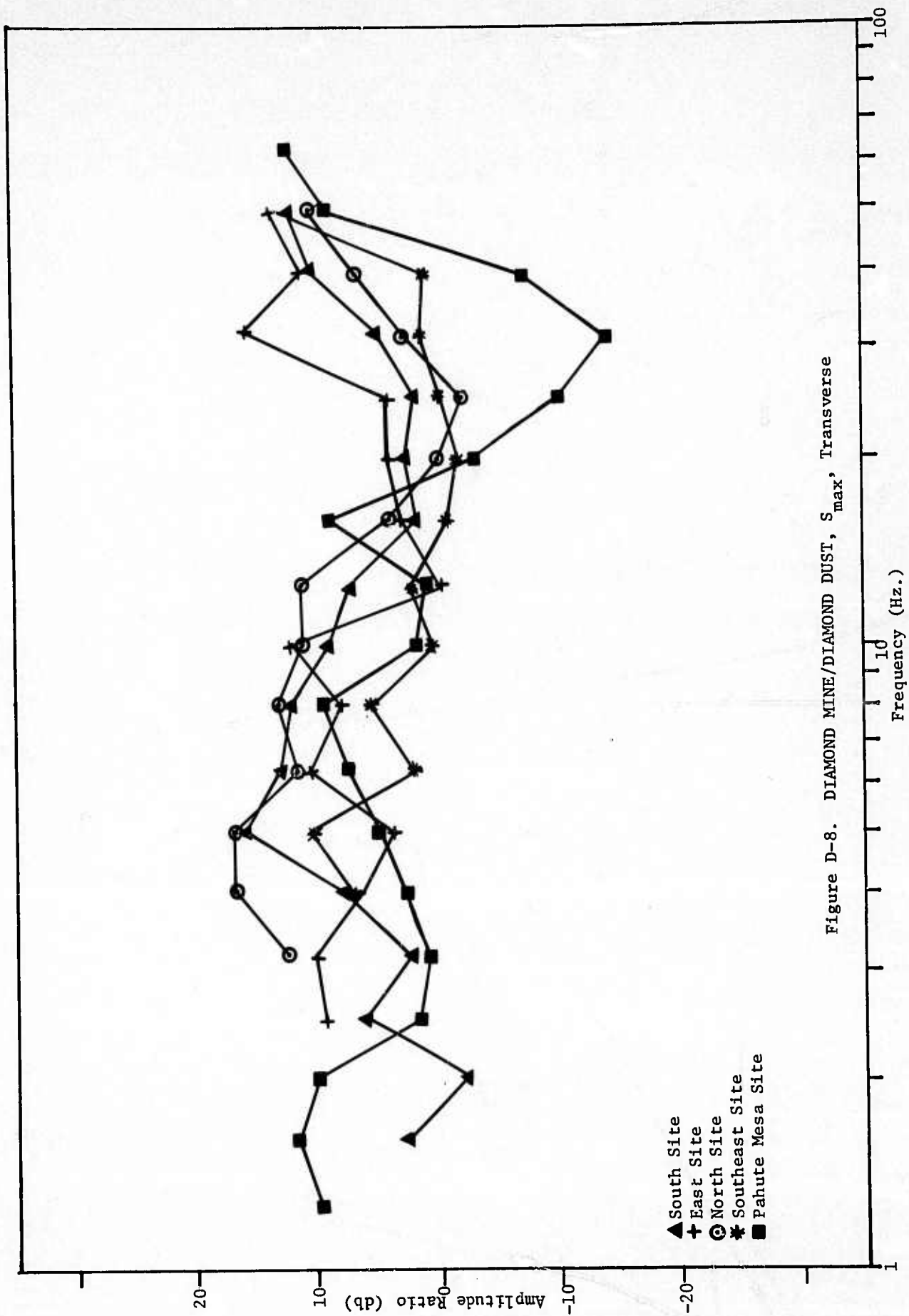


Figure D-8. DIAMOND MINE/DIAMOND DUST, S<sub>max</sub>, Transverse

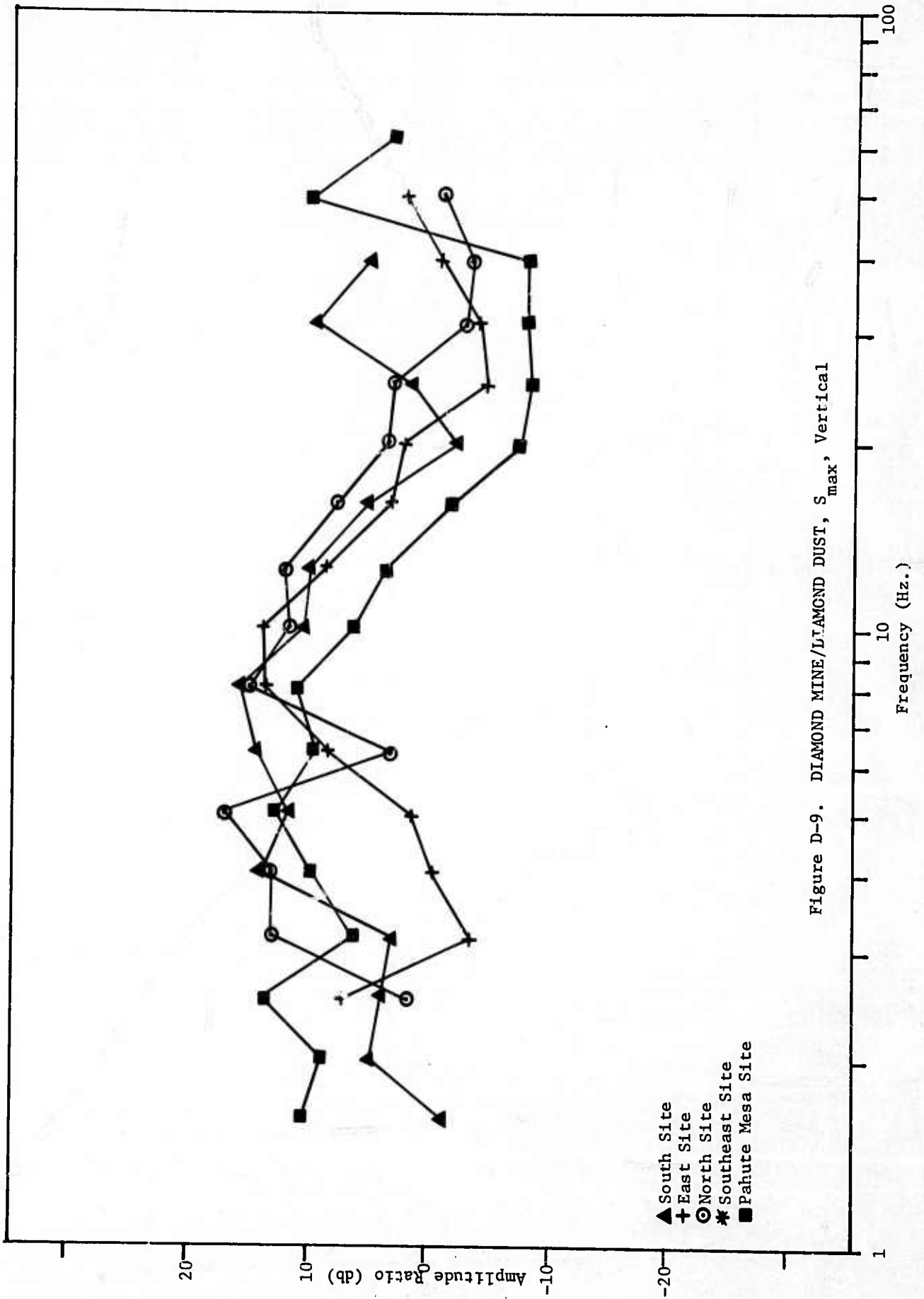


Figure D-9. DIAMOND MINE/LIAMDOND DUST, S<sub>max</sub>, Vertical

- ▲ South Site
- + East Site
- North Site
- \* Southeast Site
- Pahute Mesa Site

APPENDIX E

FORTRAN-SABR Program for Body Wave  
Energy Calculations

```

1,50L
001 C.....PROGRAM NAME: E3718, DATE 6/19/72
002 C.....PARTICLE ENERGY PROGRAM.
003 C.....USFS DATA TAPE #2, 8 CH. MULTIPLEXED.
004     COMMON IDBUF,IBUF,IDX
005     DIMENSION IDBUF(5),IBUF(1024,2),IDX(9),A(3,8),T(8),T0(8),
006     IE(8),EF(8),SHIFT(8)
007     CALL IOPEN('PTR',0)
008 S     STA             /LOAD -1
009     PAUSE
010 S     CLA             /CLAER THE ACC.
011 1     DO 3 I=1,3
012 3     READ(4,100)IDX(I),(A(I,J),J=1,8)
013     READ(4,101)T0,TS,WW
014     DO 4 I=1,8
015 4     FE(I)=0.0
016     DELTA=8./5000.
017 C.....START LOOP FOR THREE COMPONENTS: VERT. LONG. & TRANS.
018     DO 70 IDN=1,3
019     WRITE(1,102)IDX(IDN)
020     READ(4,104)SHIFT
021 C.....ZERO E(8) AND INITIALIZE T(J)S
022     ISKIP=(TS-T0(8))*625./256.
023     II=ISKIP+2
024     DIF=FLOAT(ISKIP)*DELTA
025     DO 5 I=1,8
026     T(I)=T0(I)+DIF
027 5     E(I)=0.0
028     CALL BUFIL(IDN,II)
029 C.....READ IN FIRST RECORD NEEDED
030 C.....START TRANSFORMING OF IBUF
031 10    DO 50 ISUB=1,2
032     DO 50 I=1,128
033     DO 25 J=1,8
034 C.....CHECK IF OUTSIDE WINDOW WIDTH, IF SO C=0.0
035     TT=T(J)+.00005
036     IF(TT-TS)25,14,14
037 14    IF(TT-TS-WW)17,17,25
038 C.....FORM PARTIAL SUMMATION FOR EACH OF 8 PARTS
039 17    II=8*(I-1)+J
040     X=IBUF(II,ISUB)
041     X=X-SHIFT(J)
042     E(J)=E(J)+(X*X)/T(J)
043 25    CONTINUE
044     TT=T(I)+.00005
045     IF(TT-TS-WW)40,40,30
046 C.....FORM PARTIAL SUM OF EE
047 30    DO 35 L=1,8
048     X=A(IDN,L)
049     E(L)=E(L)*X*X
050 35    EE(L)=EE(L)+E(L)

```

```

50, /L
050 35 FE(L)=EF(L)+E(L)
051 WRITE(1,103)E
052 GO TO 70
053 40 DO 45 L=1,8
054 C.....UPDATE TIME COUNTERS
055 45 T(L)=T(L)+DELTA
056 50 CONTINUE
057 C.....REFILL IBUF WITH NEXT RECORD
058 CALL BUFIL(0,ISKIP)
059 GO TO 10
060 70 CONTINUE
061 WRITE(1,103)EE
062 C.....START ALL OVER AGAIN
063 C.....AND DO ANOTHER ID
064 GO TO 1
065 100 FORMAT(14,8F10.8)
066 101 FORMAT(9E12.8,F5.0)
067 102 FORMAT(/'ID # ',14/)
068 103 FORMAT(4E16.8/)
069 104 FORMAT(8E16.8)
070 END

```

APPENDIX F

Energy Program Results as a Function  
of Site and Event

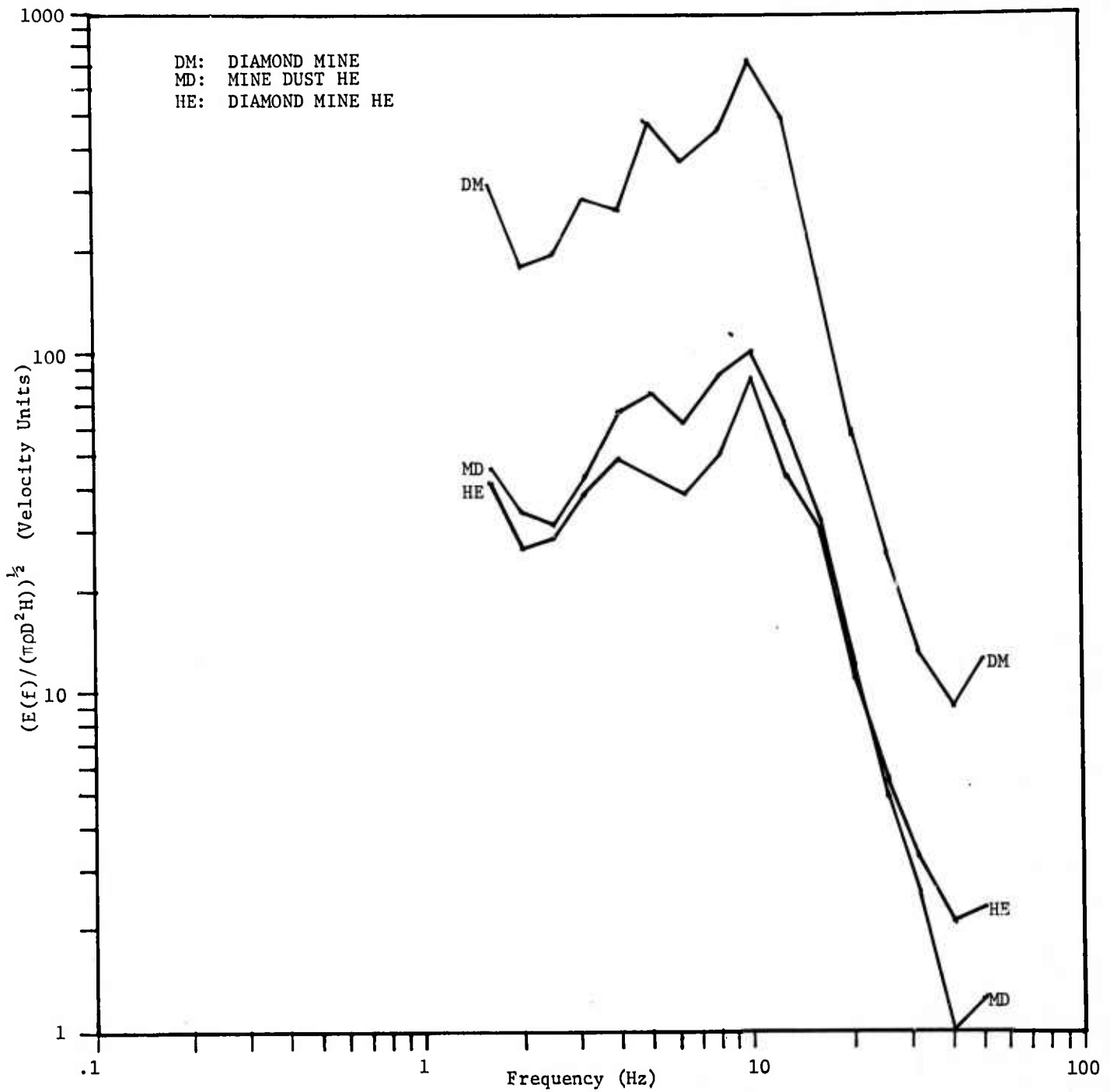


Figure F-1. Energy program output for the data recorded at the North site

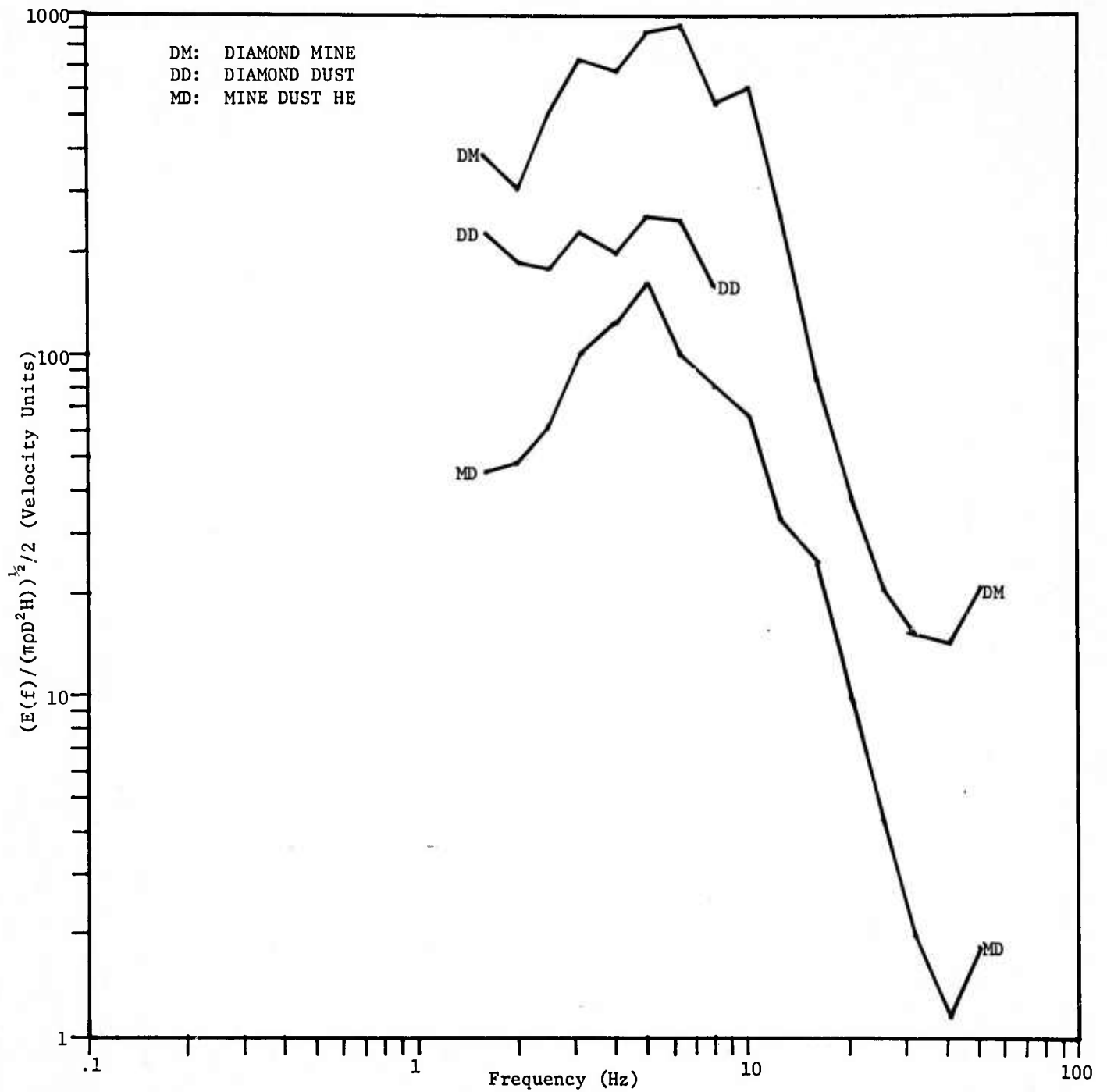


Figure F-2. Energy program output for the data recorded at the East site

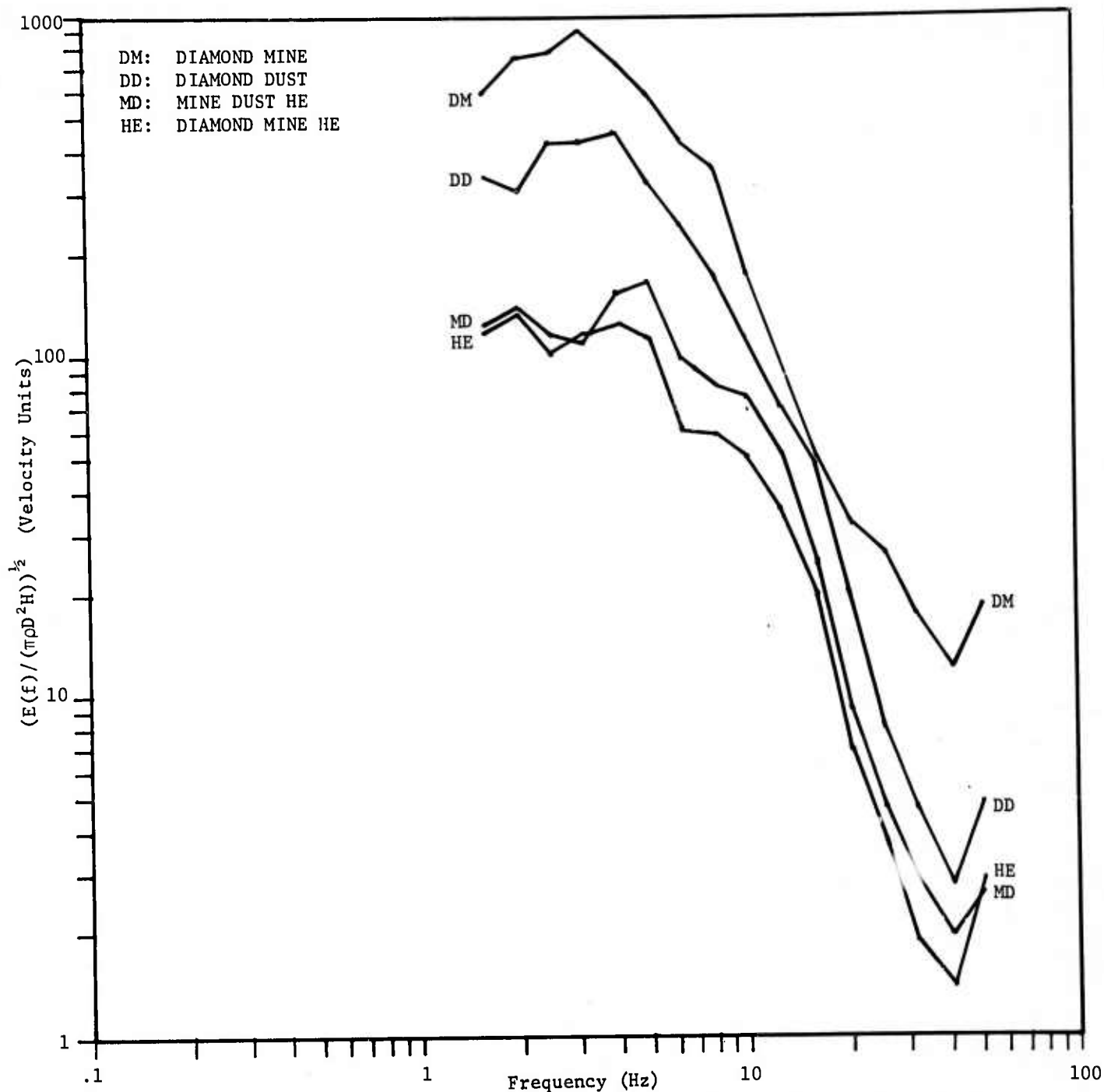


Figure F-3. Energy program output for the data recorded at the Southeast site

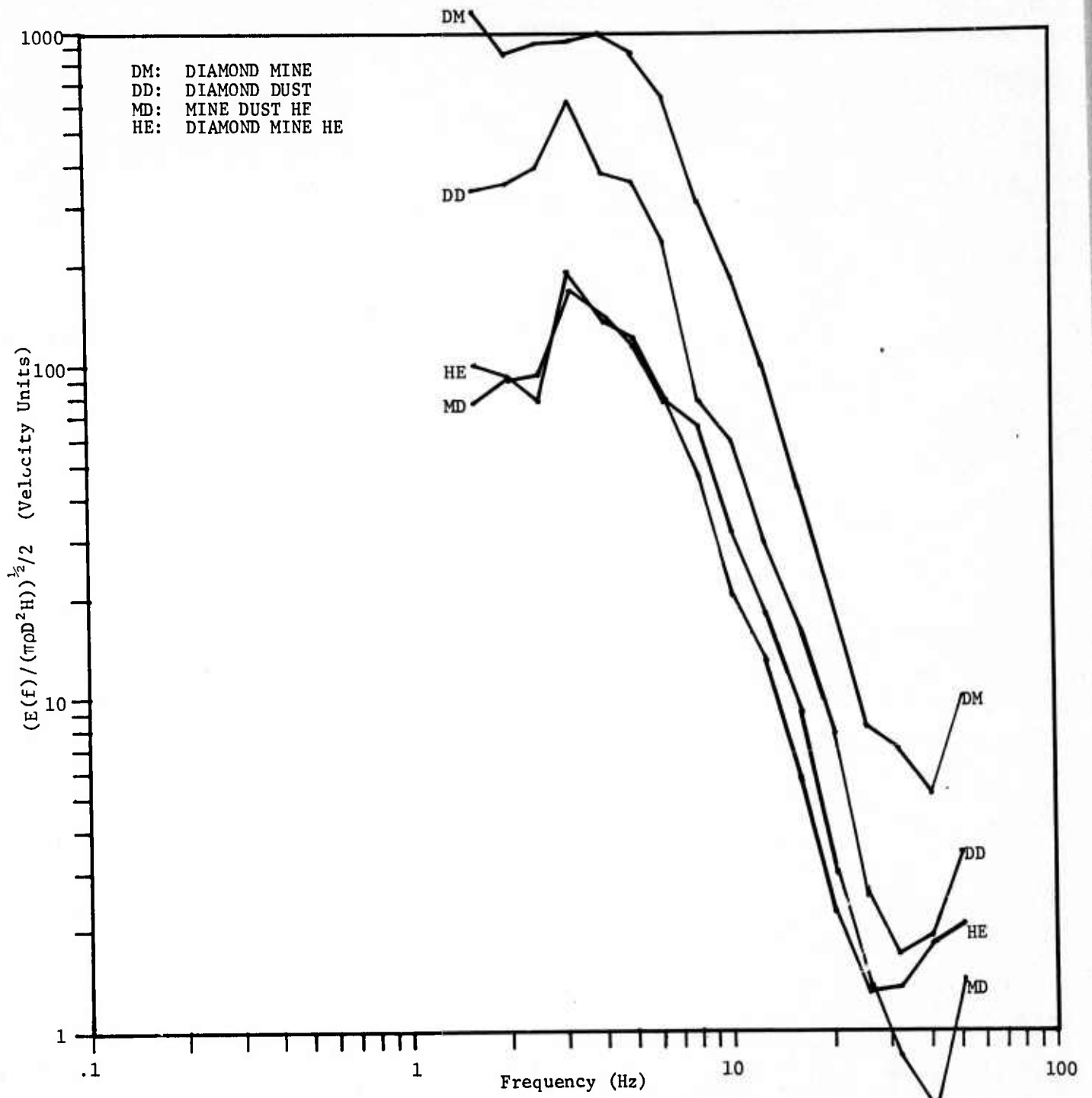


Figure F-4. Energy program output for the data recorded at the South site

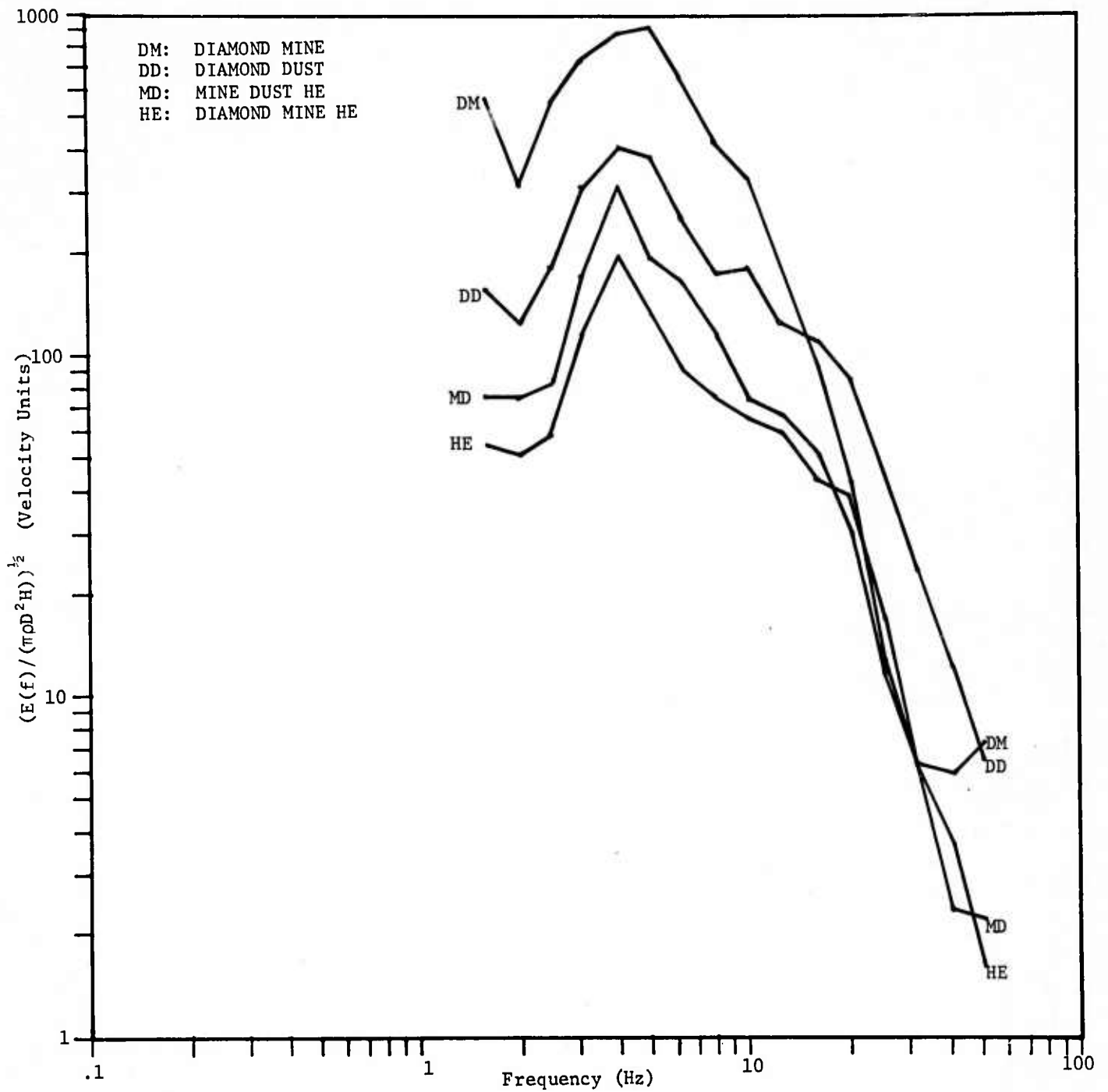


Figure F-5. Energy program output for the data recorded at the Pahute Mesa Site

APPENDIX G  
Energy Spectrum Ratios

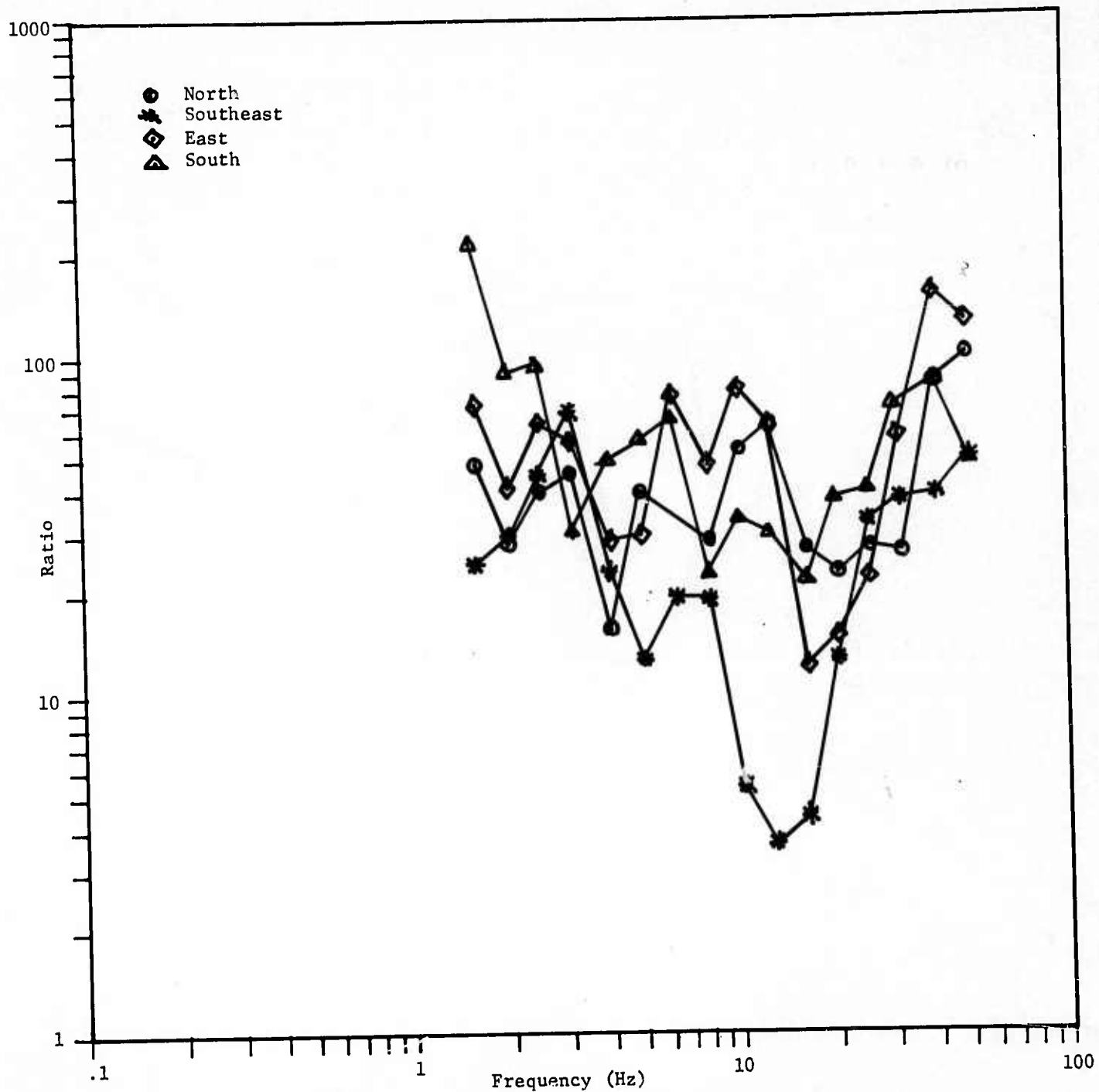


Figure G-1. DIAMOND MINE/MINE DUST HE energy Spectrum ratios

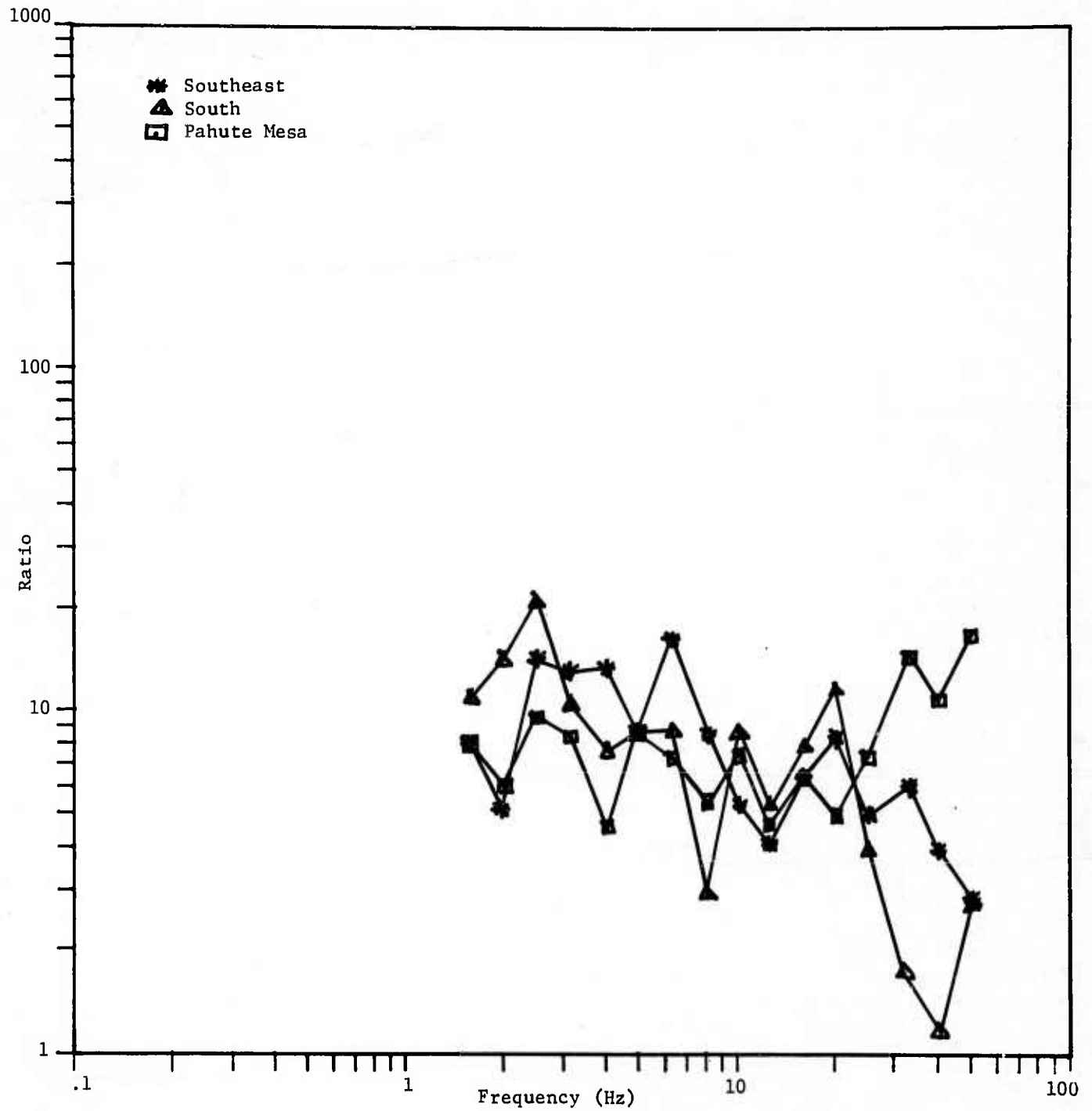


Figure G-2. DIAMOND DUST/DIAMOND MINE HE energy spectrum ratios

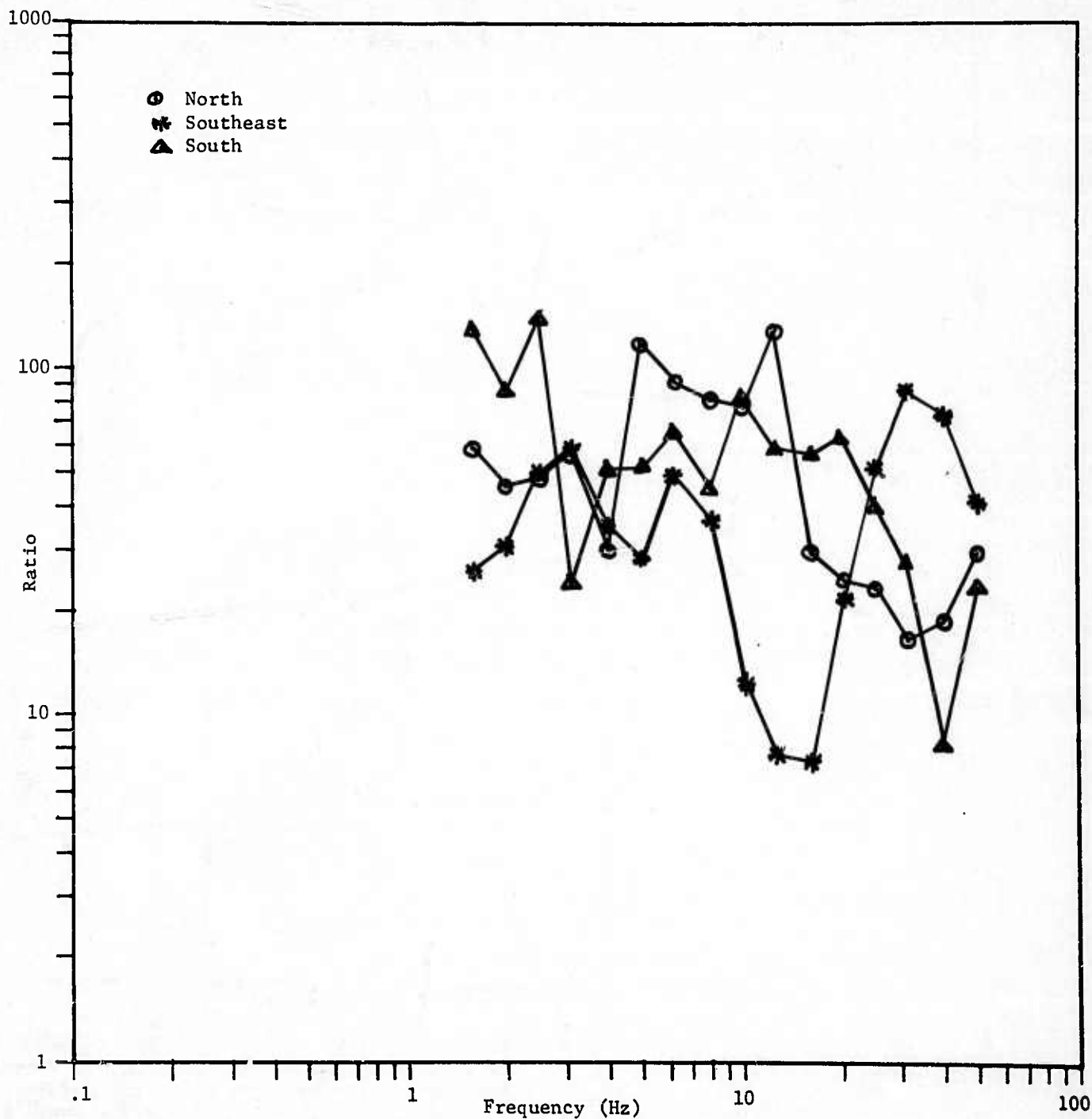


Figure G-3. DIAMOND MINE/DIAMOND MINE HE energy spectrum ratios

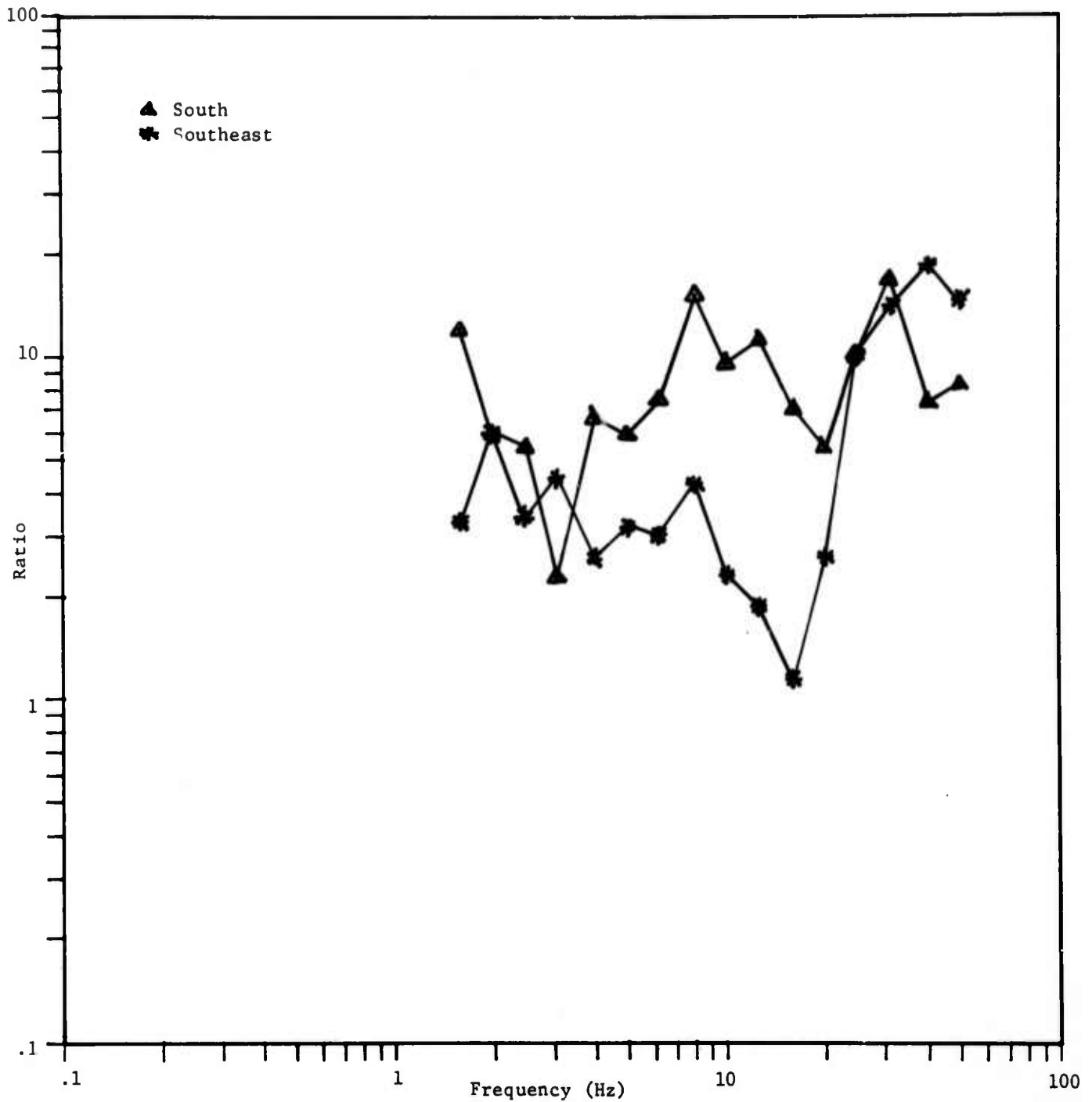


Figure G-4. DIAMOND MINE/DIAMOND DUST energy spectrum ratios

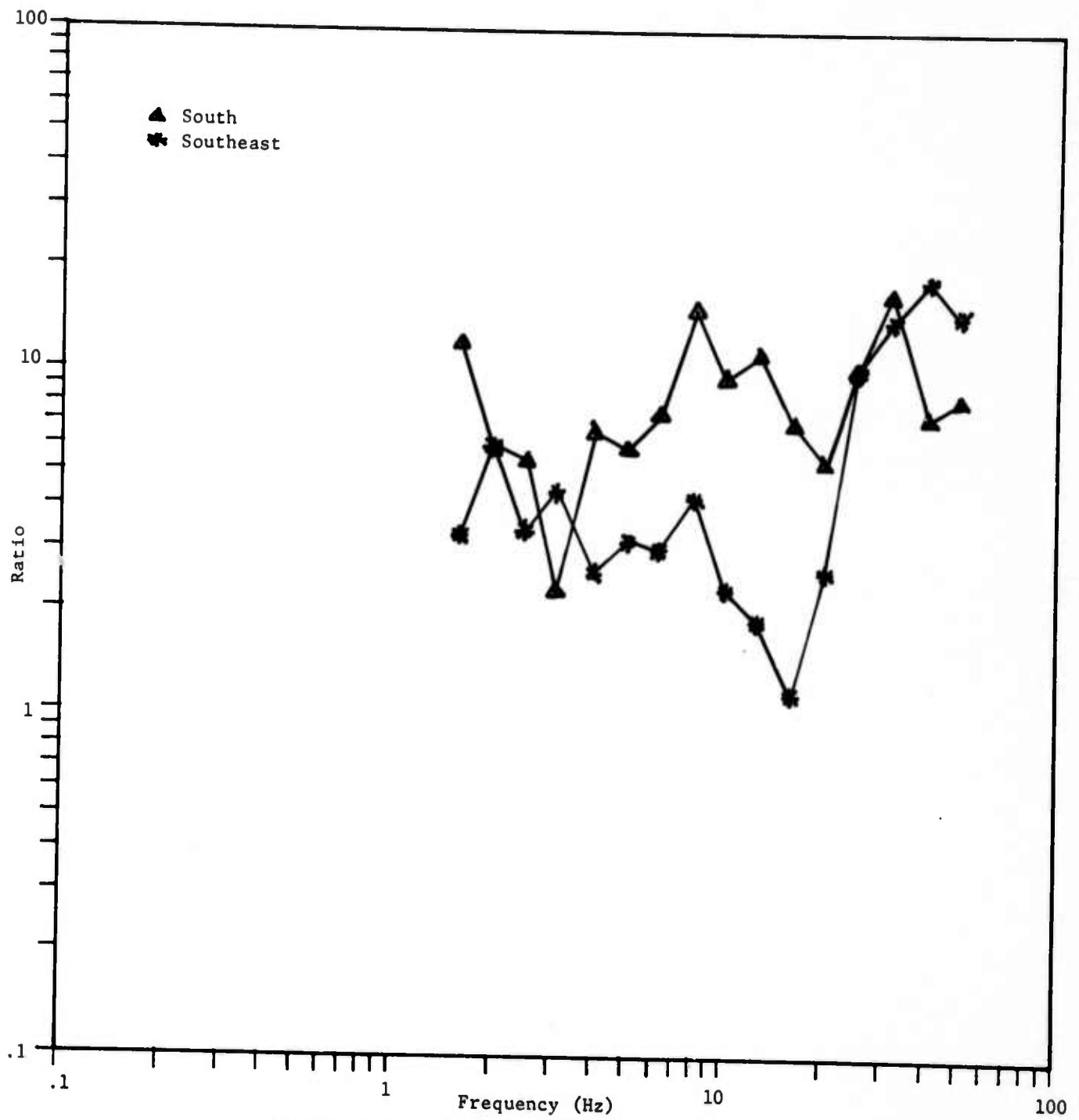


Figure G-4. DIAMOND MINE/DIAMOND DUST energy spectrum ratios

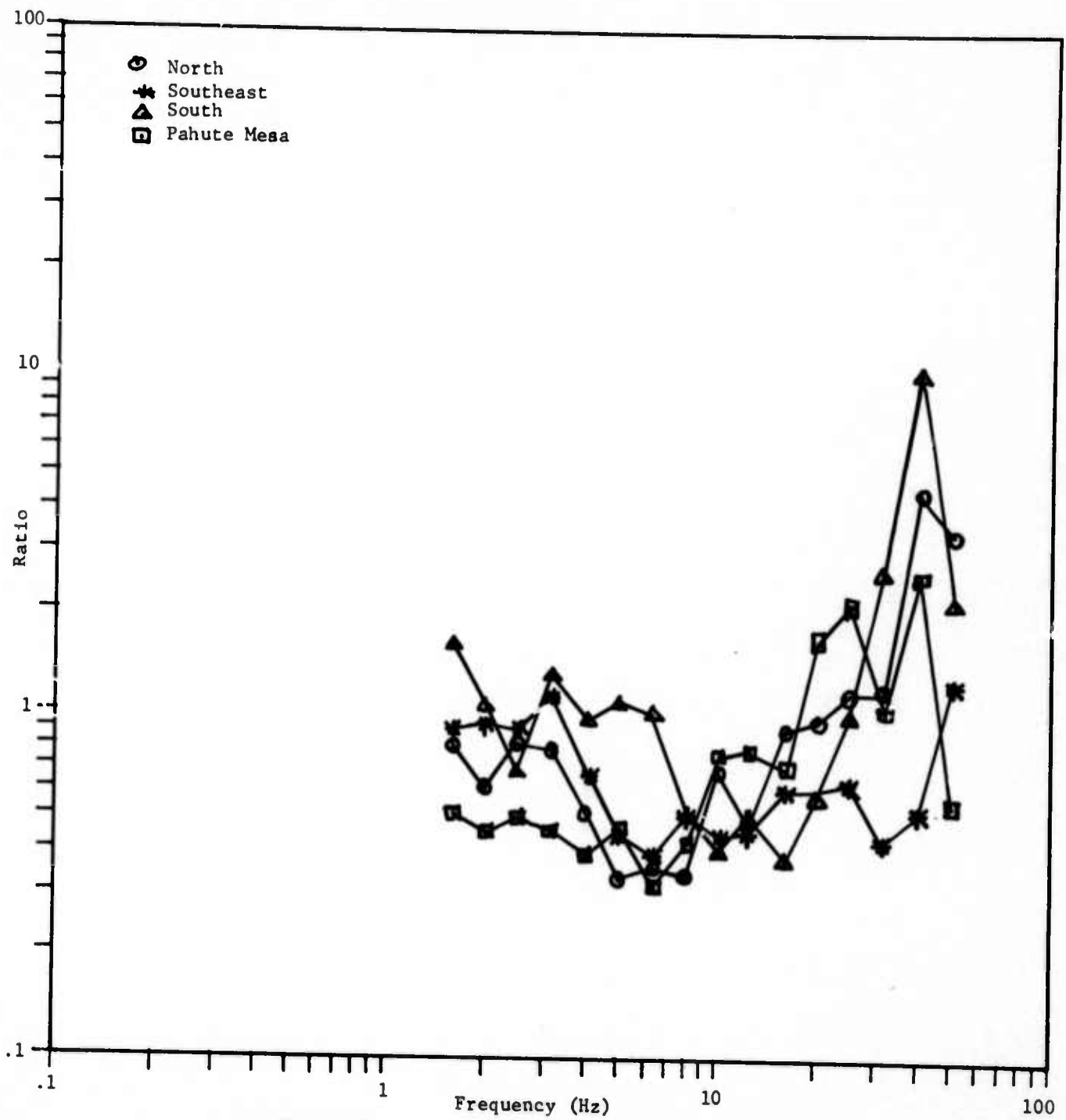


Figure G-5. DIAMOND MINE HE/MINE DUST HE energy spectrum ratios

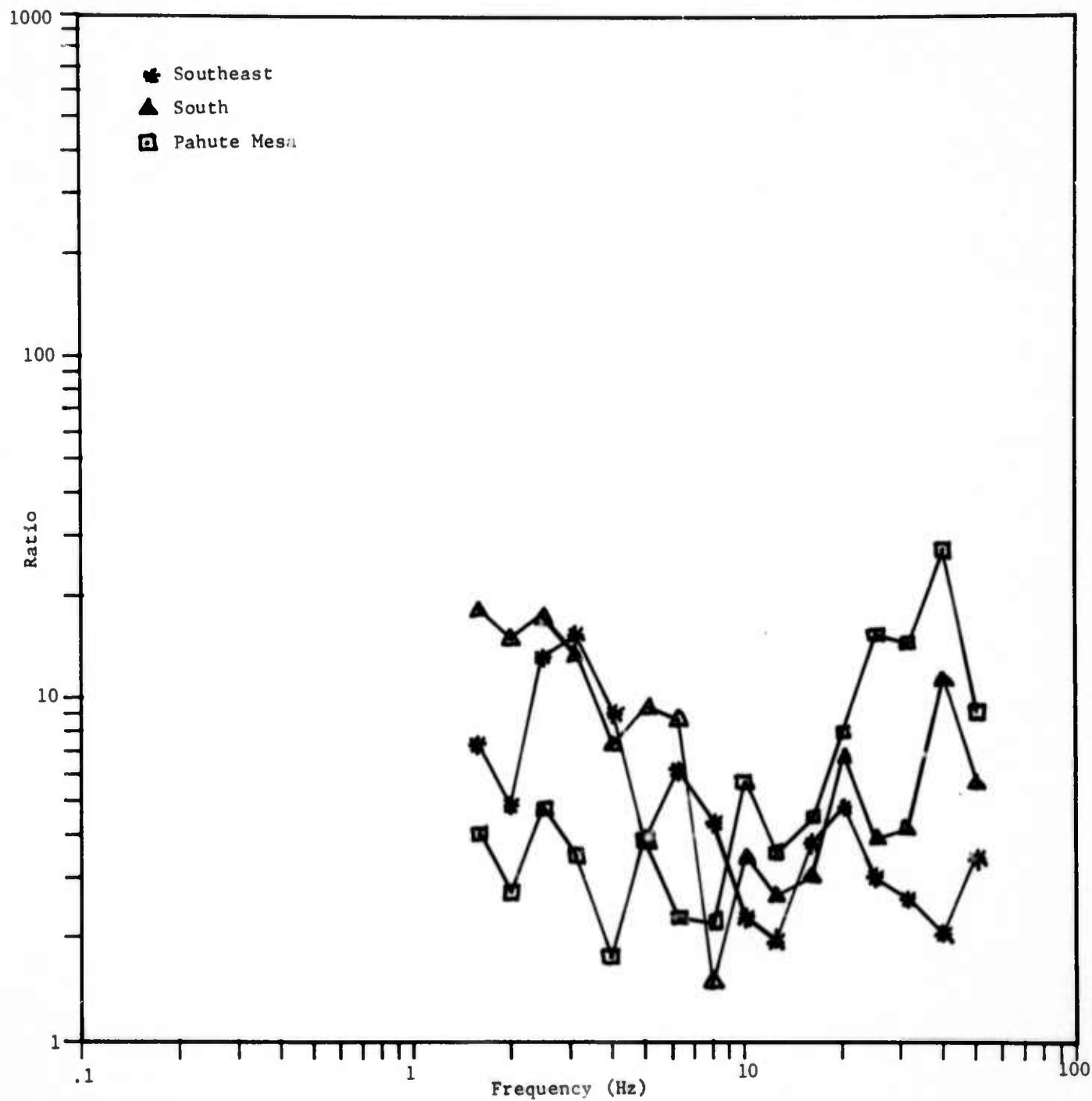


Figure G-6. DIAMOND DUST/MjME DUST HE energy spectrum ratios